NTNU

Norwegian University of
Science and Technology

Chitosan-based nanoparticles for siRNA-mediated downregulation of P-glycoprotein in rat brain endothelial cells in vitro

Hanne Auganes

Biotechnology
Submission date: May 2011
Supervisor: Kjell Morten Vårum, IBT
Co-supervisor: Sabina Strand, IBT

Norwegian University of Science and Technology
Department of Biotechnology

Preface

This Master of Science thesis in biotechnology was submitted to the institute of biotechnology belonging to the faculty of natural sciences at the Norwegian University of Science and Technology. The thesis was performed at facilities within the institute of physics in the time period September 2010 to April 2011.

I would like to express my gratitude towards my supervisor Sabina P. Strand for guidance and discussions as well as motivation, Kjell M. Vårum for being available for questioning about chitosan and its chemistry. A special thank goes out to PhD student Jostein Malmo for his time and devotion to introduce me to the techniques used and help with planning the experiments.

I would also like to thank my high school teacher in biology, Trond Herfindal who highly encouraged my ambitions to study biotechnology. Finally my family and all friends in the biotechnology class of ’11 for support and feedback throughout the years.

Trondheim, May 16th

Hanne Auganes

Abstract

Chitosans are cationic polymers desirable for use in nucleic acid delivery due to its biocompability, biodegradable and low toxic nature. The P-glycoprotein (P-gp) pump is a member of membrane transporters in brain endothelial cells which recognizes xenobiotics, extruding them from the cells. P-gp is a highly clinically relevant target as it also limits accessibility of drugs from the blood to the brain.

The overall aim of this work was to investigate the feasibility of using chitosan as a delivery vehicle for siRNA-mediated knockdown of P-glycoprotein (P-gp) efflux pump in an *in vitro* model of blood brain barrier. The human lung cancer cells (H1299) stably expressing GFP was used for screening and optimization of the delivery system and conditions. Lung cancer is often represented among multidrug resistant cell lines and is therefore also a suitable target for knockdown of transporters. The main objective was to implement this knowledge to efficiently downregulate the P-gp pump residing in the rat brain endothelial cell line RBE4.

The approach was to first establish suitable physiochemical characteristics of the chitosans like DP_n and the N/P ratios of chitosan/siRNA complexes by studying exogenous GFP and endogenous GAPDH expression and uptake of fluorescently labeled siRNA by flow cytometry. Cytotoxicity profiling of the chitosans and polyplexes was preformed with AlamarBlue, PI-staining, Cell counting and BCA assay. We further investigated the effect of chitosan mediated mdr1a-siRNA on drug efflux in the RBE4 cells using two functional assays; Rhodamine 123 efflux by flow cytometry and visualization of the anticancer drug Doxorubicin by CLSM.

We demonstrated that chitosan can be used as an efficent delivery vehicle for siRNA in both H1299 and RBE4 cells with negligible cytotoxicity in vitro. The formulated chitosan/siRNA polyplexes was found to dependent on DPn and N/P ratios in order to exert maximal effect on both uptake and knockdown. Specifically, we managed to downregulate the P-gp expression in RBE4 cells using chitosans with a high DPn complexed with mdr1a-siRNA in a low N/P ratio. Together these results elucidate the potential of chitosan mediated siRNA downregulation of the P-gp pump in RBE4 cells and further development for in vivo applications.

Table of contents

1. Introduction

Chitosan is a cationic polymer and has been widely applied for pDNA delivery; there is however a limited amount of research preformed with chitosan/siRNA polyplexes. The use of chitosan in nucleic acid delivery is desirable because of its biocompatibility and low toxicity profile. Chitin and chitosan have been a part of a research program at the institute for biotechnology at NTNU for many years and in collaboration with the St.Olavs Hospital we wanted to target a clinical target with focus on the blood brain barrier.

The P-gp pump is a member of membrane transporters in brain endothelial cells which recognizes xenobiotics, extruding them from the cells. P-gp is a highly clinically relevant target as it limits accessibility of drugs from the blood to the brain. Furthermore, overexpression of P-gp and other transporters in tumor cells is responsible for multidrug resistance in cancer. The pump is expressed by the mdr1 gene and downregulation of its expression can mediate drug accumulation in the cells.

As the RBE4 cell line was not available at the start of this thesis, we started our work by screening of different chitosan/siRNA formulations in human lung cancer cells (H1299). This cell line stably express GFP and is therefore well suited for optimization of the delivery system and conditions. Besides, lung cancer is often represented among multidrug resistant cell lines and is therefore also a suitable target for knockdown of transporters.

The overall aim of this work was to investigate the feasibility of using chitosan as a delivery vehicle for siRNA-mediated knockdown of P-gp efflux pump in an *in vitro* model of blood brain barrier. The approach was to first establish suitable physiochemical characteristics of the chitosans like DP_n and the N/P ratios of chitosan/siRNA complexes as well as cytotoxicity profiling. These preliminary studies were preformed with H1299 cells and the acquired knowledge was used with the RBE4 cells for further development.

2. Theory

2.1 RNA interference (RNAi)

RNAi interference is a part of the body's own defense machinery against unwanted and potentially harmful mobile genetic elements like transposons and viruses (Elbashir et al. 2001) . RNAi was first proposed in the nematode worm *Caenorhabditis elegans* where they fund a potent and specific genetic interference after the introduction of double-stranded RNA (dsRNA*) (*Fire et al. 1998). A schematic of the RNAi mechanism including effects of introduced short hairpin RNA and synthetic siRNA is presented in figure 2.1.

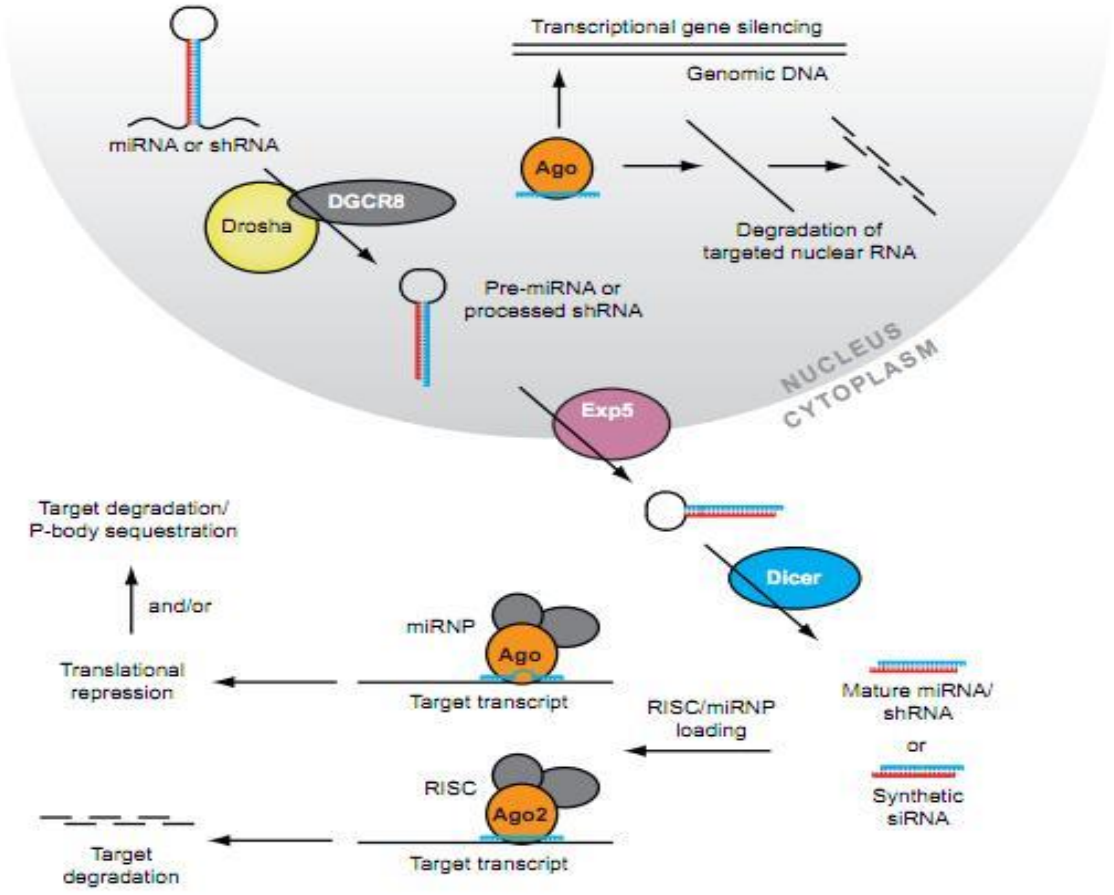

Figure 2.1 Shematics of the different RNA interference mechanisms (Martin and Caplen 2007).

Usually a large double-stranded RNA molecule is diced into small double-stranded siRNAs 21-28 base pairs long by the enzyme Dicer. They then assemble with proteins into ribonucleoprotein particles where the small interfering RNA is unwound to produce an RNA-Induced Silencing Complex (RISC) (Snustad and Simmons 2010). Argonaute 2, a multifunctional protein contained within RISC, unwinds the siRNA and leads to cleavage of the sense strand (or passenger strand) of the siRNA and further degradation (Matranga et al. 2005).

2.1.1 Short hairpin RNA (shRNA) and Small interfering RNA (siRNA)

It is possible to exploit the RNAi pathway in one of two ways: either by using a viral vector to express short hairpin RNA (shRNA) that resembles micro- RNA precursors, or by introducing siRNAs ~22 nucleotides with 3' OH dinucleotide overhangs that mimic the Dicer cleavage product into the cytoplasm (de Fougerolles et al. 2007).

After delivery of shRNA expression vectors into the cytoplasm, the vector needs to be transported into the nucleus for transcription. The primary transcripts are processed by the enzyme Drosha to form pre shRNAs. Pre-shRNAs are transported to the cytoplasm via exportin 5, to be loaded onto the Dicer complex where they are further processed to mature shRNA. Mature shRNA in the Dicer complex are associated with the RISC and results in an RNA interference function either through mRNA cleavage and degradation, or through translational suppression (Rao et al. 2009).

However, the smaller size of siRNA's and the need for cytoplasmic delivery only together with ease of availability and efficiency makes the introduction of siRNA more amenable for RNAi. siRNA can be synthetically produced and then introduced into the cells cytoplasma, thereby bypassing Dicer mechanics (Whitehead et al. 2009).

This shortcut reduces the potential for an innate immune interferon response and the shutdown of cellular protein expression that can occur following the interaction of long dsRNA with intracellular RNA receptors(Grimm et al. 2006). The activated RISC targets a sequence in a messenger RNA that is complimentary to the interfering RNA. If the sequences are perfectly base-paired, the mRNA is cleaved and the mRNA is degraded. (Snustad and Simmons 2010) The activated RISC–siRNA complex can then be recycled for the destruction of identical mRNA targets, it behaves as a catalyst.

When using appropriately designed siRNA, the RNAi machinery can be exploited to silence nearly any gene in the body, giving it a broader therapeutic potential than typical small-molecule drugs (Whitehead et al. 2009). The rest of this section will focus solely on siRNA delivery and its applications.

2.1.3 The challenges and barriers of siRNA delivery

In order for siRNA delivery to be efficient it must overcome several obstacles both outside and inside the cell. Because of its large size and negative charge, naked siRNA has a low ability to cross cell membranes. Thus, it must be complexed with a sufficient nanoparticle carrier which should express all of the qualities expected from an optimal delivery agent.

Bioconjugation of siRNAs with lipids and polymers is desirable in order to increase their thermodynamic and nuclease stability, improve the biodistribution and pharmacokinetic profiles of siRNAs, and target them to specific cell types. Although transfection efficiency of siRNAs into cultured cells is satisfactory for most in vitro applications, its therapeutic applications in vivo is more challenging (De Paula et al. 2007). Ideally, a delivery mechanism should;

1) Be capable of binding siRNAs in a reversible manner to ensure subsequent release of the siRNAs in target cells.
2) Protect siRNAs from nuclease degradation during transit through the circulation.
3) Efficiently escape from endosomal compartment.
4) Be biocompatible and biodegradable
5) Avoid rapid clearance by the liver and kidney.

Some of the limitations and obstacles of siRNA delivery are presented in figure 2.2.

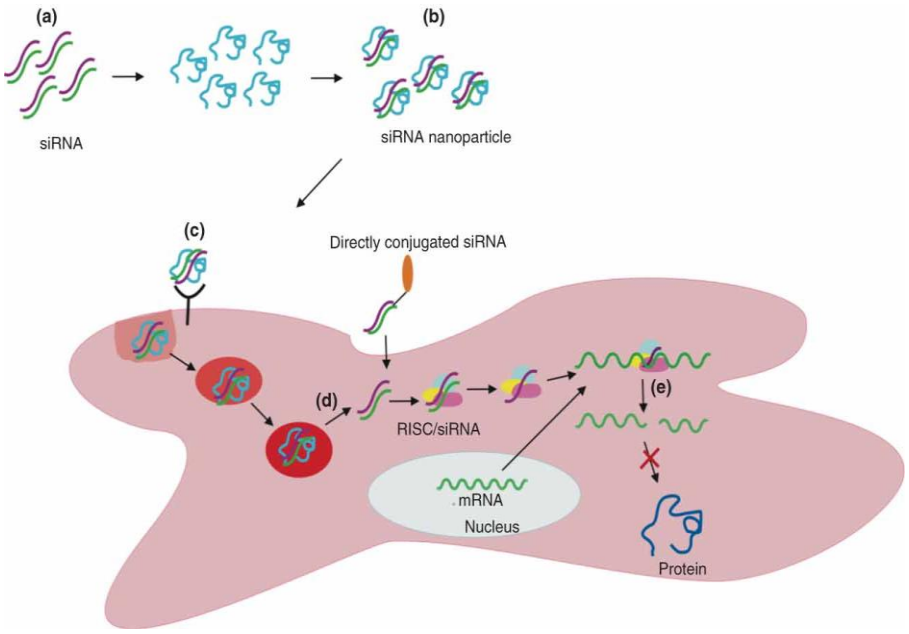

Figure 2.2 The limitations to siRNA delivery and the siRNA-induced RNAi pathway: (A) siRNA stability, (B) siRNA nanoparticle stability, (C) siRNA or siRNA nanoparticle targeting and internalization, (D) siRNA endosomal escape, and (E) siRNA off-target effects (Tokatlian and Segura 2010).

a) Interaction between nucleic acids and cationic lipids or polymers

Complex formation relies on the electrostatic interaction between the negatively charged nucleic acid and the positively charged transfection reagent. The complex enhances nucleic acid uptake by compacting the size of the nucleic acid by a phenomenon called condensation (Bloomfield 1996). Cationic polymers differ from cationic lipids in that they do not contain a hydrophobic moiety and are completely soluble in water (Elouahabi and Ruysschaert 2005). Compared with cationic liposomes, they have the advantage of compressing DNA molecules to a relatively small size (Gershon et al. 1993; Ruponen et al. 1999). This can be crucial for gene transfer, as small particle size may be favorable for improving transfection efficiency (Lv et al. 2006).

b) Cellular binding

There are several ways the siRNA delivery agents make contact with the cells; some are receptor mediated while other relies merely on electrostatic interactions. The surface charge of the delivery vehicle is an important property that affects their interaction with cells and non-cellular components. A charge acts as a double-edged sword, which aids cellular uptake but can also result in non-specific interactions with non-targets cells and extracellular components such as serum proteins and extracellular matrices. This lack of specificity is not a problem in culture when there is only one type of cell, but is a problem for systemic *in vivo* delivery (Wolff and Rozema 2007).

c) Cellular uptake

Most siRNA nanoparticles enter the cell through endocytosis, which poses a major limitation to siRNA efficiency as it must be released into the cytosol to activate the RNAi pathway. The best understood uptake pathway is clathrin-mediated endocytosis, molecules preferentially interact with generic complementary binding sites like lectin or charged interfaces (Khalil et al. 2006). Figure 2.3 illustrates the clatrin-mediated endosytosis which occurs constitutively in all mammalian cells.

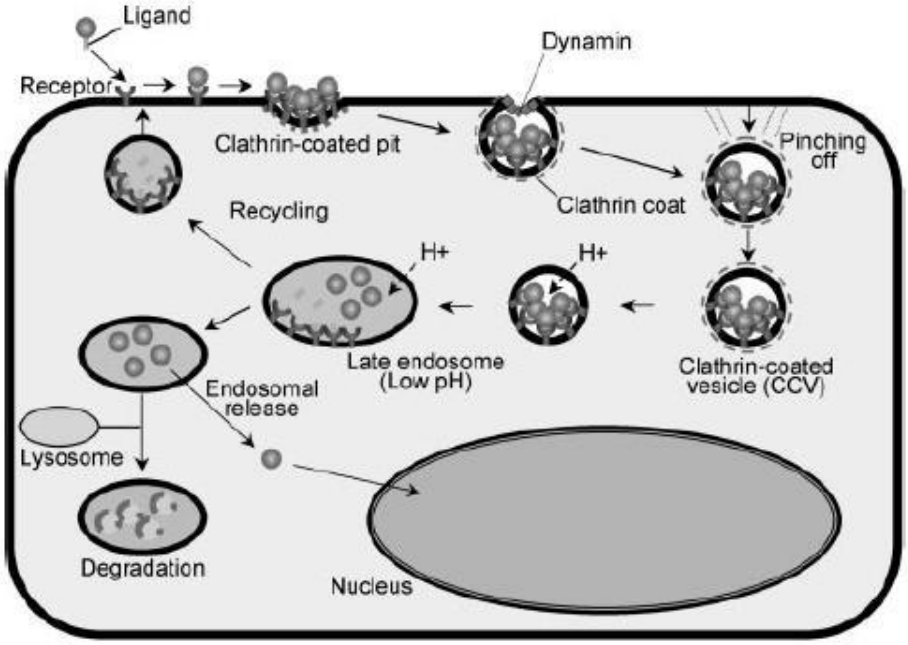

Figure 2.3 Clathrin-mediated endosytosis and pathway in the cell (Khalil et al. 2006).

In general, siRNA nanoparticles (*in vitro*) enter more than 90% of the cells through endocytosis; however, the release of the nanoparticles and/or siRNA to the cytosol occurs less readily (Tokatlian and Segura 2010). Nanoparticle capture within the endosomal–lysosomal pathway as a consequence of endocytosis is the predominant barrier for enabling interaction with cytoplasmic or nuclear targets. The inclusion of endosomal buffering and pH-activated polymers and membrane-interacting peptides capable of endosomal escape and transport to the cytosol are methods to overcome this (Howard et al. 2008).

d) Endosomal escape

If the siRNA nanocomplex is unable to exit the endosome, it will be trafficked through endomembrane compartments of decreasing pH and be subjected to degradative conditions in the lysosome.(Whitehead et al. 2009) The high charge density of cationic polymers allows them to escape from endosomes and deliver their nucleic acid cargo into the cytosol through the so-called "proton-sponge" effect. The polycationic nature of the polymer is thought to buffer low endosomal pH through enhanced influx of protons and water, resulting in endosome rupture (S. Akhtar and Benter 2007; Martinez et al. 2002).

e) siRNA off-target effects

It has been argued that off-target transcript silencing is siRNA sequence dependent and is a fundamental feature of RNAi-mediated silencing (Jackson et al. 2006). Imperfect pairing of siRNA strands with sequence motifs that reside primarily in 3′ UTR regions of cellular mRNAs can lead to microRNA-like off-target silencing (Jackson and Linsley 2010). They further suggested that many transcripts can be affected and it is inherent to any siRNA sequence, because only short regions of sequence complementarity are required for this type of off-target silencing.

Other off-target effects of siRNAs result from innate immune responses to either oligonucleotides or the delivery vehicles used to carry them to cells or tissues. Toll-like receptors (TLRs) protect the host from pathogens by detecting infectious non-self agents including double-stranded RNA (Jackson and Linsley 2010). Figure 2 shows some of the common siRNA off target effects.

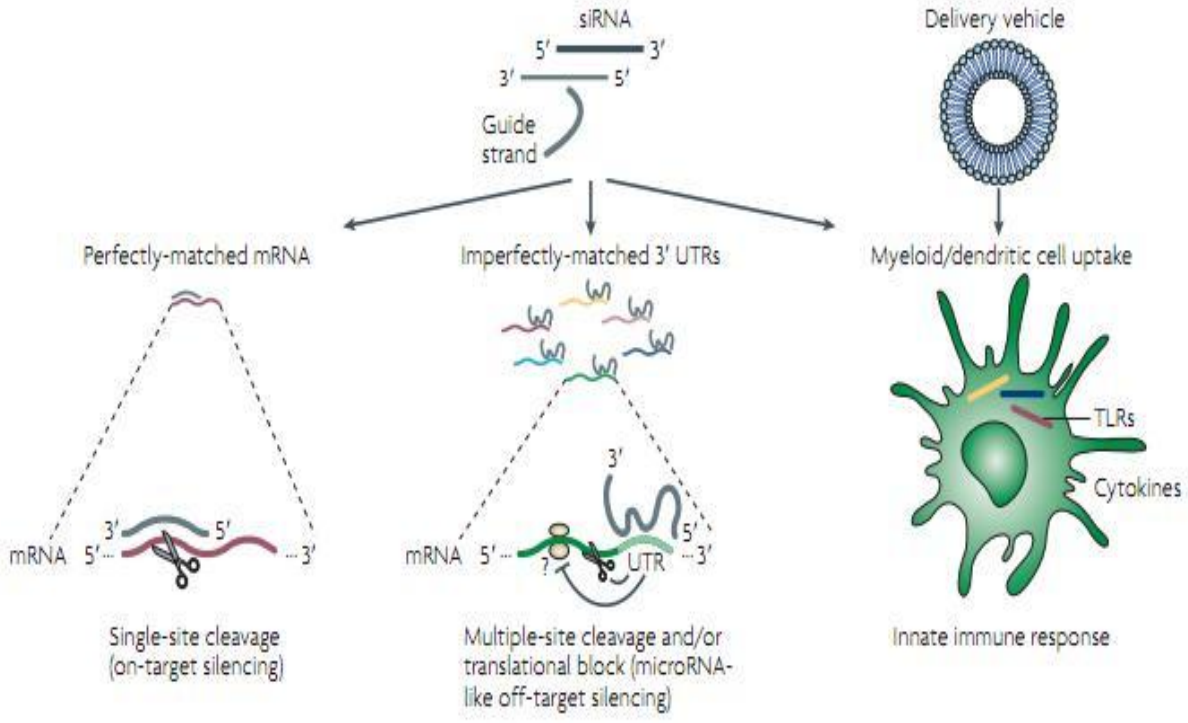

Figure 2.4 Types of off-target effects observed with siRNAs. TLR; toll-like receptor (Jackson and Linsley 2010).

Ineffective siRNAs can lead to false negative conclusions, while non-specific siRNAs can produce false-positive conclusions concerning the role of the target gene in functional assays (Jackson and Linsley 2004). These limitations in siRNA delivery can be circumvented by modifying the introduced siRNA sequence.

2.2 Chitin and chitosan

Chitin is a marine polysaccharide consider to be the second most abundant biomass resource after cellulose, and also the most unutilized (Kurita 2006). Chitosans are derived from chitin found in the exoskeleton of arthropods and in the cell wall of many fungi and is a family of cationic and linear polysaccharides. They are binary polysaccharides comprised of randomly distributed beta (1–4) linked 2-amino-2-deoxy-b-D glucose (GlcN; D-unit) and the N-acetylated analogue (GlcNAc; A-unit) (Roberts 1992).

2.2.1 Manufacturing of chitosan and its applications

Chitosan is chemically produced from chitin by alkaline de-N-acetylation and the conditions used for deacetylation determines the polymer molecular weight and the fraction of acetylated units; F_A (Dash et al. 2011). A schematic presentation of the deacetylation is presented in figure 2.3

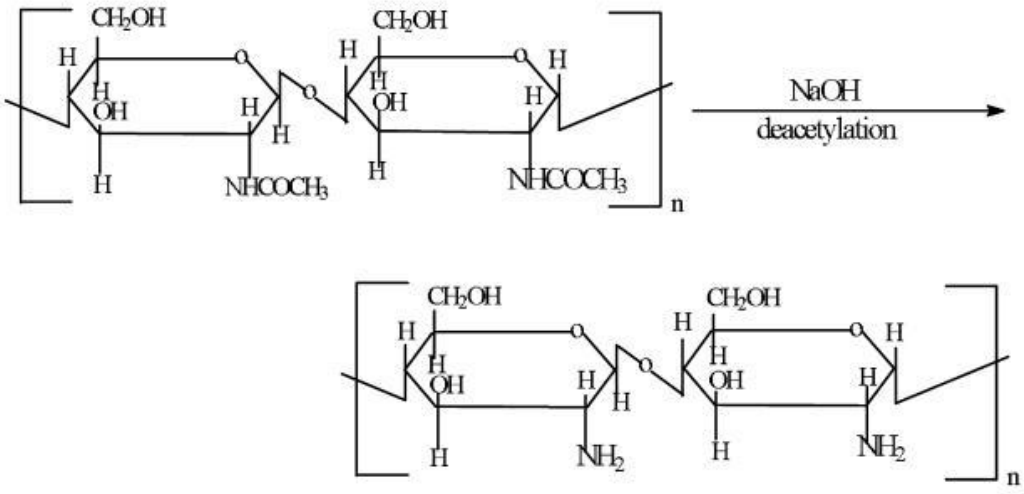

Figure 2.5 Shematic of the deacetylation of chitin to chitosan (Ravi Kumar 2000).

The application potential of chitosan is vast, in food and nutrition industries, biotechnology, material science, drugs and pharmaceuticals, agriculture and environmental protection, and recently in gene therapy (Harish Prashanth and Tharanathan 2007). An important property for biological applications is that chitosans can interact with negatively charged mucin layers on mucosal tissues or cell membrane proteoglycans in a process called muco/bioadhesion (Issa et al. 2005).

Chitosans is considered biodegradable and breaks down slowly to harmless products which are absorbed by the human body. Moreover, chitosans are biocompatible and generally have a low toxicological profile when administered to the body. This is an important aspect in regards to the metabolic fate or biodegradation which could provide fragments suitable for renal clearance or general amino acid turnover in the body (Kean and Thanou 2010). Based on these properties, chitosan is rendered as a suitable and safe delivery vehicle for nucleic acids.

2.2.2 Chitosan as a delivery vehicle for siRNA

Chitosan nanoparticles for siRNA delivery has been widely studied and modified for pDNA delivery, less research is available for the implementation of siRNA delivery. Complexes between siRNA and chitosan are formed spontaneously as a result of electrostatic interactions between the negatively charged phosphate groups of siRNA and the chitosans positively charged groups (Reischl and Zimmer 2009).

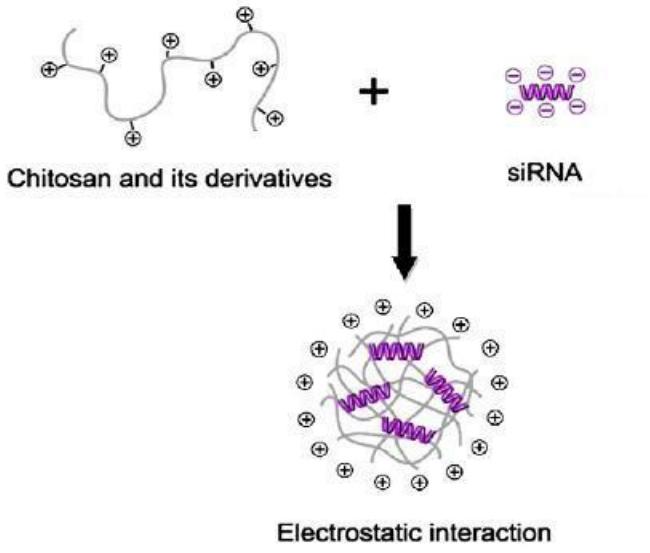

Figure 2.6 Preparation of chitosan/siRNA polyplexes based on electronegative interactions. Modified from (Mao et al. 2010).

Although most chitosans are able to compact nucleic acids into nanosized polyplexes, the stability and properties of polyplexes strongly depend on chitosan structural variables. The siRNA delivery can be varied by the molecular weight (Mw) of the chitosans which affects polymer chain entanglement, further influencing its complexing ability with siRNA (Rudzinski and Aminabhavi 2010).

The molecular weight of the chitosans are often given in statistical terms like number average and weight average (Mn and Mw), Polydispersity index (PDI) defined by Mn/Mw ratio or number average degree of polymerization (DP_n), because of its polydisperse nature (Wang et al. 2010). High Mw chitosan will entangle siRNA more readily than low Mw chitosan, which results in binding siRNA more efficiently and protecting the condensed siRNA from enzymatic degradation and serum components. (Rudzinski and Aminabhavi 2010).

Furthermore, the molecular weight will influence the size of the chitosan/siRNA polyplexes, which is an important aspect in cellular uptake. Furtehermore, the fraction of acetylated units (F_A) of chitosans determines the positive charge density and a lower F_A results in increased positive charge that enables a greater siRNA binding capacity (Liu et al. 2007). Moreover, the ratio of chitosan amino groups to RNA phosphate groups (N/P ratio) influences the ability of the particles to efficiently condense siRNA and interact with the negatively charged cell membranes (Mao et al. 2010). Together, all these properties together determine the overall charge and size of the chitosan/siRNA complex and ultimately the transfection efficiency (Rudzinski and Aminabhavi 2010).

Another factor that may influence the transfection efficiency is the pH of the system, the interactions strengths between siRNA and chitosan are pH dependent and the adhesive interactions decreases with increasing pH (Mao et al. 2010; S. Xu et al. 2007). Furthermore, the presence of serum may interfere with the transfection and chitosan/siRNA polyplexes have been shown to effectively protect siRNA from degradation of nucleases in 10% serum(Katas and Alpar 2006). Additionally, siRNA concentration, polyplex preparation techniques and route of administration are important aspects in formulation of efficient chitosan nanoparticles.

2.2.3 Chitosan/siRNA polyplex modifications

Chitosan nanoparticles have been modified and substituted in many ways in the search for an optimal gene delivery particle. One of the major obstacles concerning siRNA delivery with chitosan nanoparticles for in vivo applications is the physical and colloidal stability. This can to some extent be overcome by the incorporation of DNA and PEGylated chitosans respectively. Further, there is a need for serum stability and targeting ligands may be necessary for the correct cellular localization of the nanoparticles.

One method of preventing self-aggregation and undesired interactions with unwanted components in blood is to employ steric stabilization. Polythethylene glycol (PEG) has been conjugated to different non-viral delivery carriers, and the resulting PEGylated particles have demonstrated increased salt and serum stability (Jiang et al. 2007). Another means of copolymerization is Polyethyleneimine (PEI), which also has been used as a modifier for chitosan vector derivation but can exhibit high toxicity to cells and is need for further optimization (Wong et al. 2005).

Many of the nanoparticles developed cannot be used in clinical settings due to nonspecific delivery, which may lead to unwanted side effects. Preferably, the delivery system should show enhanced concentrations of therapeutic payloads at disease sites, minimize concerns about off-target effects, and ultimately raise the therapeutic index (Han et al. 2010; Whitehead et al. 2009). Therefore, the introduction of targeting ligands may increase the specificity and safety of the delivery agent. A novel tumor targeted delivery system for siRNA has recently been demonstrated by using an Arg-Gly-Asp (RGD) peptide-labeled chitosan nanoparticle for selective intratumoral delivery by binding to the αvβ3 integrin (Han et al. 2010)

2.3 P-glycoprotein

In this thesis we chose a target with a high clinical relevance, more specifically the down regulation of the P-glycoprotein pump in rat brain endothelial cells by chitosan-siRNA transfection. In this section we give a background for the target and its localization.

P-glycoprotein (P-gp) is a member of the ABC transporter family, expressed by the mdr1 gene The P-gp is found to be concentrated in a small number of specific sites, certain cell types in liver, pancreas, kidney, colon, show specific localization of P-glycoprotein (Thiebaut et al. 1987). They suggested that the protein plays a role in the normal secretion of metabolites and certain anti-cancer drugs into bile, urine, and directly into the lumen of the gastrointestinal tract. Additionally P-gp is found on the apical side of brain endothelial cells, mediating active efflux of xenobiotics from the cells to the blood. Figure 2.7 shows a simplified version of the function of P-gp.

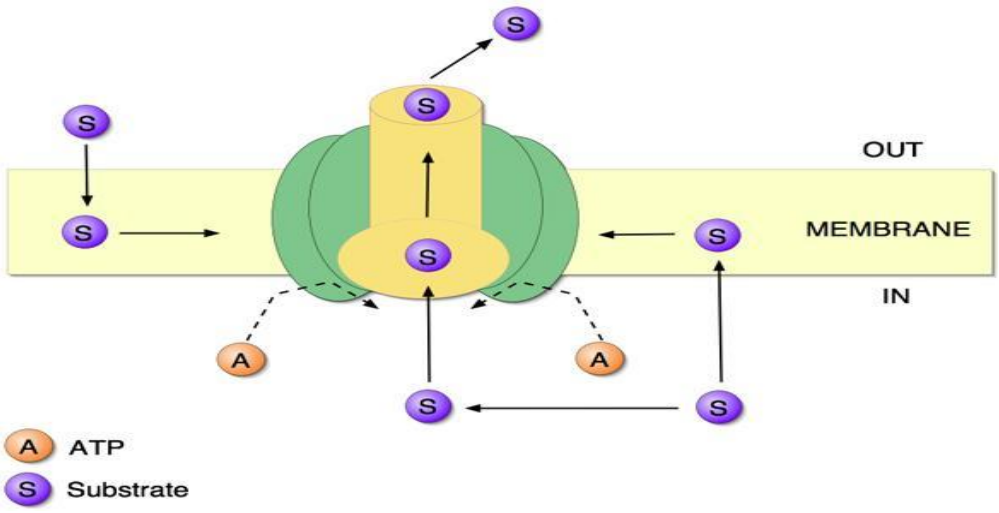

Figure 2.7 Simplified P-glycoprotein structure and function in the cell membranes (Edwards 2003).

More importantly, P-gp is often associated with multiple drug resistance (MDR) in cancer cell lines, by downregulating its expression we can dramatically improve the medical treatment.
The role of P-glycoprotein inhibitors in drug delivery have been extensively studied and reviewed, a number of inhibitors have been developed but their toxicity and unfavorable pharmacokinetics have limited their clinical use (N. Akhtar et al. 2011; Sharom 2006)

The implementation of siRNA technology to temporarily and specifically downregulate the expression of P-gp holds great potential for investigation both in vitro and in vivo. (Fuest et al. 2009; S. H. Lee and Sinko 2006). Lipid based reagents have been used to deliver naked siRNA targeting P-gp in vitro (Wu et al. 2003) and in vitro by simple IV injection of modified siRNA (Su et al. 2005). Inhibition of P-gp expression by naked siRNA transfection, siRNA incorporated plasmid transfer, and stable siRNA transfection were compared and the most dramatic silencing of P-gp was obtained in stably transfected cell lines (D. Xu et al. 2004).

This makes the P-gp pump a highly relevant clinical target for chitosan/siRNA mediated downregulation. When this thesis was written, there was no published research on the use of chitosan based nanoparticles for siRNA downregulation of the P-gp pump.

2.4 Blood brain barrier

The blood brain barrier (BBB) is formed by the blood capillary endothelial cells in the brain which are closely linked together by tight junctions. Its main purpose is to protect the central nervous system (CNS) from the harmful effects of the many toxic substances that may adversely affect brain function. This effective protection ultimately results in the limited entry of 95% of drug candidates with potential benefits for CNS diseases (Fromm 2004; Fuest et al. 2009). Diseases often accociated with the BBB and either upregulation or downregulation of P-gp expression include epilepsy, depression, brain tumors, brain HIV, Alzheimers and Parkinsons disease (Löscher and Potschka 2005).

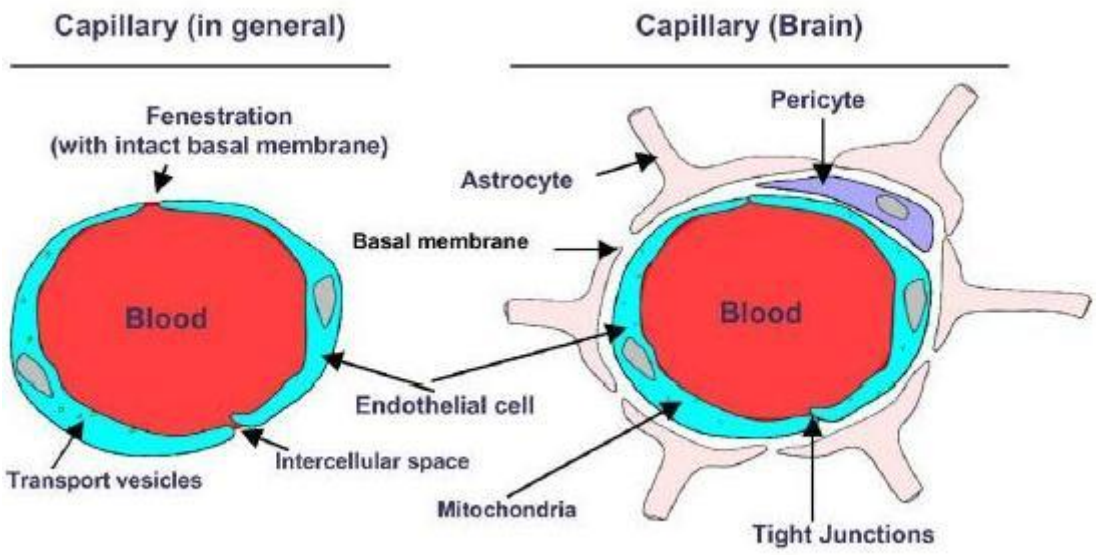

Figure 2.8 Schematic comparison of a brain capillary with a capillary in the periphery. (Löscher and Potschka 2005)

Many approaches have been made for brain drug delivery, trans-cranial/trans-nasal, BBB disruption, lipidization of small molecules, transport of large-molecule drugs with molecular Trojan horses, all with variable obstacles and results (Pardridge 2007).

The rat brain endothelial cell line (RBE4) is a suitable in vitro model for studies on BBB permeability and transport functions as it expresses many of the BBB specific properties. (Roux and Couraud 2005). Furthermore, RBE4 cell monolayers have been used to investigate transport of large molecules, potentially useful drug delivery vectors such as immunoliposomes and nanoparticles (Alyaudtin et al. 2001; Cerletti et al. 2000) More importantly, the RBE4 cells stably expresses P-gp (though downregulated) in cell culture, making it well suited for downregulation studies of the transporter (Regina et al. 1998).

Taken together, use of the RBE4 cell line as a model for BBB and investigation of chitosan mediated siRNA downregulation of the P-gp pump could provide us with the ability to increase the intracellular accumulation of drugs and thus improve treatment of the various diseases.

2.5 Fluorescence based techniques

Throughout this thesis, a majority of the techniques used for analysis is based upon the principle of fluorescence. Fluorescence can be defined as "the molecular absorption of light energy (photon) at one wavelength and its re-emission at another, usually longer, wavelength".

The fluorescence process can be broken down into three phases:
1. **Excitation** - absorption of light of an appropriate wavelength by fluorophore.
2. **Excited state** - fluorophore undergoes vibrational and conformational changes.
3. **Emission** - photon of light is emitted.

The fluorescence process is cyclical therefore a fluorophore can be excited repeatedly (GE-Lifesciences). Specific biological and inorganic materials have the capacity to absorb light of a particular wavelength, this energy excites electrons of a low energy state to a higher state, loss of energy is emitted as fluorescent light which can be detected be photomultiplier tubes in the case of flow cytometric instruments (Warnes). A Jablonski energy diagram i presented in figure 2.9.

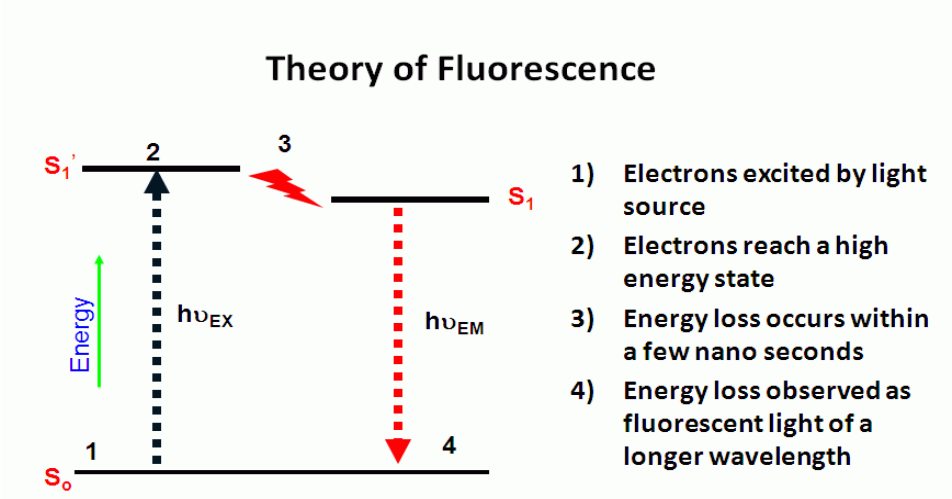

Figure 2.9 Jablonski energy diagram of fluorescence (Warnes).

In this thesis we use flow cytometry for estimation of knockdown and uptake in cells as well as confocal laser scanning microscopy for vizualisation of intracellular drug accumulation. These methods will be described briefly in the following sections.

2.5.1 Flow cytometry

Flow cytometry is a technology that simultaneously measures and then analyzes multiple physical characteristics of single particles, usually cells, as they flow in a fluid stream through a beam of light. The properties measured include a particle's relative size, relative granularity or internal complexity, and relative fluorescence intensity. These characteristics are determined using an optical-to-electronic coupling system that records how the cell or particle scatters incident laser light and emits fluorescence. A flow cytometer is made up of three main systems: fluidics, optics, and electronics (Rahman).

• *The fluidics system* transports particles in a stream to the laser beam for interrogation. Essentially, the fluidics system consists of a central channel/core through which the sample is injected, enclosed by an outer sheath that contains faster flowing fluid. As the sheath fluid moves, it creates a massive drag effect on the narrowing central chamber. This alters the velocity of the central fluid whose flow front becomes parabolic with greatest velocity at its center and zero velocity at the wall. The effect creates a single file of particles and is called hydrodynamic focusing (USU)

• *The optics system* consists of lasers to illuminate the particles in the sample stream and optical filters to direct the resulting light signals to the appropriate detectors. The cells in the sample are accelerated and individually pass through a laser beam for interrogation. Light scattering occurs when a particle deflects incident laser light.(Rahman)

Light that is scattered in the forward direction, typically up to 20° offset from the laser beam's axis, is collected by a lens known as the forward scatter channel (FSC). The FSC intensity roughly equates to the particle's size and can also be used to distinguish between cellular debris and living cells. Light measured approximately at a 90° angle to the excitation line is called side scatter. The side scatter channel (SSC) provides information about the granular content within a particle. Both FSC and SSC are unique for every particle, and a combination of the two may be used to differentiate different cell types in a heterogeneous sample. (Rahman)

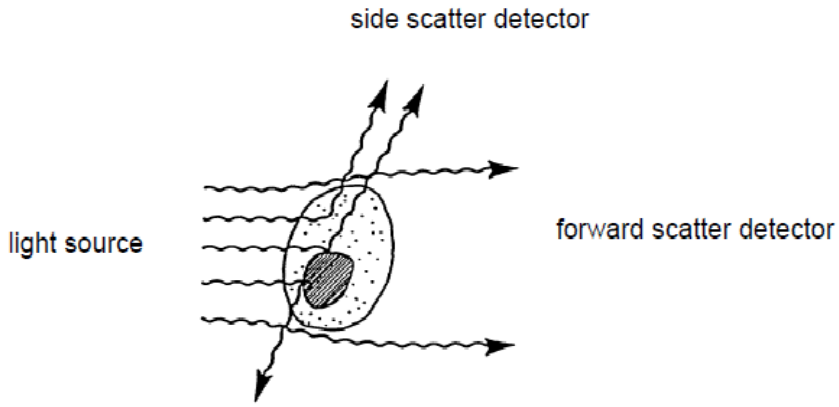

Figure 2.10 Light scattering properties of a cell (USU).

• *The electronics system* converts the detected light signals into electronic signals that can be processed by the computer. The detectors produce electronic signals (voltages) proportional to the optical signals striking them by photodetectors and then assigned a channel number on a data plot.(51) List mode data are collected on each particle or event. The characteristics or parameters of each event are based on its light scattering and fluorescent properties. The data are collected and stored in the computer. This data can be analyzed to provide information about subpopulations within the sample (BD-biosciences).

An important principle of flow cytometry data analysis is to selectively visualize the cells of interest while eliminating results from unwanted particles e.g. dead cells and debris. This procedure is called gating. Cells have traditionally been gated according to physical characteristics. For instance, subcellular debris and clumps can be distinguished from single cells by size, estimated by forward scatter. Also, dead cells have lower forward scatter and higher side scatter than living cells

Single-parameter histograms are graphs that display a single measurement parameter (relative fluorescence or light scatter intensity) on the x-axis and the number of events (cell count) on the y-axis. The histogram is useful for evaluating the total number of cells in a sample that possess the physical properties selected for or which express the marker of interest. Cells with the desired characteristics are known as the positive dataset (Rahman).

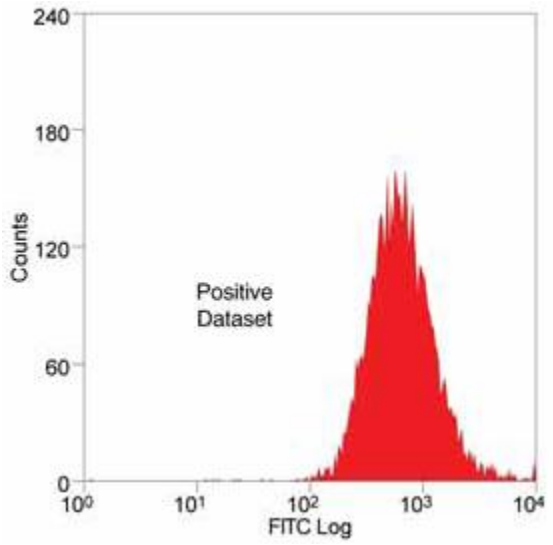

Figure 2.11 Example of a single parameter histogram (Rahman).

2.5.2 Confocal laser scanning microscopy

A confocal microscope creates sharp images of a specimen that would otherwise appear blurred when viewed with a conventional microscope. This is achieved by excluding most of the light from the specimen that is not from the microscope's focal plane. The image has less haze and better contrast than that of a conventional microscope and represents a thin cross-section of the specimen. The confocal microscope incorporates the ideas of point-by-point illumination of the specimen and rejection of out-of-focus light(Semwogerere)

The confocal principle in epi-fluorescence laser scanning microscope is diagrammatically presented in Figure 2. Coherent light emitted by the laser system (excitation source) passes through a pinhole aperture that is situated in a conjugate plane (confocal) with a scanning point on the specimen and a second pinhole aperture positioned in front of the detector (a photomultiplier tube). As the laser is reflected by a dichromatic mirror and scanned across the specimen in a defined focal plane, secondary fluorescence emitted from points on the specimen (in the same focal plane) pass back through the dichromatic mirror and are focused as a confocal point at detector pinhole aperture.

The significant amount of fluorescence emission that occurs at points above and below the objective focal plane is not confocal with the pinhole (termed Out of- Focus Light Rays in Figure 2). Because only a small fraction of the out-of-focus fluorescence emission is delivered through the pinhole aperture, most of this extraneous light is not detected by the photomultiplier and does not contribute to the resulting image. (Claxton)

The detected light originating from an illuminated volume element within the specimen represents one pixel in the resulting image. The computer can generate a three-dimensional picture of a specimen by assembling a stack of these two-dimensional images from successive focal planes. In addition, confocal microscopy provides a significant improvement in lateral resolution and the capacity for direct, non-invasive serial optical sectioning of intact, thick living specimens with an absolute minimum of sample preparation.

As laser scanning confocal microscopy depends on fluorescence, a sample usually needs to be treated with fluorescent dyes to make things visible. However, the actual dye concentration can be very low so that the disturbance of biological systems is kept to a minimum. Some instruments are capable of tracking single fluorescent molecules. Additionally transgenic techniques can create organisms which produce their own fluorescent chimeric molecules, such as a fusion of GFP, Green fluorescent protein with the protein of interest. (Quanta-tech).

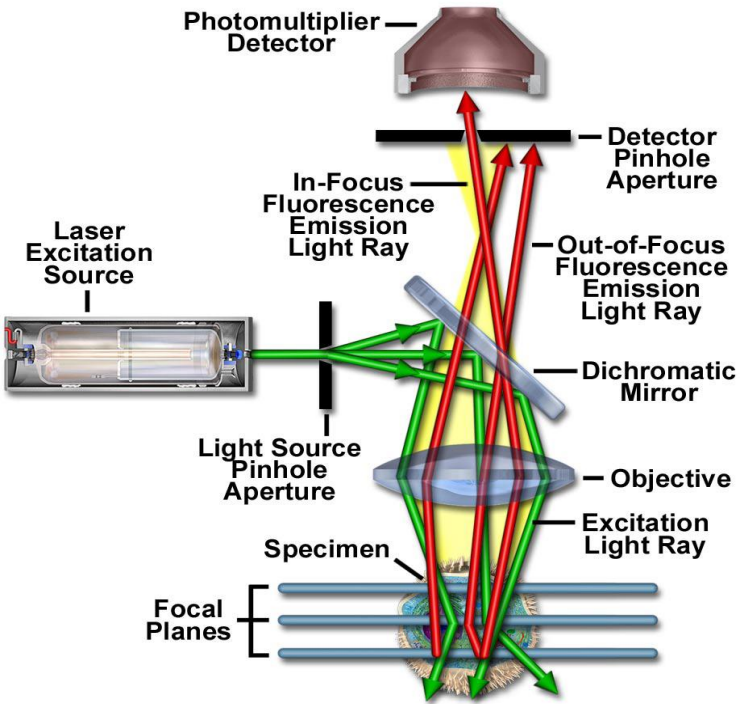

Figure 2.12 Schematic diagram of the optical pathway and principal components in a laser scanning confocal microscope (Claxton).

3. Materials and methods

3.1 Materials

The human lung cancer cell line (H1299) was a gift from Jørgen kjems, inst. for molecular biology at the University of Århus, Denmark. The rat-brain endothelilial cell line (RBE4) was a gift from Tore Syvertsen, inst. for nevromedisin at St Olav hospital, Norway.

The linear chitosans used in this thesis were developed by the department of biotechnology, Norwegian University of Science and Technology and supplied by the courtesy of post doc Sabina P. Strand. Producers and production numbers of all reagents used are given in appendix A, some physiochemical properties of the chitosan used are given in table 2.1.

Table 3.1 Physical and chemical properties of the chitosans used in this study. DPn, Mn, Mw and PDI.

Notation	**Mn (kDa)**	**Mw (kDa)**	**DPn**	**PDI**
DP_n 54	10.8	16.4	54	1.52
DP_n 200	39.8	74.5	199	1.87
DP_n 250	49.5	100.3	247	2.03
DP_n 300	64.1	141.6	320	2.21
DP_n 400	75.1	203	375	2.70

3.2 Cultivation and passaging of cell lines

The H1299 cells were cultivated in RPMI medium (Sigma) supplemented with 1% non-essential amino acids NEAA (Gibco), 100U/mL Penicillin/100µg/mL streptomycin; PEST (sigma) or 300µg/mL G418 (Sigma). The RBE4 cells were cultivated in αMEM (Gibco) supplemented with 1% NEAA, 10% heat inactivated fetal bovine serum; FBS (Gibco), PEST or 300µg/mL G418 and 100ng/mL growth factor bFGF. The same passaging procedure was performed for both cell lines (H1299 and RBE4):

For cell passaging the cells should be ~95 % confluent. Old medium was removed from the flask and the cells were rinsed with 10-13 mL of warm phosphate buffered saline; PBS (Gibco) by swinging gently and removing it. 2-3 mL trypsin/EDTA (Sigma) was added on the roof for detachment of cells and poured out leaving ~1mL, incubated at 37°C and 5% CO_2 for 2-3 min. The flask was shaken carefully with hand palm for detachment and checked under the microscope. In order to inactivate the trypsin, 7 mL growth medium was added and mixed well by pipetting up and down 10-20 times. The cell suspension was transferred to a 50 mL tube (possibly adding more medium in order to reach a total volume of 10mL) and mixed well again for equal cell distribution.

Further, a small volume was transferred to an eppendorf tube for cell counting in a bürker counting chamber and calcultation of medium required for re-suspending the cells in a suitable concentration (eg. $1x10^6$ cells/mL). The 50 mL tube was centrifuged for 5 min at 1500 rpm, the medium removed and the pellet re-suspended in the calculated volume of medium. An appropriate amount of cells (typically $1x10^6$ cells/mL) was transferred to a new labeled flask with 14 mL medium and put on incubation at 37°C in a humidified atmosphere with 5% CO_2. The cells were checked regularly (preferably every day) and the medium changed when necessary, the cells grew confluently after 3-4 days.

3.3 Seeding cells in 96/24- well plates

Seeding was performed after cell passaging, using the remaining cell suspension with $1x10^6$ cells/mL. The suspension was further diluted with medium containing PEST to appropriate concentration (typically 7500-45000 cells/mL). The cells were seeded in the 94/24 tissue culture well plates (collagen coated for RBE4 cells) by pipetting the desired volume (100/600 µL) of the cell suspension in each well and incubated at 37°C and 5% CO_2. The cells were ready for transfection 24-48 hrs after seeding.

3.4 Polyplex formation and transfection

Before any transfection experiment, the quality of the seeded cells was checked. The medium was poured out of the pre-seeded plates onto tissue paper and washed with 200 µL/well pre-heated hank's balanced salt solution; HBSS (Gibco). The plate was incubated at 37°C and 5% CO_2 until the time of transfection (15-20 min). Formulation of polyplexes can be found in appendix B.

The mixtures were prepared by first adding MQ water to the tubes followed by siRNA. Chitosan was added while stirring with a vortex mixer (~1200 rpm). The complexes were incubated 30 min before the tonicity of the formulations was adjusted (1:1) with hypertonic OptiMEM pH 7-7.2 (OptiMEM (Gibco)+ 270mM Mannitol (AnalaR® + 20mM HEPES (Sigma)) for a osmolarity of 300 mOsm/kg and pH 7.2. 50 µL of transfection mixture was added to each well in the 96 well plate and incubated at 37°C and 5% CO_2 for 4-5hrs. The transfection mixture was poured out and replaced with 200µL/well growth medium containing PEST. For uptake experiments, preparation and analysis was performed right after incubation with complexes while 24-120hrs for knockdown and cytotoxicity experiments

Prosedure for other transfection reagents used:
Turbofect^{TM} (Fermentas) transfects the same way as for chitosans with the exeption of using OptiMem instead of MQ water and hypertonic OptiMem when preparing the polyplexes,
Lipofectamine^{TM} *RNAiMAX* (Invitrogen) polyplexes were prepared the same way as Turbofect, but siRNA-OptiMem and chitosan-Optimem were mixed in separate tubes and combined by pipetting.

3.5 GFP knockdown measured by flow cytometry

The H1299 cells express enhanced green fluorescent protein (eGFP) with a halftime of 2hrs, the eGFP gene is incorporated into the cell line by transfection. In order to investigate efficient transfection and knockdown in the cells, the GFP expression was analysed after transfection with GFP-siRNA by flow cytometry. ~7500 cells/well were seeded in 96 well plates (or 45000 for 24-well plates). The cells were transfected the next day as described previously and incubated for 5hrs before replacing the complexes with 200 µL medium and further incubated for 48hrs. In order to prepare the samples for flow analysis the cells were washed twice with 200µL PBS and 25µL trypsin/EDTA was added for detachment of cells. After incubation at 37°C and 5% CO_2 for 2-3 min, 150µL ice-cold PBS with 5% FBS was added and the cells were re-suspended carefully. The samples was transferred from the wells into flow tubes by filtering through 40 µm nylon mesh (BD) filter caps and kept on ice before analysis.

A Gallios flow cytometer (Beckman Coulter) equipped with the 488nm laser line, a 525/40 band pass filter and channel FL 1 for collection of emitted light. A dot plot of forward scatter vs side scatter was used to determine a collection gate for the cells, leaving out dead cells, debris and cellular aggregations. The gate was set according to the positive cells (untreated) in order to exclude autofluorescence and 10 000 gated events was counted for each sample.

3.6 Alexa 647-siRNA uptake measured by flow cytometry

In order to determine cellular uptake of the polyplexes, the cells were transfected with fluorescent siRNA and ananlysed by flow cytometry. ~10 000 cells/well was seeded in 96 well plates (or 60000 cells/well in 24-well plates) and incubated for 24hrs. The cells were transfected as usual with Alexa647-labelled siRNA, after incubating for 4hrs the polyplexes were removed and washed with 200µL PBS. 200 µL medium containing PEST was added and the cells were incubated for 30 min. The medium was removed and replaced with 200 µL medium containing heparin (1mg/mL) to dissociate and remove the cell surface-associated complexes and incubated for another 30 min. The medium was removed and the cells washed twice with 200 µL PBS before adding 25mL trypsin for detachment of cells. After incubating 2-3 min the cells were re-suspended in 150µL ice-cold PBS with 5% FBS.

The suspension was transferred from the wells into flow tubes by filtering through 40 µm nylon mesh (BD) filter-caps (combining two wells for 96-well plates, one for 24-well plates). The samples were put on ice before running flow measurements using the 488nm laserline and a 660/20 band pass filter, emitted light was collected at channel FL6. The gate was set according to samples of untreated cells as negative controls to set a threshold for fluorescence above the levels of autofluorescence and the cell count set to 10 000 gated events per sample.

3.7 GAPDH knockdown assay

KDalert™ GAPDH assay kit (Applied Biosystems) was used to facilitate identification of optimal siRNA delivery conditions by assessment of GAPD expression and knockdown. The assay measures the conversion of NAD+ to NADH by GAPDH in the precence of phosphate and G-3-P (Glyceraldehyde-3-phosphate), the rate of NADH production is proportional to the amount of GAPDH enzyme present.

Approximately 5000 cells/well were seeded in 96-well plates and transfected as previously described. Medium was removed from the well plates 48hrs after transfection and 100-150µL lysisbuffer was added to each well. The plate was sealed with parafilm and put in the refrigerator for 20 min. During the lysis reaction, a mastermix was prepared by using calculated amounts of solutions A, B and C needed for each well (Sol. A : 88,8 µL + 5%, Sol. B: 0,68 µL + 5% Sol C: 0,47 µL + 5%).

The solutions were mixed by stirring on a vortex mixer. The well plate was taken out of the refrigerator and the cell lysate was pipetted up and down five times. 10 µL of the lysate was transferred to ½ area well plates, 10 µL MQ water was added to three wells not containing cells for blank measurements. 90 µL mastermix was added to each well and absorbance was measured at 615 nm after 5, 10, 15, 20, 25, and 30 minutes on a UV/VIS plate reader (SpectreMax Plus^{384}, Molecular Devices). The blank measurement values were subtracted from the sample values and presented as percent GAPDH of untreated cells.

3.8 Cytotoxicity assays

3.8.1 AlamarBlue assay for estimation of metabolic acivity

AlamarBlue® is a cell health indicator used to establish metabolic activity and relative cytotoxicity of agents by flurometric/colometric measurements. The assay incorporates an oxidation-reduction indicator that both fluoresces and changes color in response to chemical reduction of growth medium resulting from cell growth. The compound resazurin is reduced to the highly fluorescent resafurin and the absorbance is monitored at 570nm and 600nm (Al-Nasiry et al. 2007).

The cells were seeded in 96 well plates with RPMI (H1299 cells) or MEMα (RBE4 cells) medium. The next day cells were transfected as usual and incubated at 37°C and 5% CO_2 for 4hrs. 1% Triton X 100 lyses the cells and was added to untreated cells; it shows if the assay works and was used as a positive control. The polyplexes/medium/triton was removed after 4hrs and 200µL medium was added, 24hrs after transfection the medium was changed. 48hrs after transfection the cells were washed two times with PBS and 10 µL alamarBlue reagent mixed with 100 µL DMEM (without phenol red) for each well was added (including wells without cells for blank measurements), incubated at 37°C and 5% CO_2 for 4hrs. After incubation the plate was analyzed on a UV/VIS plate reader at absorbances 570 and 600 nm.

3.8.2 Propidium iodide staining for cell viability

Propidium iodide is membrane impermeant and thereby excluded by viable cells but can penetrate the cell membranes of dying or dead cells (Nocker et al. 2006). It is a fluorescent compound and by monitoring the fluorescence intensity by flow cytometry it is possible to distinguish viable from dead cells.

In order to stain and evaluate cell viability the transfected samples were treated with 1 µg/mL propidium iodide (PI) prior to flow analysis. The samples were analysed using a 488 laser line and emitted light collected through channel FL3. The gate was set according to samples of untreated cells as negative controls to set a threshold for fluorescence above the levels of autofluorescence from viable cells. The cell count was set to 10 000 gated events per sample

3.8.3 Bicinchoninic acid (BCA) assay for total protein determination

The BCA protein assay kit ™ from Pierce combines the reduction of Cu^{2+} to Cu^{1+} by protein in an alkaline medium with the highly sensitive and selective colorimetric detection of the cuprous cation (Cu^{1+}) by bicinchoninic acid. The BCA/copper complex exhibits a strong linear absorbance with increasing protein concentrations (Krohn 2001).

The medium was removed from the wells and the cells were washed with 200 uL PBS before addition of 100 µL ice-cold Reporter lysis buffer (Promega). Samples for the standard curve was prepared by diluting bovine serum albumin (BSA) stock solution (2mg/mL) in lysis buffer in the range 0 - 2000 µg/mL. The plates were thawed at 37°C and 5% CO and the bottom of the wells were scraped for 5-10 seconds in order to obtain a homogenous cell lysate. 10 µL of the cell lysates and standards were transferred to a ½ area 96-well plate, blank samples contained only lysis buffer. Amount of BCA working reagent A and B were calculated for lysates, standards and blank, mixed (50:1) and 100 µL of the solution were added to each well.

The plate was wrapped in aluminum foil and incubated at at 37°C and 5% CO for 30 min. Absorbance was measured at 570 nm using a UV/VIS plate reader. The blank measurements were subtracted from the sample values and protein concentration was calculated from the standard curve, presented as ug/mL cell lysate.

3.9 Rhodamine 123 efflux assay

Rhodamine is a fluorescent dye and a substrate for the P-gp pump, intracellular accumulation of Rhodamine can be used as a measurement of the pumps efflux activity and thus knockdown efficiency. Verapamil is a well known inhibitor of the P-gp pump and was used as positive control.

Approximately 10 000 cells were seeded in 96-well plates and the assay was performed 48hrs after chitosan/siRNA transfection of RBE4 cells. The cells were washed with warm PBS, 50 µL of 10 µM Verapamil solution in Optimem was added to the cells that should be inhibited with Verapamil. 50 µl Optimem was added to the rest of the cells followed by incubation at 37°C and 5% CO_2 for 45 min. After incubation, 50 µL of 10 µM Rho123 solution in Optimem was added (not removing Optimem with/without Verapamil). The plate was wrapped in Al-foil and incubated for 15 min. After incubation, the solutions were removed and the cells washed with warm PBS. 200 µl of growth medium was added placed on incubation for 2hrs at 37°C and 5% CO_2.

The cells inhibited with Verapamil were incubated in growth medium containing 5 µM Verapamil. After incubation the cells were washed rapidly with 200 µL cold PBS, detached with 25µL trypsin and re-suspended in 150uL ice-cold PBS with 4% FBS. The samples were filtered into flow tubes though filter caps while being kept on ice. It was important to keep the cells on ice while preparing the samples and not running all the samples at the same time on the flow cytometer in order to avoid leakage of Rho12. The samples were run using the argon 488nm laserline and the emission was collected at the FL1 channel. The gate was set according to samples of untreated cells as negative controls to set a threshold for fluorescence above the levels of autofluorescence and the cell count set to 10 000 gated events per sample

3.10 Confocal laser scanning microscopy of RBE4 cells

The anticancer drug Doxorubicin is a substrate for the P-gp pump and allows for visualization of intracellular accumulation in the treated cells. The cells were seeded in collagen coated eight-chamber microscopic slides (Ibidi GmbH), 18750 cells/chamber. The cells were transfected as usual with 125 µL polyplexes/well and incubated for 5 hrs before the medium was changed, and again after 24hrs. Cells for positive control were treated with 5µM Verapamil in αMEM for 30 min before the cells were treated with αMEM supplemented with 50µM Doxorubicin (stock solution 3443µM) and incubated for 2hrs.

Medium was removed and 150 ul CellMask plasma membrane stain 5µg/mL (Invitrogen) was added and incubated for 5 min in 37°. CellMask was removed and the cells washed with 300uL PBS three times and 300 uL medium was added right before microscopy.
Doxo-accumulation was studied and merged with cellmask to show confluence. A LSM 510 (Carl Zeiss Jena GmbH, Germany) confocal microscope with a c-Apochromat 40x/1.2 NA W corr objective was used to investigate the cells.

Doxorubicin was excited using the 488-nm argon laser line and CellMask using the 633-nm HeNe laser line. The emitted light was collected using 500-550 nm band pass and 651-704 nm long pass filters. Resolutions of 512 x 512 pixels was used for all of the images, image acquisition and processing were conducted using the LSM Image Browser (Zeiss) software program.

4. Results

This section begins with a general screening of chitosan/siRNA polyplexes transfection in the human lung cancer cell line (H1299) as a model-cell line in the anticipation of rat brain endothelial cells (RBE4). Uptake and knockdown efficiency was investigated followed by cytotoxicity screening of the chitosan/siRNA polyplexes. The following sections will focus on the RBE4 cells where general uptake and knockdown was investigated as well as cytotoxicity. Further, knockdown of the mdr1a/b mRNA coding for the P-glycoprotein pump was determined by drug efflux /retention studies and confocal laser scanning microscopy.

Commonly used abbreviations in the graphical presentation of the results throughout this section includes; C for chitosan followed by DPn, T for targeting, NT for non-targeting, N for naked, Turbo for Turbofect and R-Max for RNAiMAX. All raw and supplemental data for the results can be found in the indicated appendices.

4.1 DPn and N/P ratio screening in H1299 cells

The human lung cancer cell line H1299 and was used in order to establish and select the optimal DP_n and N/P ratio for further studies. Transfection and assay procedures were performed with these cells for training and anticipation of rat brain endothelial cells RBE4.

4.1.1 Uptake of chitosan/siRNA polyplexes in H1299 cells

The first barrier nanoparticles encounter is the cell wall and its subsequent entry into cells by endosomal encapsulation. In this experiment different chitosan/siRNA polyplexes were compared in terms of their ability to deliver siRNA by using fluorescently labeled Alexa 647 siRNA.

The chitosans chosen for formulation with GFP-siRNA were all linear with DP_n 54, 200, and 300 with $F_A = 0$. The siRNA concentration was 45nM and the N/P ratios were 10 and 30 for each sample. The commercial transfection reagent Turbofect was included for comparison and naked siRNA served as negative control as it was not expected to enter the cells.

The cells were transfected as described previously and the cellular uptake of the chitosan/ siRNA complexes in H1299 cells was investigated 4hrs after transfection by flow cytometry. The results are presented in figures 4.1 and 4.2, supplemental data for the presented figures can be found in appendix C.

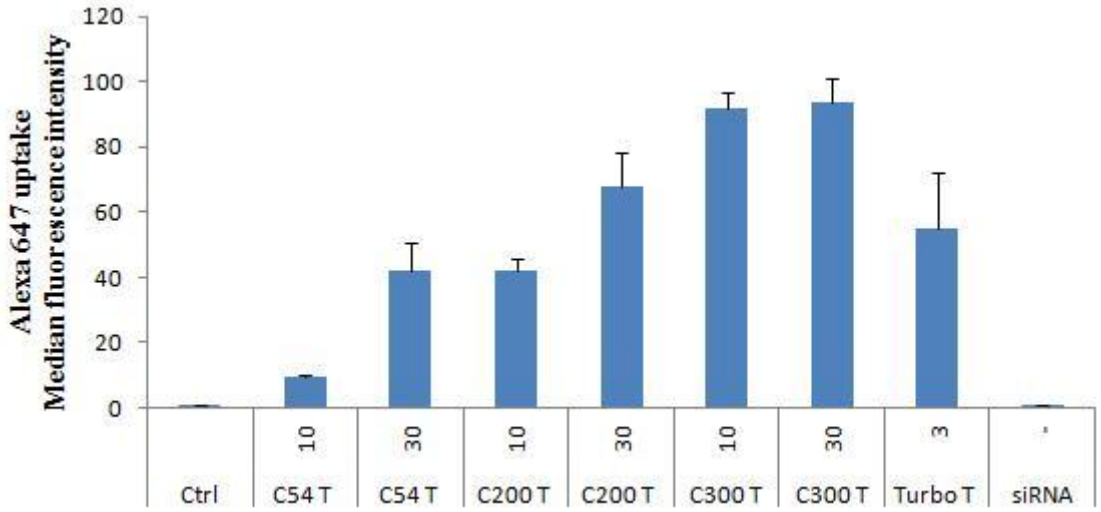

Figure 4.1 The relative amount of internalized siRNA in H1299 cells treated with chitosans DP_n 54, 200, 300 complexed with Alexa647-siRNA in N/P ratios of 10 and 30. The results are presented as percent median FI of control. Each data point is the mean value ± standard deviation (n=3).

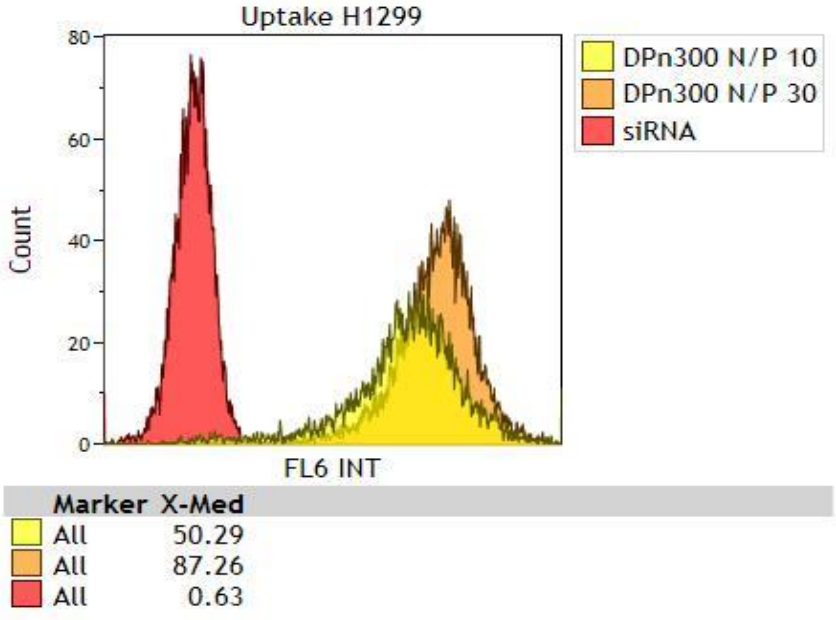

Figure 4.2 Fluorescence intensity overlay-plots for cells treated with chitosan DP_n 300 complexed with Alexa647-siRNA in N/P ratios of 10 and 30 compared to untreated control cells. Results are presented as fluorescence intensity plotted against cell count (number of events) followed by its median value. Cell count was set to 10000 and measured through channel FL6.

The chitosan-siRNA complexes all showed increasing uptake efficiency with higher DP_n and N/P ratio, naked siRNA did not mediate uptake on its own. This is similar to the observed knockdown efficiency in cells treated with DP_n 300. Samples with N/P ratios of 30 had the highest uptake closely followed by N/P 10, the longer chitosans worked better with lower N/P ratios compared to chitosan with a low DP_n. Both the untreated cells and the cells treated with naked siRNA resulted in a median fluorescence close to zero, thus confirming uptake specificity.

4.1.2 GFP knockdown in H1299 cells

H1299 cells express green fluorescent protein (GFP) which can be efficiently downregulated by the introduction of siRNA. This stable reporter gene should thus give a representative picture of transfection efficiency by measurement of the median fluorescent intensity.

The chitosans chosen for formulation with GFP-siRNA were all linear with DP_n 54, 200, and 300 with $F_A = 0$. The antiGFP-siRNA concentration 45nM and the N/P ratios were 10 and 30 for each sample. Additionally, chitosan polyplexes with non-targeting siRNA were used in order to distinguish sequence-specific silencing from non-specific effects. Commercially available Turbofect^{TM} transfection reagent was included for comparison of transfection success and knockdown efficiency. Untreated cells served as negative control, the gate was set according to these in order to define GFP positive cells.

The cells were transfected as previously described and the median fluorescence intensity (FI) was measured by flow cytometry 48hr after transfection. The results are presented in figure 4.3 and 4.4, supplemental data for the presented figures can be found in appendix C.

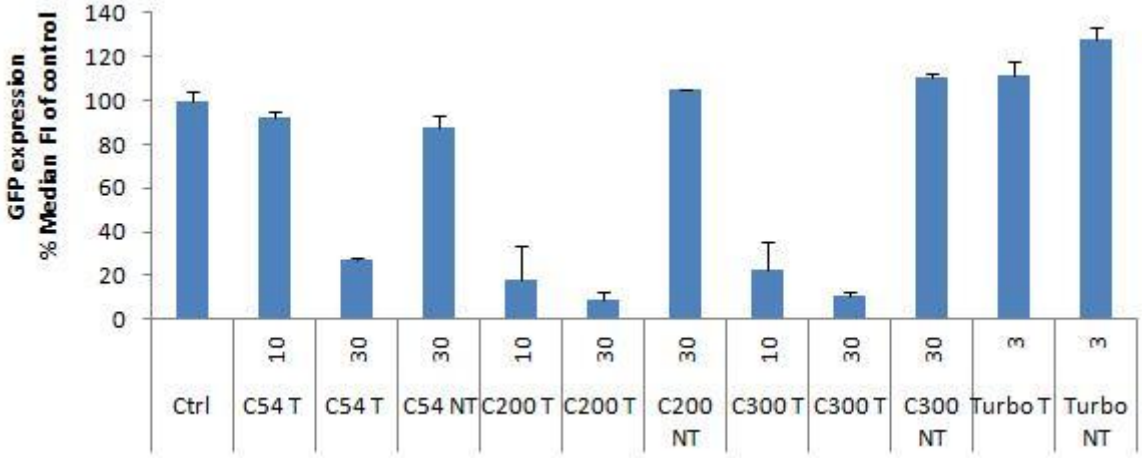

Figure 4.3 GFP expression in H1299 cells measured by flow cytometry. The cells were transfected with chitosan DP_n 54/200/300 complexed with antiGFP-siRNA in N/P ratios of 10 and 30, non-targeting controls and turbofect. Untreated cells were set as baseline control and the results are presented as percent median FI of control. Each data point is the mean value ± standard deviation (n=3).

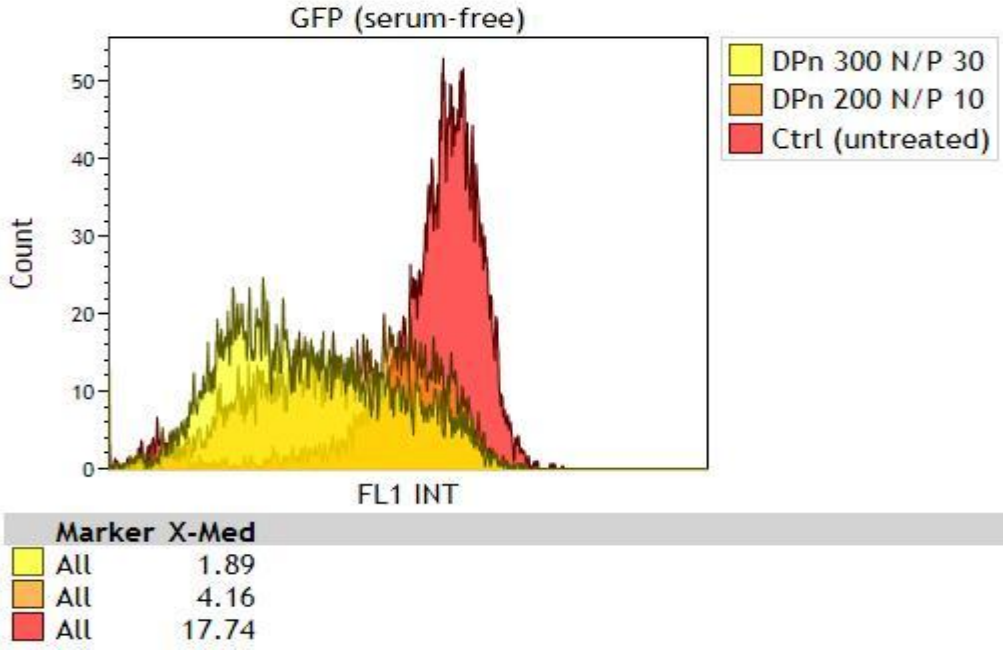

Figure 4.4 Fluorescence intensity overlay-plots for cells treated with chitosan DP_n 200 complexed with antiGFP-siRNA in N/P ratios of 10 and 30 compared to untreated control cells. Results are presented as fluorescence intensity plotted against cell count (number of events) followed by its median value. The cell count was set to 10000 events and measured through channel FL1.

It can be observed from figure 4.3 that the chitosans with high DP_n and N/P ratios displayed the best knockdown efficiency with a median FI ~15% of untreated cells. N/P ratios of 30 seemed to be twice as efficient as the ones with N/P 10, exept for DP_n 54 where a N/P ratio of 10 had little effect compared to N/P 30. The commercial Turbofect transfection reagent had no apparent effect on knockdown, it rather showed an increase in median fluorescence, even with non-targeting siRNA.

We also wanted to investigate the effect of serum addition at transfection. The mere intention was to see if the complexes could successfully form and in what way may affect the transfection efficiency. Therefore 10% FBS was added to OptiMem at transfection using the same sample formulations and analysed after 48hrs by flow cytometry. The results are presented in figure 4.5 and 4.6, supplemental data for the presented figures can be found in appendix C.

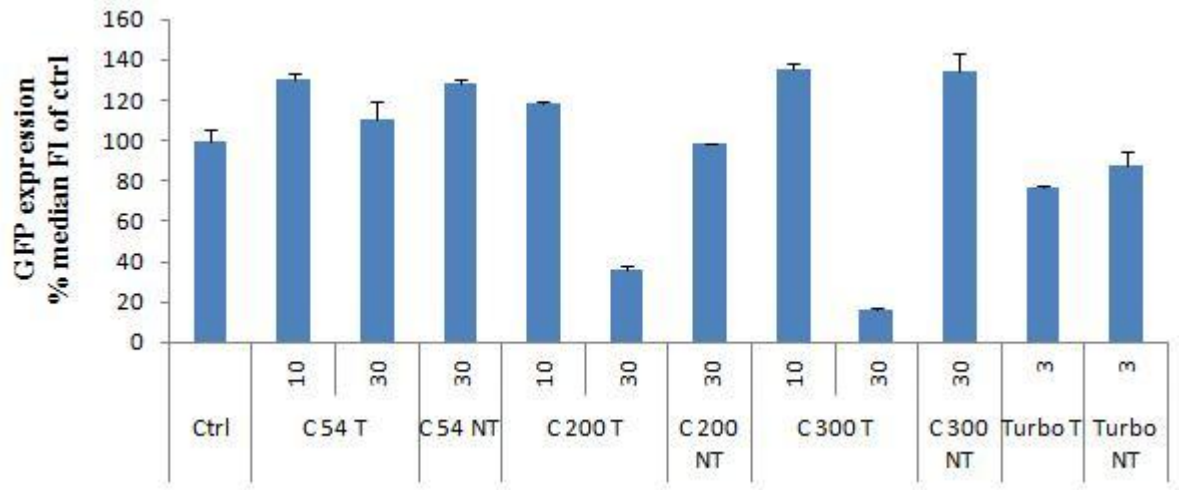

Figure 4.5 GFP expression in H1299 cells measured by flow cytometry. The cells were transfected in the precence of 10% serum with chitosans DP_n 54/200/300 complexed with antiGFP-siRNA in N/P ratios of 10 and 30. Untreated cells were set as baseline control and the results are presented as percent median FI of control. Each data point is the mean value ± standard deviation (n=3).

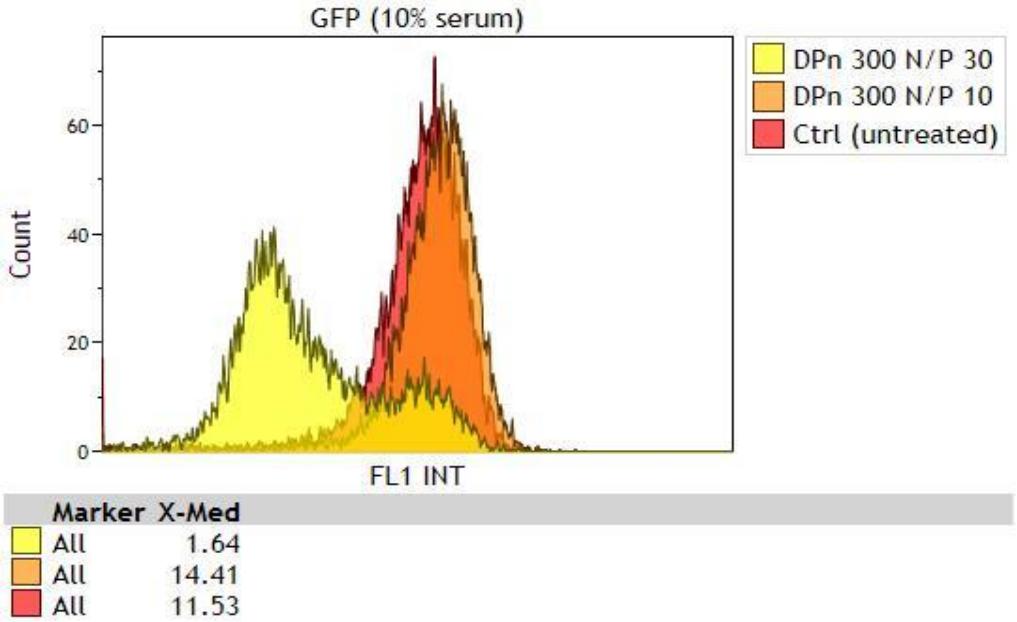

Figure 4.6 Fluorescence intensity overlay-plots for cells transfected in 10% serum with chitosan DP_n 300 complexed with GFP-siRNA in N/P ratios of 10 and 30 compared to untreated control cells. Results are presented as fluorescence intensity plotted against cell count (number of events) followed by its median value. Cell count was set to 10000 and measured through channel FL1.

Presence of serum at transfection seemed to negatively affect the knockdown efficiency of all chitosans with N/P 10, it never reached below the threshold value of the control cells (untreated). The same is observed for LIN54 with N/P 30 which were expected to exhibit a low yet distinguishable knockdown. Longer chitosans (200/300) with N/P 30 showed a similar reduction of GFP expression as the previous experiment without transfection with serum.

Cells treated with Turbofect displayed a reduction in GFP expression, also the samples with non-targeting siRNA. This may be related to toxicity as in some of the preliminary experiments (not included) were it killed most of the transfected cells. It must however be taken into consideration that this is two individual GFP experiments and they are therefore subject to variability in sample preparation and analysis.

4.1.3 GAPDH knockdown in H1299 cells

GFP is artificially introduced whereas GAPDH is endogenously expressed in most mammalian cell lines. The RBE4 cells intended for use in the further studies do not express GFP, therefore GAPDH was chosen for analysis. The method was first performed with H1299 cells in order to confirm transfection with chitosan/siRNA polyplexes.

The polyplex formulations chosen for this experiment were the same as for the previous studies. The knockdown was determined by measuring the reduction in GAPDH enzyme activity in cells transfected with GAPDH siRNA relative to untreated cells which served as a negative control.

The cells were transfected as described previously and analysed by absorbance measurements on a UV/VIS plate reader after 48hrs. The results are presented in figure 4.7, supplemental data for the presented figure can found in appendix C.

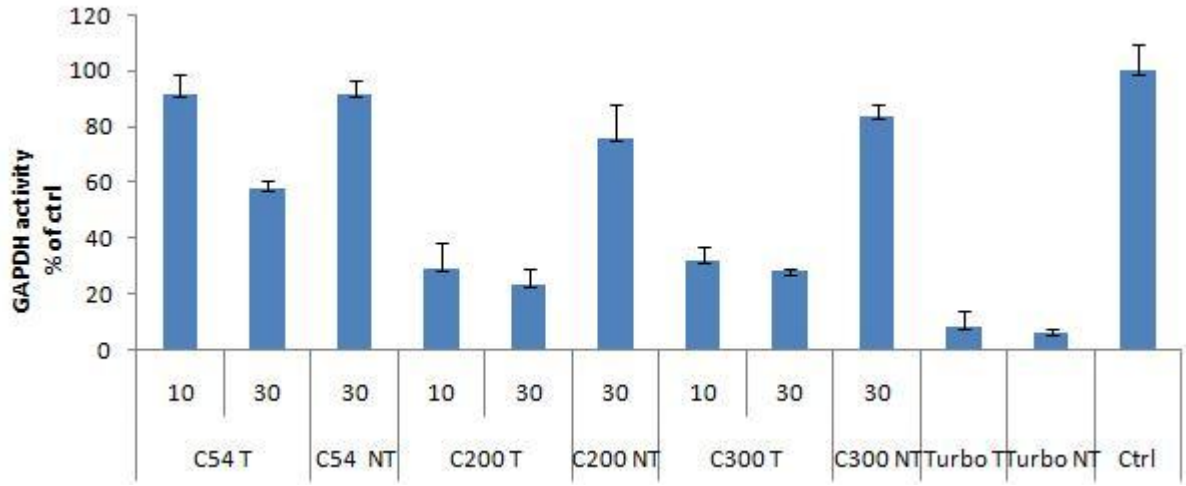

Figure 4.7 Enzymatic activity of GAPDH in H1299 cells treated with chitosans DP_n 54/200/300 complexed with GAPDH-or nontargeting siRNA in N/P ratios of 10 and 30 and turbufect. Untreated cells were set as baseline control and the results are presented as percent of control. Each data point is the mean value ± standard deviation (n=3).

From the results in figure 4.7, chitosans with a higher degree of polymerization showed a more efficient knockdown of GAPDH activity. There were only subtle differences between DP_n 200 and DP_n 300 chitosans with a reduction of ~40% of control. DP_n 54 with N/P 10 had a reduction similar to the non-targeting sample, suggesting little or no effect on knockdown. There was little observed difference between the chitosans with N/P ratios of 10 and 30, which corresponds with the previous GFP expression studies. The knockdown efficiency therefore seems to depend in a higher degree on the DP_n rather than the N/P ratio of the chitosans. The reduction of GAPDH activity in samples treated with non-targeting siRNA indicates that the chitosan may have a negative effect on the cells and suggests the need for further studies on cytotoxicity of the chitosans.

4.2 Cytotoxicity of chitosan and chitosan-siRNA polyplexes.

When developing nucleic acid delivery systems, it is important that the components are biocompatible and display a low cytotoxicity. Here we take advantage of the body's own machinery via RNAi and the fact that chitosans break down to charbohydrates and components that can be extruded from the body. Therefore it is expected that the chitosan nanoparticles will exhibit a tolerable toxicological profile in the H1299 cell line.

It was desirable to investigate the possible long term cytotoxicity of the chitosan-siRNA polyplexes and naked chitosans on the H1299 cells. Over a five-day period the transfected cells were subjected to analysis by four different cytotoxicity assays:

- Alamar blue assay for determination of metabolic activity.
- PI staining for membrane permeability and thus cell viability.
- Cell count for estimation of cell proliferation.
- BSA assay for determination of total protein concentration.

Only chitosan with DP_n 200 and N/P 10 and 60 was chosen for investigation, due to the higher possibility of observed cytotoxicity with longer chitosans. Samples with naked chitosan and naked siRNA were included for determination of possible cytotoxic effects alone. Commercial RNAiMAX was used for comparison of its cytotoxicity relative to the chitosan and chitosan/siRNA polyplexes. The cells were transfected as normal and subjected to analysis after 24, 48 ,72, 96 and 120hrs.

4.2.1 AlamarBlue assay

Estimation of metabolic activity in the different samples were analysed by the alamarBlue assay. The cells were transfected with the complexes described above and analysed 24, 48, 72, 96 and 120hrs after transfection with a UV/VIS plate reader at 570 and 600 nm. The results are presented in figure 4.8, supplementary data for the figure can be found in appendix D.

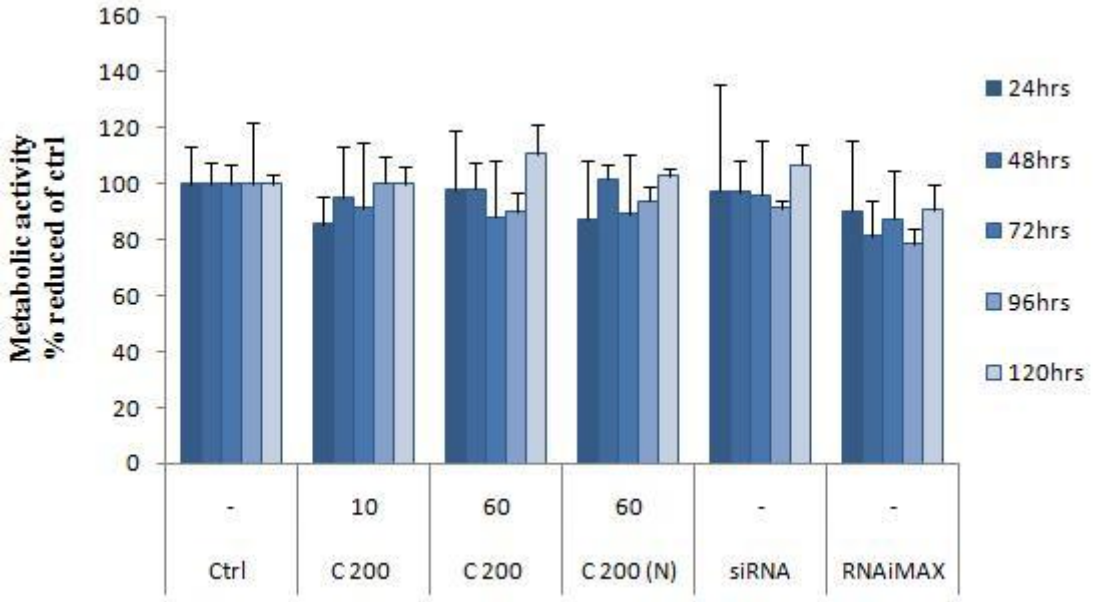

Figure 4.8 Metabolic activity of H1299 cells over 120hrs measured by alamarBlue assay. Cells were treated with chitosan DP_n 200 complexed with non-targeting siRNA in N/P ratios of 10 and 60, naked chitosan and siRNA, RNAiMAX. Untreated cells were set as baseline control and the results are presented as percent reduction of control. Each data point is the mean value ± standard deviation (n=4).

The results in figure 4.8 show that chitosan DP_n 200 polyplexes with N/P 10 and 60 both exhibited negligible reduction in metabolic activity of the cells. The amount of reduction in relation to untreated control had a maximum ~10% for all samples containing chitosan/siRNA polyplexes, the same is observed for the naked chitosan sample. The cells treated with naked siRNA displays comparable values to the untreated control cells. The commercial RNAiMAX transfection reagent displayed the most prominent reduction in metabolic activity, reaching ~20% reduction and therefore displays a higher toxicological profile in this experiment.

4.2.2 Propidium iodide staining

In order to stain and determine the amount of dead cells in the samples/evaluate cell viability the cell samples were treated with propidium iodide (PI) prior to flow analysis. PI is membrane impermeant and generally excluded by viable cells but can penetrate cell membranes of dying or dead cells. The samples were transfected as initially described and treated with PI directly prior to flow analysis after 24, 48, 72, 96 and 120hrs. The results are presented in figure 4.9, supplemental data for the figure can be found in appendix D.

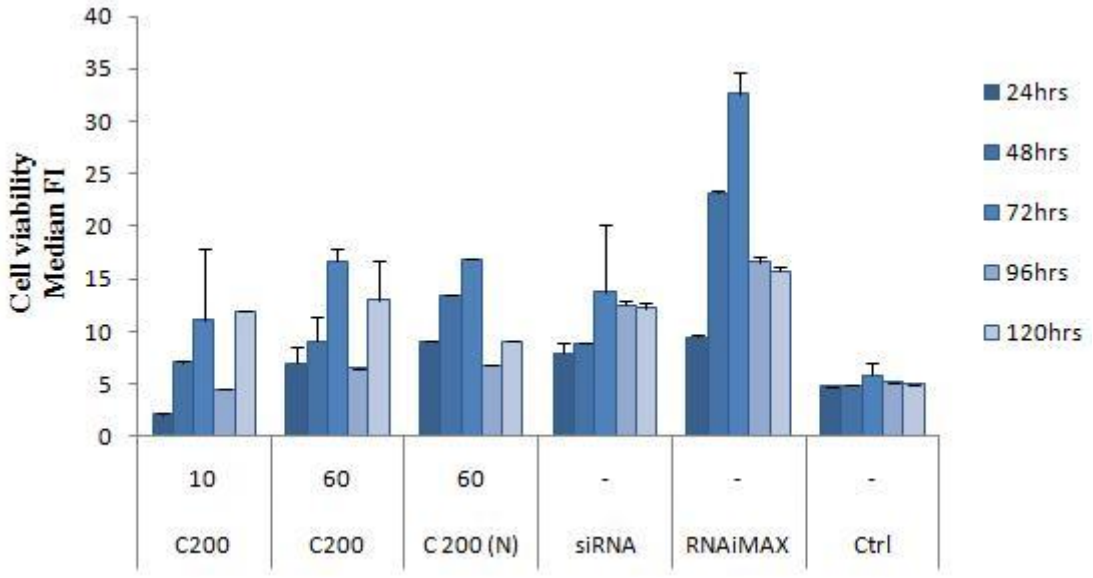

Figure 4.9 Cell viability in H1299 cells assayed by PI staining followed by flow cytometry over 120hr. Cells were treated with chitosan DP_n 200 complexed with non-targeting siRNA in N/P ratios of 10 and 60, naked chitosan and siRNA, RNAiMAX. Untreated cells were set as baseline control and the results are presented as median fluorescent intensity. Each data point is the mean value ± standard deviation (n=3).

The observed results in figure 4.9 show an increase in PI permeability during the three first days followed by a reduction the last two days. There is no difference between chitosan polyplexes with N/P 10 and 60 as well as naked chitosan. Interestingly the chitosan treated samples displays similar permeability as naked siRNA. Untreated cells show a stable viability during exposure to PI throughout the 5-day period. RNAiMAX samples displayed a greater increase in PI permeability during the three first days.

4.2.3 Cell counting

The same samples were assessed for proliferation by cell counting in bürker chambers over a five day period after transfection. It was expected that cells treated with complexes and naked chitosan would have the greatest growth retention and thereby have fewer cells pr mL than the samples with naked siRNA and the untreated cells. The results are presented in figure 4.10, supplemental data for the figure can be found in appendix D.

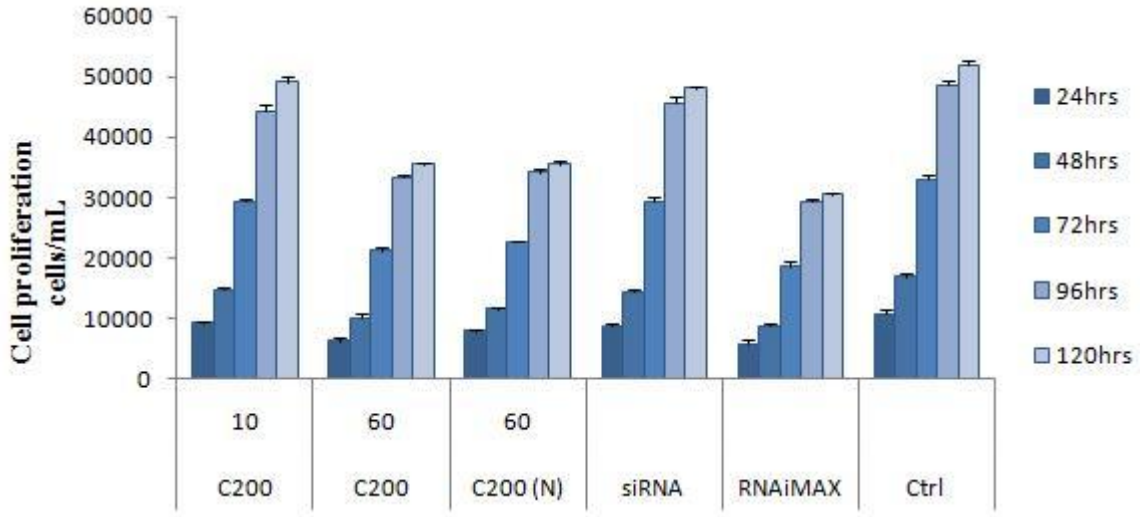

Figure 4.10 Proliferation in H1299 cells by cell counting over 120hrs. Cells were treated with chitosan DP_n 200 complexed with non-targeting siRNA in N/P ratios of 10 and 60, naked chitosan and siRNA, RNAiMAX. Untreated cells were set as baseline control and the results are expressed as cells/mL. Each data point is the mean value ± standard deviation (n=3).

The results in figure 4.10 reflect a steady cell proliferation which reaches a plateau after four days. The samples treated with chitosan N/P 10 shows little reduction in growth compared to the untreated cells, the same is observed for naked siRNA. However, both the naked chitosan and the chitosan- siRNA complexes have an inhibitory effect when the N/P ratio is increased to 60. Treatment with RNAiMAX gave the most pronounced growth retention which also correlates to results obtained in the previous cytotoxicity experiments.

4.2.4 Bicinchoninic acid (BCA) assay

BCA assay was used for total protein determination in the samples. The cells were transfected as previously described and analysed at 570nm on a UV/VIS plate reader 24, 48, 72, 96 and 120hrs after transfection. The result is presented in figure 4.11, Supplemental data for the figure can be found in appendix D.

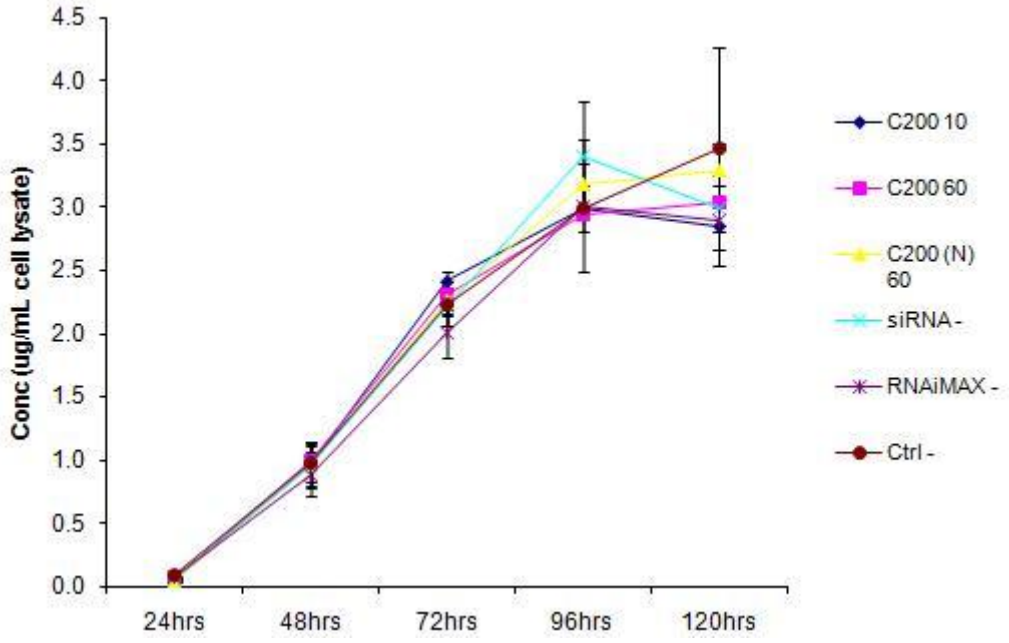

Figure 4.11 Total protein concentration in H1299 cells determined by BSA assay over 120hrs. The cells were treated with chitosan DP_n 200 complexed with non-targeting siRNA in N/P ratios of 10 and 60, naked chitosan and siRNA, RNAiMAX. Untreated cells were set as baseline control and the results presented as change in protein concentration (µg/mL cell lysate). Each data point is the mean value ± standard deviation (n=4).

There is a linear increase in protein concentration which stagnates during the last 24hrs, these results correlates well with the cell count study. The samples are not easy to distinguish from another but there are notable differences between the extremities. RNAiMAX results in a continuous though negligible lower protein concentration than the other samples. Untreated control and naked siRNA shows a slightly higher concentration.

4.3 Investigation of general uptake and knockdown in RBE4 cells

The preceding work on H1299 cells was done in order to establish efficient chitosan/siRNA polyplex formulation for use in the RB4 cell line. For demonstration of efficient uptake and knockdown feasibility of the chitosan nanoparticles in the RBE4 cells, knockdown of GAPDH and uptake of fluorescently labeled Alexa 647 siRNA was investigated.

4.3.1 Analysis of uptake in RBE4 cells by flow cytometry

By using fluorescently labeled Alexa 647 siRNA complexed with chitosans, the uptake efficiency of the nanoparticles into RBE4 cells was investigated by flow cytometry.
Based on the preliminary experiments with H1299 cells, chitosans with high Dpn and both a high and low N/P ratio was chosen for investigation of uptake in RBE4 cells. The chitosans used in this experiment was DP_n 250, 300, 400 and 810, complexed with Alexa 647 siRNA all with N/P ratios of 10 and 60. The samples were analysed 4h after transfection by flow cytometry. The results are presented in figure 4.12, supplemental data for the figure can be found in appendix C.

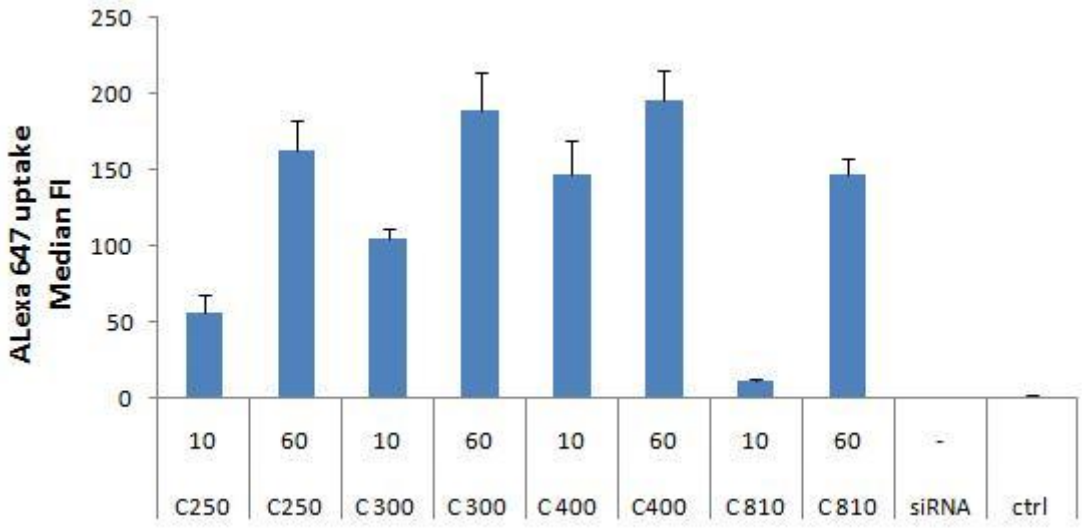

Figure 4.12 Relative amount of internalized siRNA in H1299 cells measured by flow cytometry. The cells were treated with chitosans DP_n 250,300,400,810 complexed with Alexa647-siRNA in N/P ratios of 10 and 30. The results are expressed as median of fluorescence intensity (FI). Cells treated with siRNA were set as baseline control and the results are presented as median FI of control. Each data point is the mean value ± standard deviation (n=3).

The results presented in figure 4.12 shows an increasing uptake efficiency of chitosan/siRNA polyplexes with increasing DPn of the chitosans. This result corresponds with the previous result with H1299 cells. The difference in uptake efficiency is much more evident between the chitosans with N/P ratios of 10 than the ones with a N/P ratio of 60. The chitosan with DPn 810 did not display the same level of internalization of polyplexes as the others, with a negligible effect at N/P 10.

4.3.2 GAPDH knockdown in RBE4 cells

The RBE4 cell line does not have the exogenous GFP gene, but do express GAPDH. The assay has been previously tested on H1299 cells (fig 4.7). The cells were transfected as described previously and analysed by flow cytometry after 48hrs. The results are presented in figure 4.13, supplemental data for the figure can be found in appendix C.

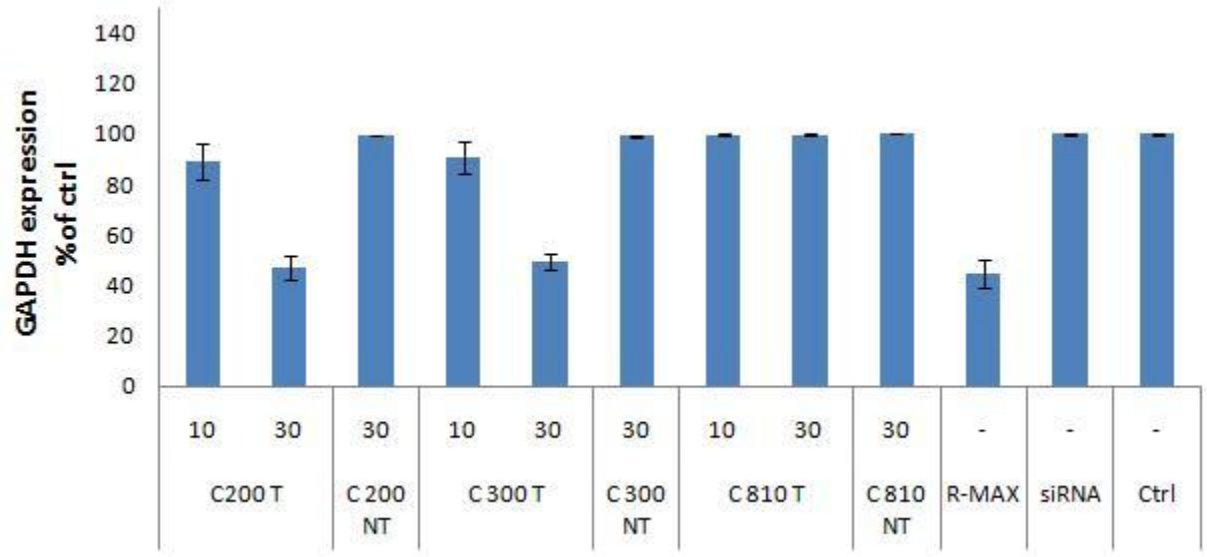

Figure 4.13 Enzymatic activity of GAPDH in RBE4 cells treated with chitosans DPn 200,300,810 complexed with GAPDH-siRNA in N/P ratios of 10 and 30, non-targeting samples and RNAiMAX. Untreated cells were set as baseline control and the results are presented as percent of control. Each data point is the mean value ± standard deviation (n=3).

The results presented in figure 4.13 show that chitosan polyplexes with DP_n 200 and 300 has the same effect on knockdown at N/P 60, with a ~50 % decrease of untreated control. This is comparable to the commercial RNAiMAX which show only a slightly higher effect on knockdown. The chitosan with DP_n 200 and 300 with N/P 10 did not give a sufficient knockdown, only a mere ~10% of control.

4.3.3 Investigation of metabolic activity in RBE4 cells

The alamarBlue assay was chosen in order to check for possible cytotoxicity of the chitosan nanoparticles on the RBE4 cells. The assay has been previously tested on the H1299 cells where a maximum reduction of ~15% in metabolic growth was found in the chitosans with DPn 200 and N/P 60 after 48 hrs.

Chitosans with DP_n 200 and 300 with N/P 10 and 60 was chosen for this experiment with an additional naked chitosan sample for both chitosans. The siRNA used was non-targeting as for the same experiment with H1299 cells (fig 4.8). Samples containing only siRNA were again used to show that does not mediate transfection on its own. RNAiMAX was included on the basis of comparison with a commercial reagent which in previous experiments has been seen to exhibit a higher toxicity profile. Triton lyses the cells and gives a direct indication that the assay works.

The cells were analysed 48hrs after transfection with a UV/VIS plate reader at 570 and 600 nm. The results are presented in figure 4.14, supplemental data for the figure can be found in appendix D.

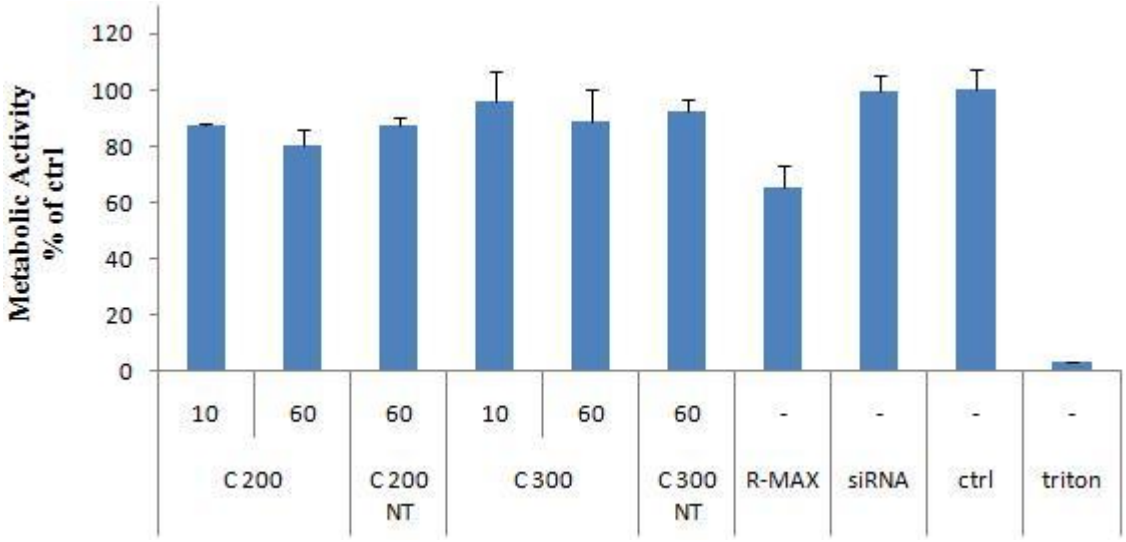

Figure 4.14 Metabolic activity of RBE4 cells measured by alamarBlue assay. Cells were treated with chitosans DP_n 200, 300 complexed with non-targeting siRNA in N/P ratios of 10 and 60, non-targeting siRNA and naked siRNA, RNAiMAX. Untreated cells were set as baseline control and the results are presented as percent reduction of control. Each data point is the mean value ± standard deviation (n=4).

The results in figure 4.14 show that both chitosan nanoparticles with DP_n 200/300 had a reduction of ~10-20% in metabolic activity at N/P 60. The samples with N/P 10 showed a reduction of ~5-10% while the naked chitosan exhibited a somewhat lower toxicity at N/P 60 than the same samples complexed with siRNA. The triton treated samples showed a reduction of ~95 % of untreated control, indicating that the samples were lysed and that the assay worked.

The commercial reagent RNAiMAX was again more toxic to the cells than chitosan with a mere ~35% reduction in metabolic activity. Samples treated only with naked siRNA gave no observed difference from the untreated control cells.

4.4 Rhodamine efflux in RBE4 cells after targeting the mdr1 gene

Rho 123 was used as a functional assay for determination of P-gp knockdown. Rhodamine is a substrate and functional reporter for the P-gp pump and intracellular accumulation of Rhodamine should reflect low efflux and thus efficient knockdown of the P-gp gene. In these experiments the Rho123 assay was used in order to investigate efficient knockdown of the mdr1 gene expression compared to the commercially available Verapamil, which is a known inhibitor of the P-gp pump.

4.4.1 Knockdown of P-gp in RBE4 cells

Intracellular Rho 123 accumulation in cells can be used as assay for determining knockdown of the P-gp pump. The chitosans chosen for use in this assay were DP_n 300 and DP_n 400 all complexed with mdr1a/b in N/P ratios of 10. The calcium-channel blocker Verapamil is a specific inhibitor of P-gp modulated efflux and was used as positive control.

The cells were transfected as usual and after 48hrs subjected to rho123 influx and Verapamil inhibiton prior to flow analysis. The results are presented in figure 4.15 and 4.16, supplemental data for the figures can be found in appendix E.

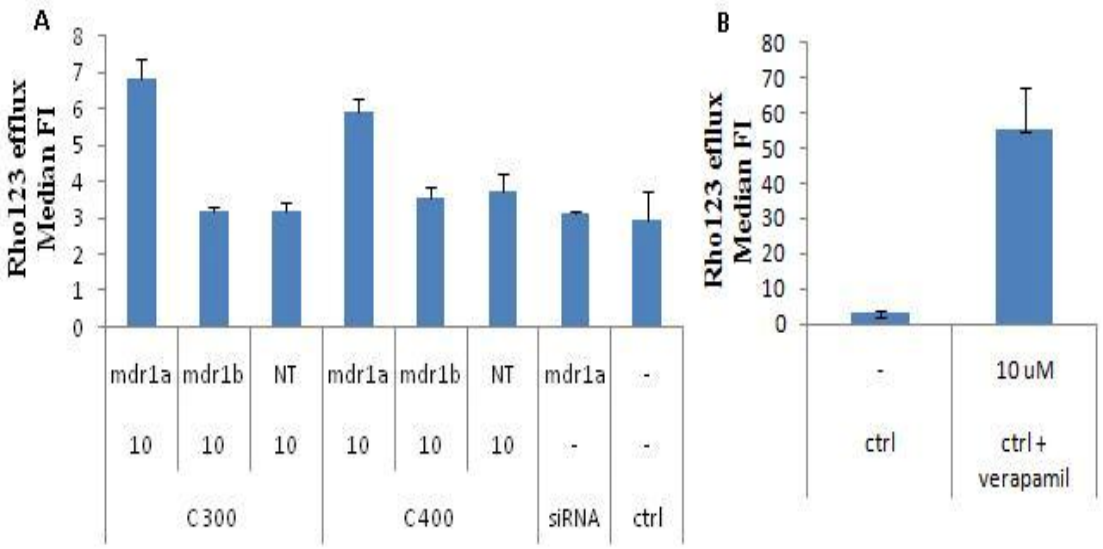

Figure 4.15 Rhodamine 123 efflux in RBE4 cells measured by flow cytometry. *A)* Cells were treated with chitosans DPn 300/400 and complexed with mdr1a/b-siRNA in a N/P ratio of 10. *B)* comparison of untreated cells and cells treated with 10µM Verapamil. The results are presented as percent reduction of control. Each data point is the mean value ± standard deviation (n=3).

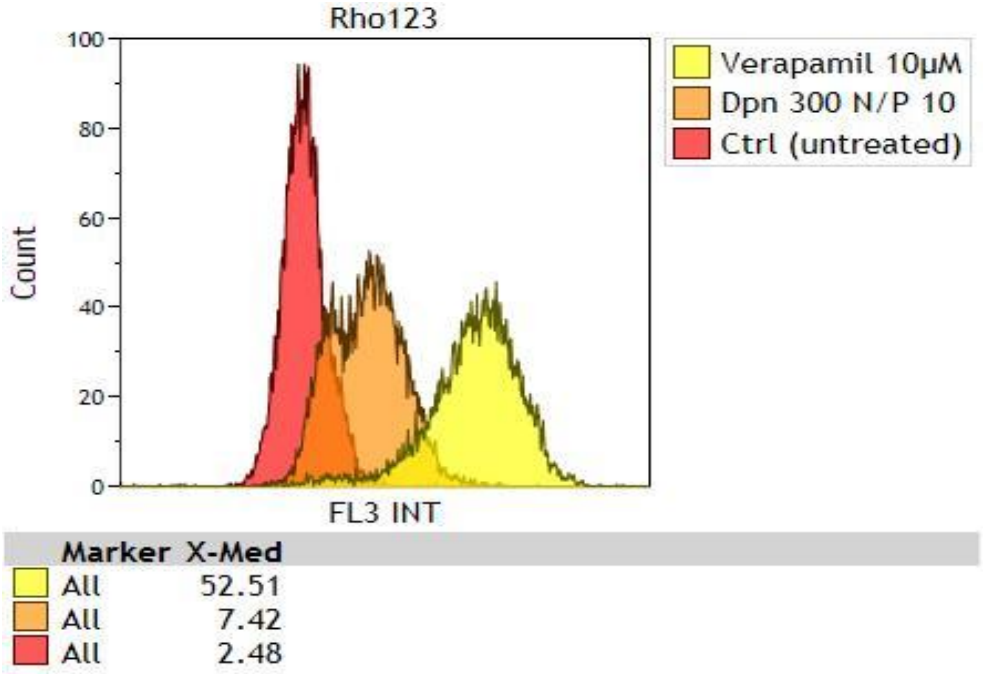

Figure 4.16 Overlay flow cytometry plots of fluorescence intensity in cells treated with chitosan Dpn 300 complexed with mdr1a-siRNA in an N/P ratio of 10, Verapamil treated cells and untreated control cells. Results are presented as fluorescent intensity plotted against cell count (numer of events). Cell count was set to 10000 events and measured through channel FL6.

There is an increased intracellular accumulation of Rhodamine after treatment with mdr1a siRNA polyplexes while mdrb1 only had a minor effect compared to untreated control. Non-targeting control and naked siRNA cells displayed negligible effects on Rho123 retenton in the cells and are comparable to the untreated control cells.

These results reflect a 2/3 fold chitosan-mdr1a siRNA downregulation of the P-pg pump. However, the Verapamil treated cells displayed a much higher inhibition of the pump. Verapamil treated cell resulted in a median fluorescent value so high that is would be difficult to display the effects of chitosan/siRNA polyplexes.

4.4.2 Rho123 accumulation with increasing Verapamil concentration

It was desirable to investigate the effect on knockdown of Pgp with different Verapamil concentrations as well as rate of efflux of Rhodamine. Based on the preliminary experiments there was a difference in Rhodamine accumulation/efflux at 5uM and 10 uM Verapamil. Therefore cells were treated with 5, 10, 25, 50 and 250 uM Verapamil to see if there was any plateau where the cells stop taking up more Rhodamine. The results are presented in figure 4.17 and 4.18, supplemental data for the figures can be found in appendix E.

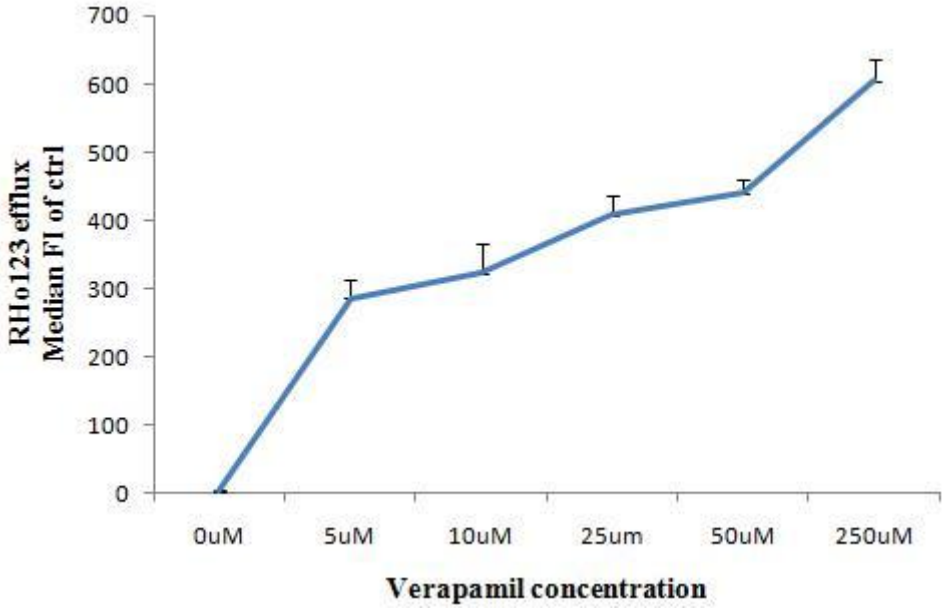

Figure 4.17 Effect of Verapamil concentration on Rhodamine 123 efflux in RBE4 cells measured by flow cytometry. Cells were treated with 0, 10, 25, 50 and 250µM Verapamil prior to and during Rho123 influx. Results are presented as median fluorescent intensity of untreated control cells (0µM). Each data point is the mean value ± standard deviation (n=3).

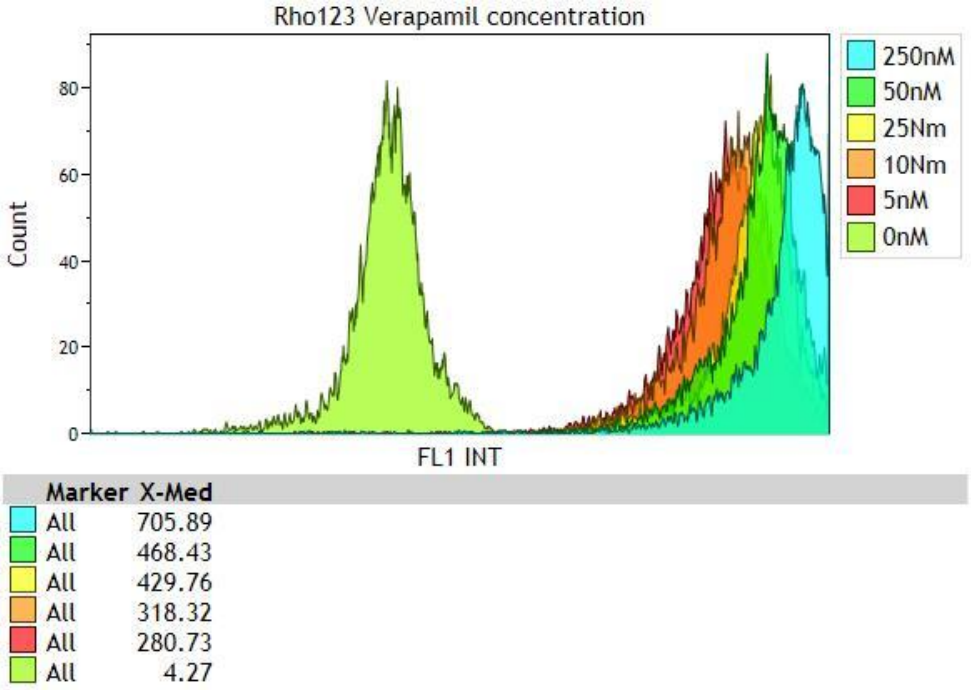

Figure 4.18 Overlay-plots of Rho123 fluorescence intensity in cells treated with 0, 5, 10, 25, 50 and 250uM Verapamil. Results are presented as fluorescence intensity plotted against cell count (number of events). The cell count was set to 10000 events and measured through channel FL1.

It can be observed from figure 4.16 and 4.17 that the Verapamil effect on Rho123 efflux in the cells is concentration dependent. The intracellular Rhodamine increases continuously with higher concentrations and does not reach a plateau where the cells are saturated with the drug.

4.4.3 Verapamil concentration-time effect on Rho123 efflux

It was evident that there is an increase in intracellular Rhodamine with increasing Verapamil concentrations, an important factor for further use of the assay and comparison with published results.

In order to investigate the rate of Rhodamine efflux, the incubation time (2hrs) with medium/Verapamil was left out of the assay and the cells were not kept on ice. The samples resuspended in HBSS instead of PBS and directly analysed with flow cytometry after 1, 1.5 and 2hrs. The results are presented in figure 4.19, supplemental data for the figure can be found in appendix E.

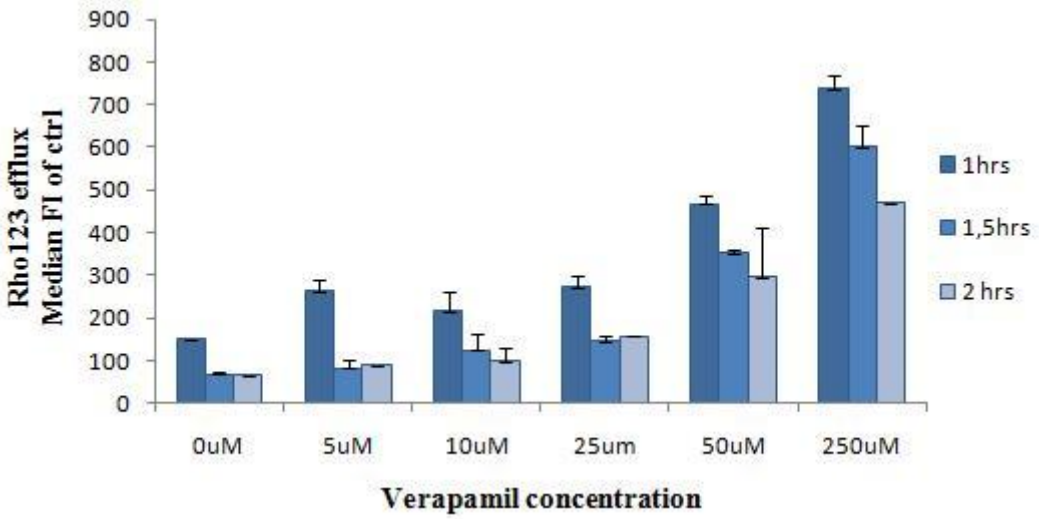

Figure 4.19 Rho123 efflux in RBE4 cells treated with 0, 5 ,10, 25, 50 and 250µM Verapamil measured by flow cytometry after 1, 1,5 and 2hrs. Untreated cells were set as baseline control and the results are presented as percent median fluorescent intensity (FI) of control. Each data point is the mean value ± standard deviation (n=3).

There was a rapid increase in Rhodamine efflux after 1.5 hrs, indicating that the P-gp pumps are efficiently pumping out Rhodamine in the absence of Verapamil inhibitor. The untreated control cells had initially more intracellular Rhodamine than in the previous Verapamil experiment. The median fluorescence decreased with time, but it did not reach the same low level even after 2hrs. The decrease in intracellular Rhodamine seemed to stabilize after 2hrs, but only one parallel of the samples had enough viable cells for analysis.

4.4.5 Effect of siRNA consentration on Rho123 efflux

In gene therapy application, the siRNA concentration plays a significant and limiting role in both polyplex stability and possible off-target effect. It was therefore of interest to investigate how far down on the concentration scale efficient knockdown was still apparent.

Two dilution series were made with mdr1a and non-targeting siRNA respectively, prepared from an initial 96nM concentration after complexation with chitosan (N/P 30) by dilution with MQ water before 1:1 addition of hypertonic OptiMem. The resulting concentrations used were; 96, 48, 24, 12, 6 and 3nM. The cells were transfected as usual and after 48hrs subjected to rho123 influx and Verapamil inhibiton prior to flow analysis. The results are presented in figures 4.20 and 4.21, supplemental data for the figures can be found in appendix E.

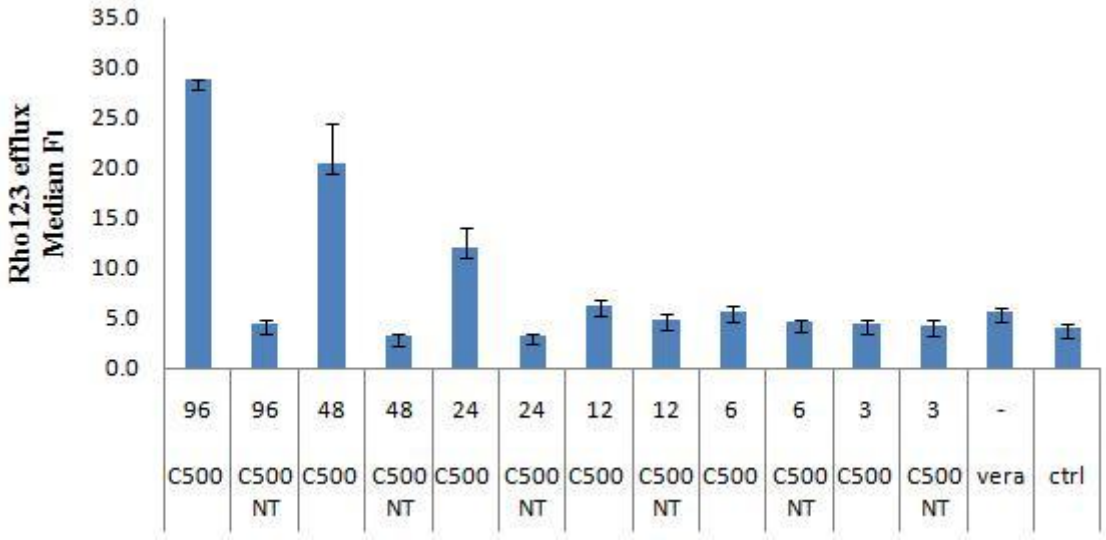

Figure 4.20 Effect of siRNA concentration on Rho123 efflux in cells treated with chitosan DP_n 500 complexed with mdr1a-siRNA or nontargeting siRNA with an N/P ratio of 30. siRNA concentrations used were 96, 48, 24 12, 6 and 3nM. Untreated cells were set as baseline control and the results are presented as percent median fluorescent intensity (FI) of control. Each data point is the mean value ± standard deviation (n=3).

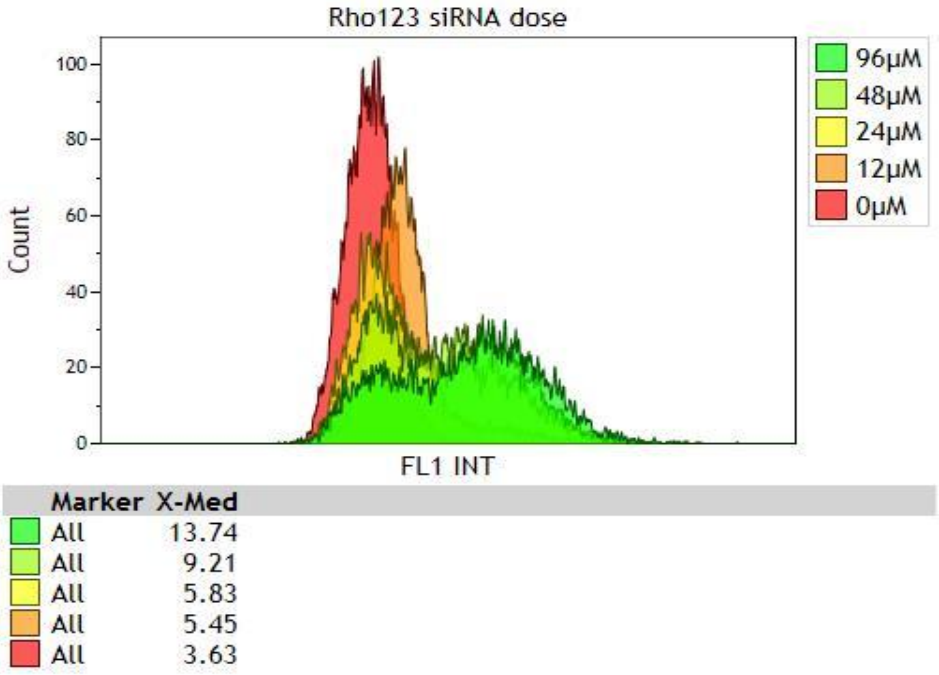

Figure 4.21 Overlay-plots of intracellular Rho123 fluorescence intensity in cells treated with chitosan DPn 500 complexed with mdr1a-siRNA or non-targeting siRNA in an N/P ratio of 30. siRNA concentrations used were 96, 48, 24, 12 and 6nM. Results are presented as fluorescence intensity plotted against cell count (number of events). The cell count was set to 10000 events and measured through channel FL1.

It is evident from the results that the siRNA concentration affects the knockdown efficiency in a concentration-dependent manner (fig.4.19 and 4.20). It displays a decrease in median FI of ~10 for each concentration division. However, when the concentration reaches 12,6 and 3nM, there is little observed difference between them and the untreated control. Interestingly, the Verapamil treated control samples failed to display any effect on the Rho123 retention in the cells, as seen in the preceding experiments. All of the non-targeting samples showed negligible deviations from the untreated control cells.

4.5 Doxorubicin accumulation in RBE4 cells visualized by CLSM

Doxorubicin is a common cancer drug that works by intercalating the DNA in the nucleus and is also a known substrate of the P-gp pump. The purpose of this experiment was to investigate the accumulation of Doxorubicin after transfection with mdr1a siRNA for inihibion of the p-gp pump. The P-gp pump inhibitor Verapamil was included to compare the effects on Doxorubicin retention in the cells.

Chitosans with DP_n 400 and N/P 30 was chosen for investigation based on preliminary screening studies, the mdr1a siRNA was used for complexation based on the same studies. The cells were transfected as usual and the cells analysed by CLSM after 48hrs of incubation and treatment with 50 µM Doxorubicin and CellMask. The results are presented in figure 4.21.

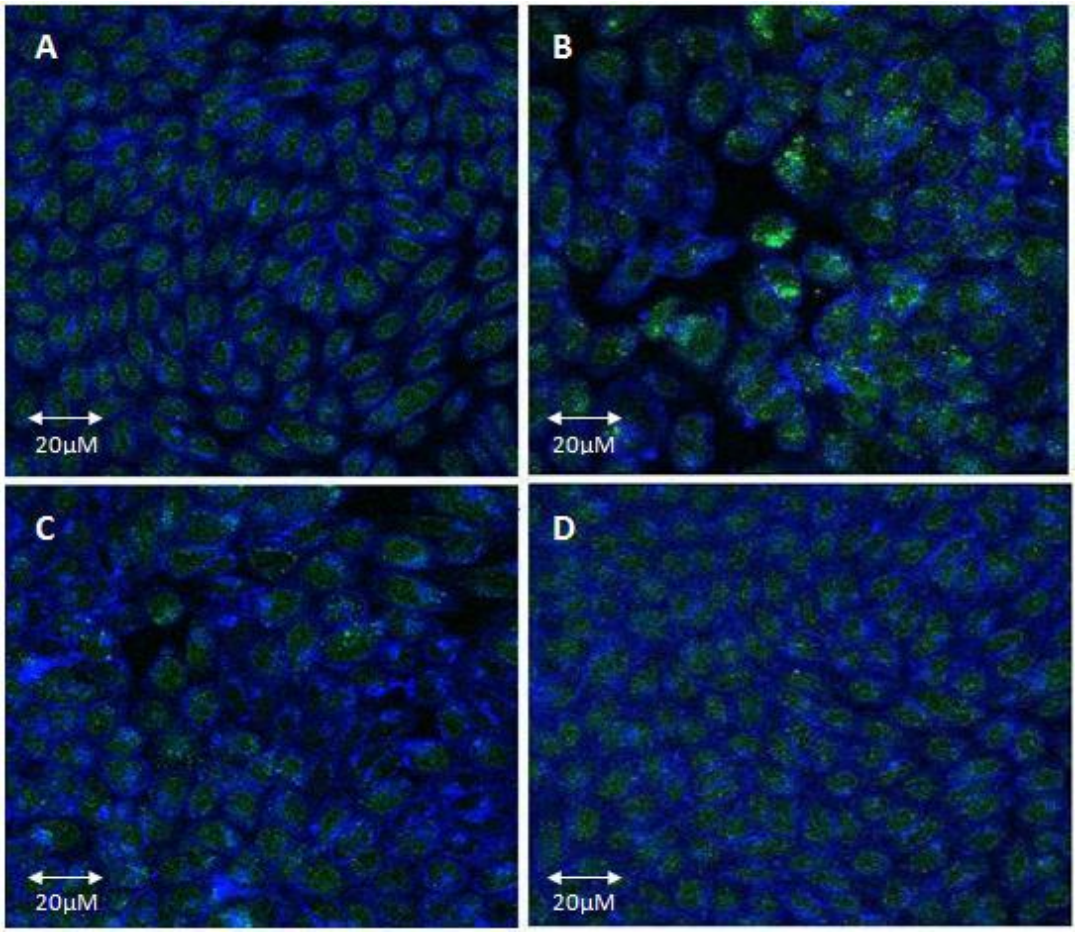

Figure 4.22 Doxorubicin accumulation in RBE4 cells 48hrs after transfection analysed by CLSM. A) untreated control cells B) C) chitosan Dpn 400 complexed with non targeting-siRNA in N/P ratio 30. CellMask plasma membrane stain is visualized as blue and Doxorubicin is presented as green fluorescence.

The observed results are presented in figure 3.17 and show an increased accumulation of Doxorubicin in the cells treated with chitosan-mdr1a siRNA polyplexes compared to both control and non-targeting sample. Verapamil treated cells showed little difference from the untreated control cells, as previously seen in the siRNA concentration experiment.

The fluorescence intensity of the chitosan-siRNA treated cells is variable, but with an overall higher amount of observed accumulated Doxorubicin. There is no directly observed nucleus localization of the Doxorubicin, and the accumulation is likely to reside in the endosomes.

5. Discussion

Chitosan is considered as a biocompatible and safe polymer for nucleic acid delivery and has been widely applied for pDNA, less research has been performed using siRNA. In this study, we set out to investigate the feasibility of using chitosan as a delivery vehicle for siRNA-mediated knockdown of P-gp efflux pump in an *in vitro* model of blood brain barrier.

P-glycoprotein (P-gp) was chosen as a target for RNAi mediated knockdown using chitosan as a novel delivery vehicle. P-gp is a highly clinically relevant target as it limits accessibility of drugs from the blood to the brain. The P-gp pump is a member of membrane transporters in brain endothelial cells which recognizes xenobiotics, extruding them from the cells. The P-gp pump is expressed by the mdr1 gene and downregulation of its expression could mediate drug accumulation in the cells.

As the RBE4 cell line was not available at the start of this thesis, we started our work by screening of different chitosan/siRNA formulations in human lung cancer cells (H1299). We established suitable physiochemical characteristics of the chitosans like DP_n and the N/P ratios of chitosan/siRNA complexes in both cell line. These preliminary studies were preformed with H1299 cells and the acquired knowledge was used with the RBE4 cells for further development.

It was found that chitosans with a high DPn were efficient at both high and low N/P rations while low DPn chitosans were less efficient at low N/P ratio. Furthermore, the cytotoxicity profiling showed negligible effects on cell proliferation and activity. We managed developed a chitosan/siRNA polyplex delivery particle suitable for the targeting and downregulation of mdr1 mRNA and hence P-gp in rat brain endothelial cells *in vitro*.

5.1 Screening of DPn, N/P ratio and cytotoxicity in H1299 cells

The need for optimization of chitosan length and charge interactions with nucleic acids have been verified by many studies (Koping-Hoggard et al. 2004; Lai and Lin 2009; Strand et al. 2008) It was therefore evident to start the experiments by screening for the most efficient formulation of polyplexes by varying the DP_n and N/P ratios of the linear chitosans.

5.1.1 Uptake efficiency of chitosan/siRNA polyplexes in H1299 cells

The first barrier encountered by the chitosan/siRNA polyplexes *in vitro* is binding to the cellular membrane and subsequent endocytosis. It has been suggested that chitosan of the appropriate Mw should be selected to achieve the desirable particle size because the transfection efficiency depends highly on the particle size which subsequently determines their cellular uptake (Mao et al. 2010).

The level of cellular uptake of the chitosan polyplexes were determined by measuring fluorescently labeled Alexa siRNA in the transfected cells (fig 4.1). In general, there was an observed increase in fluorescence intensity using formulations with increasing DP_n and N/P ratio. However, the chitosans with a low DPn seems to be dependent on a high N/P ratio for efficient uptake while the chitosans with a high DPn were just as efficient at low N/P ratios. This has also been shown by others where the use of a low N/P ratio seemed to function better with longer chitosans in transfection studies (Liao et al. 2010; Rojanarata et al. 2008).

This could be due to poor physical stability of the nanoparticles at low N/P ratios leading to increased disassociation. This has previously been demonstrated by Liu et al (2007) where chitosans with a low Mw (10 kDa) resulted in the formation of large aggregates and almost no knockdown because it could not complex and compact siRNA into stable particles (Liu et al. 2007) The reason for this may be a lack of sufficient charge interactions between the chitosan amino groups and the siRNA phosphate groups. It can be argued that the use of a low chitosan DPn and hence Mw together with a low N/P ratio with siRNA will lead to a further instability and disassociation.

5.1.2 siRNA knockdown of GFP expression

Uptake efficiency does not always equal knockdown efficiency, even though the nanoparticles enter the cells the siRNA needs to be liberated from the endosomes in order to exert its effect, so called uptake and release. Knockdown of the exogenously introduced GFP gene in H1299 cells was investigated by flow cytometry after transfection with and without addition of 10% serum.

The results from transfection in serum-free medium (Optimem) showed an increasing downregulation of gene expression with increasing DP_n and N/P ratio of the chitosan/anti-GFP siRNA polyplexes (fig 4.3). Furthermore, there were minor observed differences between the N/P ratios for the longest chitosans. The cells treated with the lowest chitosan DPn and N/P ratios showed negligible effect on knockdown. These results correspond with the uptake experiment, confirming the importance of optimized polyplex formulation in regards to DPn and N/P ratio.

Moreover, this result is in agreement with previously reported results where chitosan/anti-GFP siRNA polyplexes showed an efficient GFP knockdown of in H1299 (Howard et al. 2006). Together, these results again indicate that chitosans with a high DP_n are more efficient in mediating knockdown in H1299 cells and that low N/P ratios works better when the length of the chitosans are increased.

5.1.3 Chitosan/siRNA polyplex stability in serum

Development of siRNA delivery systems that are stable even in serum is very important for the practical applications of gene therapy *in vivo* (Mao et al. 2010). We wanted to investigate the possible effects of serum addition at transfection on knockdown efficiency in the H1299 cells. Earlier published studies has shown that chitosan nanoparticles were stable in medium containing up to 10% serum for chitosan–siRNA complexes (Katas and Alpar 2006). They also found that further incubation of the polyplexes in 50% serum rendered the siRNA stable against nucleases for several hours.

When the cultivated H1299 cells were transfected in presence of 10 % serum (fig 4.5), the chitosan/anti-GFP siRNA polyplexes with N/P ratios of 10 displayed a lower knockdown efficiency compared to the same samples in the serum-free transfection. This suggests that the serum had a slight negative effect on chitosan complexes with low N/P ratios. However, the chitosan polyplexes with N/P 30 displayed a comparable knockdown efficiency, although not to the same level. Together, these result show that the H1299 cells can be efficiently transfected in the presence of low serum concentrations.

However, in regards to BBB application, the serum percentage in blood is normally ~55% (Manzone et al. 2007). Therefore, transfection studies with a higher concentration of serum addition should be performed to further establish stability of the chitosan/siRNA polyplexes. A recent study have shown that fluorescence fluctuation spectroscopy allows quantitatively monitoring of the disassembly of siRNA containing nanoparticles in full serum (Buyens et al. 2010). This approach may be useful for further studies on the intravascular behavior of the chitosan/siRNA polyplexes.

5.1.4 Knockdown of GAPDH expression

To investigate the knockdown of an endogenous target beside GFP, GAPDH was chosen as a target for RNAi. The results of GAPDH knockdown in H1299 cells showed that the longest chitosans polyplexes (DP_n 200/300) mediated similar downregulation of the enzyme, as well negligible difference between N/P ratio 10 and 30 (fig 4.7). The shortest chitosan displayed modest effect on knockdown, this again indicates that chitosans with DP_n 54 is not sufficiently long enough to mediate optimal transfection efficiency, especially with a low NP ratio.

Interestingly, the non-targeting samples displayed 10-25% reduction in apparent GAPDH expression. This may be due to non-specific effects of either the chitosan or the siRNA used and elucidates the need for investigation of possible cytotoxicity of the components. However, the experiments shows that the GAPDH assay worked well with the transfected H1299 cells and should also be compatible with the RBE4 cells.

When relating the results to the GFP experiments, the GAPDH knockdown did not display the same maximal effect, 90 and 85% respectively. Variance in protein half life may account for the observed differences, GFP is known to have a half life of 2hrs while GAPDH has a half life of 72 hrs (Franch et al. 2001; Howard et al. 2006). Since the cells were analysed 48 h after transfection, some GAPDH enzyme may still be present from before the transfection.

The commercial transfection reagent Turbofect used in the experiments was very unstable in its knockdown and uptake efficiencies and was also seemingly toxic to the cells. This correlates with previously reported studies, where chitosan–DNA nanoparticles carried lower cytotoxicity than the commercial carriers such as Turbofect transfection reagents (Mohammadi et al. 2011).

5.1.4 Cytotoxicity assays with H1299 cells

Chitosans generally exhibit a good biocompatibility, it has been shown by several studies that chitosan/siRNA polyplexes display a low cytotoxicity (Corsi et al. 2003; M. Lee et al. 2001; Thanou et al. 2002). However, Liu et al (2007) found that chitosan/siRNA polyplexes with N/P ratios of 50 exhibited 20-40% cytotoxicity in H1299 cells. It is therefore important specifically investigate the possible cytotoxicity of the chitosan/siRNA polyplexes in the cell lines used.

The chitosans chosen for these studies had a high DP_n and were complexed with siRNA in low and high N/P ratios because of the increased possibility of toxic effect with a higher concentration of chitosan. It has been reported previously that excess chitosan in nanoparticles formed at high N/P may decrease cell viability related to the possible toxicity associated with high-molecular weight chitosan (Richardson et al. 1999).

The alamarBlue assay was used to determine if any changes in metabolic activity occurred over the 5-day period. There was a negligible observed decrease in metabolic activity and no direct time-dependent decrease in activity (fig 4.8). The chitosan complexes displayed the same effect on knockdown as for naked chitosan. The samples treated with naked siRNA did not display the same decrease in metabolic activity, comparable to untreated control. The AlamarBlue assay has not been reported for use with chitosan/siRNA previously, a recent study did however evaluate the cytotoxicity of linear, selfbranced and trimethylated chitosan-pDNA polyplexes in the HeLa cell line (Malmo et al. 2011). They found that the cells treated with linear chitosans retained a high metabolic activity with no significant changes.

Evaluation of cell viability was done by propidium iodide-staining followed by flow analysis. PI is cell-impermeable and therfore only dead cells with damaged/disintegrated cell membranes will be stained. The results showed an increasing PI permeability over the first three days with a decline the next two days (fig 4.9). Chitosan with N/P ratio 60 showed the same level of cell death for both siRNA complexes and naked chitosans. RNAiMAX resulted in the highest level of PI-positive cells, and thus correlates with the alamarBlue assay. The observed decline in cell permeability the last two days may be attributed to the growth of new and viable cells which are not affected by the initial transfection procedure. This would then compete for the number of PI-positive cells, resulting in a "false" observed decrease in permeability.

Investigation of cell proliferation was studied by cell counting (fig 4.10) and reflected the results seen in the previous cytotoxicity assays. The chitosan complexes showed similar growth retention while naked siRNA gave comparable results to the untreated control cells. This is expected since naked siRNA is subject to degradation by endogenous enzymes, and is too large and too negatively charged to cross cellular membranes (Whitehead et al. 2009). Cells treated with RNAiMAX complexes had the greatest growth retention, again suggesting toxic nature of the transfection reagent.

The BCA assay was used to estimate the concentration of protein in the samples by comparison with a standard curve based on absorbance readings. The samples gave comparable results to the cell count, with a linear increase in protein concentration reaching a small plateau at the end of five days (fig 4.11). This also corresponds to the metabolic activity and PI staining with a similar effect of chitosans and RNAiMAX resulting in the greatest reduction.

The commercial transfection reagent RNAiMAX had the most pronounced effect in all the assays, indicating that the reagent is more toxic to the cells. This has been shown in other cell lines where RNAiMAX resulted in a 1/3 decrease in cell growth relative to novel delivery lipids (NDL's) and untreated controls at 1/4 of the recommended concentration (Rossomando 2010). In summary, the four different cytotoxicity assays all displayed comparable negligible effects of the naked chitosan and chitosan/siRNA complexes on the H1299 cells. The subtle changes observed may be attributed to the growth of new cells, exceeding the surface layer capacity and thus restricting metabolic activity, proliferation and hence protein concentration at the end of the five days.

5.2 Screening of DP_n , N/P ratio and cytotoxicity in RBE4 cells

The previous transfection studies on H1299 cells set the basis for development of chitosan/siRNA polyplexes that efficiently transfected the RBE4 cells. The experiments started with screening of general uptake and knockdown efficiency of the selected chitosan/siRNA polyplexes as well as its cytotoxicity.

The aim of the following sections was to specifically downregulate the mdr1a/b mRNA which codes for the P-glycoprotein pump in brain endothelial cells. We investigated the effect of mdr1a siRNA on drug efflux in the RBE4 cells using two functional assays; Rhodamine 123 efflux by flow cytometry and visualization of the anticancer drug Doxorubicin by CLSM.

5.2.1 Uptake of chitosan/siRNA polyplexes in RBE4 cells

In order to establish efficient uptake of polyplexes into the RBE4 cells, fluorescent Alexa siRNA was used (fig 4.12). The results showed increasing uptake efficiency with higher DPn and N/P ratios which correlated with the previous mentioned studies with H1299 cells (fig. 4.1). There were however a greater difference between the effects of N/P ratios when using the same chitosan, this is expected since the ratios are 10 and 60 as opposed to 10 and 30 used with the H1299 cells.

All chitosans with different high DPn values displayed similar efficiencies when complexes in N/P ratios of 60, indicating that the chitosan length plays a minor part in mediating transfection when using high N/P ratios. The chitosan with DP_n 810 did however not display the same uptake efficiency as the others, indicating that the chitosan was compromised in some way before or during the transfection. Altogether, the results indicated efficient uptake of chitosan/siRNA polyplexes in the RBE4 cell line.

5.2.2 GAPDH knockdown in RBE4 cells

The observed result from knockdown in RBE4 cells showed nearly 1/2 reduction in enzyme expression for chitosans with high DP_n complexed in N/P ratio 30. However, only negligible reduction in enzyme activity was observed for formulations with N/P 10, this can again be attributed to a lower stability of the polyplexes. However, this is not comparable to the high DP_n chitosans in H1299 cells, where both NP 10 and 30 exhibited similar effect on knockdown (fig 4.7).

Direct conclusions can however not be drawn by comparing different cell lines, they may possess different uptake and cellular processing of the polyplexes (Malmo et al. 2011) Furthermore, aggregates, enodocytic mechanisms and intracellular trafficking may influence the uptake efficiency. Taken together, these studies confirm efficient uptake and knockdown ability of the chitosan/siRNA complexes in RBE4 cells. It may however be speculated that polyplexes formulated with low N/P ratios are not as efficient in transfecting the RBE4 cell line, despite using chitosan with a high DPn.

5.2.3 Cytotoxicity of siRNA-chitosan nanoparticles on RBE4 cells

By measuring the reduction in metabolic growth using the alamarBlue assay, cytotoxicity of chitosan nanoparticles, naked chitosan and siRNA was investigated in RBE4 cells (fig 4.14). The results showed comparable values to that of the H1299 cells with a maximum reduction with chitosan nanoparticels of ~20% of untreated control. The commercial RNAiMAX displayed an even greater reduction than the chitosan/siRNA polyplexes, again reflecting the toxic nature of the transfection reagent. These result correlates with the previous study in H1299 cells, where the chitosans with the highest DPn complexed with non targeting siRNA at N/P ratio 60 had a maximum observed reduction in metabolic activity.

Taken together, the chitosans used throughout this thesis seems to exhibit tolerable toxicity in both the H1299 and RBE 4 cell lines. The observed concentration effect of the chitosans indicates a need for using a minimum N/P ratio in further development of polyplexes.

5.3 Rhodamine efflux in RBE4 cells

We needed a functional assay for estimation of P-gp knockdown. Rhodamine is a well known substrate for the P-gp pump and by investigating its intracellular accumulation in cells we could determine the knockdown effect of chitosan-mdr1a/b polyplexes. In order to establish effective gene knockdown of the P-gp pump in vitro, the Rhodamine efflux in transfected cells were compared to Verapamil positive control which have been studied by others (Kasinathan et al. 2010; Pautina 2010).

Only the mdr1a siRNA displayed an effect on Rhodamine efflux, mdr1b siRNA had no apparent effect compared to untreated control (fig 4.15). Even though the mdr1b has been showed to be upregulated in cultured RBE4 cells (Loscher 2005), it did not seem to be functional in this study. This may be attributed to the localization of the mrd1b gene which primarily resides in the astrocytes (Begley et al. 2000).

The chitosan/mdr1 polyplexes were formulated with an N/P ratio of 10, even though low N/P ratios have shown to work well with high DPn chitosans, they may be unstable and higher ratios should be investigated. The cytotoxicity studies showed negligible negative effects at N/P 60, thus increasing the chitosan concentration should not compromise cell viability.

Furthermore, Rhodamine has also been suggested to be a substrate for the multidrug resistance protein *Mrp*1 (Minderman 1996; Twentyman et al. 1994; Zaman et al. 1994). *Mrp*1 protein, mRNa and activity has been shown to be upregulated in rat or human endothelial cell lines during culture (Regina et al. 1998; Seetharaman et al. 1998). Because Verapamil is a known inhibitor of both P-gp and Mrp1 (Loscher 2005), it can be suggested that the effect of Rhodamine retention in the cells not treated with the inhibitor is counteracted by the efflux by *Mpr*1. This indicates the need for further study on the possible anti synergistic effects of the two mRNAs.

The median fluorescent intensity of chitosan/mdr1a-siRNA treated cells did however not reach the same level as for Verapamil control. This indicated the need for siRNA dosage-experiments as well as Verapamil concentration investigation for assay adjustment. Pautina et al (2010) performed a similar experiment where Vepapamil displayed a much more pronounced effect on intracellular accumulation than the siRNA mediated knockdown, using the same concentration of the inhibitor (Pautina 2010).

We wanted to look further into the use of Verapamil as a positive control in the Rho123 assay. When the Verapamil concentration effect was investigated it showed a linear increase in intracellular Rhodamine accumulation (fig 4.17). This has also been shown by another study where addition of Verapamil significantly increased R123 uptake in a concentration-dependent manner (Yang 2010). This suggests that the Rhodamine 123 efflux assay is highly dependent on Verapamil concentrations and makes it difficult to compare the results with previous publications.

We also wanted to measure the rate of efflux using the same concentrations by excluding ice and post-Rho123 efflux incubation from the assay. The results showed a rapid decline in intracellular Rhodamine with time for all concentrations and increasing dell death which confirmed the need of ice (fig 4.19). The untreated control cells also contained Rhodamine which graduately became depleted; this is probably due to the lack of incubation after treatment with Rhodamine. The untreated cells have functional P-gp pumps and may not have enough time to pump the Rhodamine out before analysis, therefore resulting in higher values than previously seen. Also, a high sample number limited the measurements since the cells died over time in the absence of ice.

Furthermore, the siRNA concentration is a limiting factor in clinical applications of RNAi. Throughout the work presented in this thesis, we used a constant siRNA concentration of 45nM, commonly used siRNA concentrations in published studies is 50nM (Dehousse et al. 2010; Tahara et al. 2010). The possibility of off-target or non-spesific effects increases when excess amounts of siRNA are delivered to the body. A major problem with increasing the siRNA concentration in the polyplex formulations for transfection is the increased excess of siRNA that may interfere with uptake and induce immunological responses.

We therefore investigated the knockdown efficiency of the P-gp pump at different mdr1a-siRNA concentrations to determine a minimum concentration for sufficient knockdown.
The results reflected a linear decrease in knockdown for each 1:2 dilution from 96nM to 12nM where it reached a halt and did not change significantly between 12, 6 and 3 nM (fig 4.20). The three lowest concentrations did not display more than ~5% knockdown compared to the untreated control cells, this suggest that a minimum threshold for siRNA concentration lies between 48 and 12nM for this particular chitosan.

Taken together, the Rho123 assay reflected a 2-3 fold increase in intracellular accumulation after introduction of mdr1a siRNA compared to untreated control. This confirms knockdown of the mRNA coding for the P-gp pump but needs further development for sufficient effect. Verapamil is a strong inhibitor of the P-gp pump directly, but also other transporters in the endothelial cell membranes. This makes it difficult to compare the effect on cells treated with chitosan/siRNA polyplexes with Verapamil treated cells.

5.4 CLSM analysis of Doxorubicin accumulation in RBE4 cells.

The anticancer drug Doxorubicin works by intercalating with DNA in the nucleus and is also a known substrate of the P-pg pump (Loscher 2005). By visualizing the intracellular accumulation of Doxorubicin in cells by CLSM, it was possible to determine efficient knockdown of P-gp and resulting retention of the drug.

The results in reflected an increased accumulation of Doxorubicin in cells treated with chitosan-mdr1a siRNA polyplexes, confirming knockdown of P-gp (fig 4.22). It was difficult to determine whether the Doxorubicin is located in the nucleus or still residing in the endosomes, this could have been resolved by additionally staining of the nucleus membrane.
Unfortunately, it was not possible to compare the results with the Verapamil treated cells; there is a possibility that the stock solution of Verapamil was too old or compromised in some way. Even though the Verapamil inhibition failed to work, the difference in Doxorubicin accumulation between chitosan/mdr1a-siRNA transfected cells and untreated control cells still gives a good indication of efficient knockdown.

Like Rhodamine, Doxorubicin is also a common substrate of the MDR transporter *MRP1* which resides in the RBE4 cells (Loscher 2005). This can possibly be working as an additional efflux mechanism and thus counteract the effect of reduced P-gp expression in the cells. It once again shows the substrate-overlap between the two MDR transporters and poses an additional problem of efficient retention. Verapamil is also an inhibitor of MRP1, so the drug retention in the cells treated with the inhibitor was expected to be higher.

Throughout this thesis we have used functional assays that indicate that the P-gp function is disabeled. However, we have no direct evidence for knockdown. In order to confirm the findings, western blot or immunostaining for protein determination and PCR for mRNA expression should be performed. It must be taken into consideration that the RBE4 cells expresses very low levels of P-gp in culture (Hosoya et al. 2000), therefore these studies are yet to be successful in our research group.

5.6 Summary

The chitosan/siRNA polyplex formulations used throughout this thesis displayed an efficient uptake and knockdown as well as low cytotoxicity in both H1299 and RBE4 cells.

- There was an observed correlation between chitosan DPn and N/P ratios of polyplexes on both uptake and knockdown efficiency. Chitosans with a low DPn generally needed a high N/P ratio while chitosans with higher DPn worked well at low N/P ratios.
- The H1299 cells were transfected efficiently in the presence of serum, although knockdown levels were lower at low N/P ratios
- The chitosan/siRNA polyplexes exhibited negligible cytotoxicity in both cell lines at high N/P ratios.

The P-gp expression in RBE4 cells were efficiently downregulated after chitosan-mdr1a-siRNA transfection, but not mdr1b.

- Rhodamine accumulation in the RBE4 cells increased 2-3 fold in chitosan/mdr1a-siRNA transfected cells compared to untreated control cells.
- Verapamil inhibition was too efficient to compare with chitosan transfection, possibly due to dual inhibition. It also displayed a concentration and time dependent efficiency on Rhodamine accumulation.
- The mdr1a-siRNA concentration was a limiting factor in the knockdown of P-gp, a minimum concentration for efficient knockdown was found to lie between 12-48nM.
- The visualization of intracellular Doxorubicin in the RBE4 cells gave a good indication of efficient reduction in P-gp expression in cells transfected with chitosan/mdr1a-siRNA.

6. Concluding remarks

We have shown that chitosan can be used as an efficent delivery vehicle for siRNA in both H1299 and RBE4 cells with negligible cytotoxicity in vitro. The formulated chitosan/siRNA polyplexes was found to dependent on DPn and N/P ratios in order to exert maximal effect on both uptake and knockdown.

Specifically, we managed to downregulate the P-gp expression in RBE4 cells using chitosans with high a DPn complexed with mdr1a-siRNA in a low N/P ratio. Together, the results presented in this thesis elucidate the potential of chitosan mediated siRNA downregulation of the P-gp pump in RBE4 cells and further development for in vivo applications.

7. Future directions and considerations

There is still much to be revealed about the chitosan/siRNA polyplexes in general and in relation to blood brain barrier and P-plycoprotein applications *in vitro*. Furthermore, modifications to the proposed delivery system may be needed for use *in vivo.*

7.1 Chitosan/siRNA polyplexes

In order to quantitatively confirm mRNA and protein reduction after administration of chitosan/siRNA polyplexes, PCR and western blot/immunohistochemical staining needs to be performed. For evaluation of possible off target effects, a wide microarray analysis of gene expression can give a more accurate picture.

When these parameters are firmly established, testing in vitro using animal models like rat or mice can be performed. However, chitosan/siRNA polyplexes are in need of further development for *in vivo* applications and targeting to tissue. Structural modifications like copolymerization and functional group modification or ligand conjugation may be beneficial in increasing transfection and uptake efficiency as well as steric stability and serum compatibility.

Nanoparticles that are polycation-nucleic acid composites are known to be unstable in biological fluids such as blood. One method of preventing self-aggregation and undesired interactions with unwanted components in biological fluids is to employ steric stabilization. Polythethylene glycol (PEG) has been conjugated to different non-viral delivery carriers, and the resulting PEGylated particles have demonstrated increased salt and serum stability (Jiang et al. 2007). Another means of copolymerization is Polyethyleneimine (PEI), which also has been used as a modifier for chitosan vector derivation but can exhibit high toxicity to cells and is need for further optimization (Wong et al. 2005).

Many of the nanoparticles developed cannot be used in clinical settings due to nonspecific delivery, which may lead to unwanted side effects. Preferably, the delivery system should show enhanced concentrations of therapeutic payloads at disease sites, minimize concerns about off-target effects, and ultimately raise the therapeutic index (Han et al. 2010; Whitehead et al. 2009). Therefore, introduction of targeting ligands may increase the specificity and safety of the delivery agent. A novel tumor targeted delivery system for siRNA has recently been demonstrated by using an Arg-Gly-Asp (RGD) peptide-labeled chitosan nanoparticle for selective intratumoral delivery by binding to the αvβ3 integrin (Han et al. 2010)

7.2 P-gp and the blood brain barrier

Knockdown of efflux pumps such as P-gp is very important in cancer treatment because many cancer types become resistant to cytostatic drugs in their presence. By downregulating their expression we can dramatically improve the medical treatment. As previously mentioned, more information regarding the disassembly of chitosan/siRNA polyplexes in blood needs to be established for applications in viro. It can be suggested that to overcome the BBB, one should develop a chitosan nanoparticle that targets more than one transporter, by combining several siRNAs. A drawback from this approach may be the increased access of harmful toxic substances to the brain when shutting down several MDR proteins.

Another approach could be to engineer nanoparticles with dual drug and siRNA delivery, previously shown in a cancer cell line (Meng et al. 2010). In this regard the P-gp expression has a long half-life of about 16-72 hrs depending on cell line (Stierlé 2004), which ultimately raises the question of whether the existing P-gp would pump out the drug before efficient knockdown occurs. Furthermore, it brings into question what the optimal transfection duration is in order to reach satisfactory knockdown of P-gp expression before administration of a drug. Kinetic studies needs to be performed to investigate the temporal effects of chitosan/siRNA delivery in cells. Moreover, the possible off target effects and cytotoxicity need to be evaluated in order to apply the current knowledge to *in vivo* testing.

Additionally, there may be a functional impact of polymorphisms in the human MDR1 gene, there has been reported more than 50 single nucleotide polymorphisms and insertion/deletions, some associated with alteration of P-gp expression and/or function (Brinkmann and Eichelbaum 2001; Löscher and Potschka 2005) This poses an additional limitation of the RBE4 cell line model, because is not known whether functionally relevant polymorphisms also occurs in the mdr1a gene (Löscher and Potschka 2005; Volk and Löscher 2005). These polymorphisms may lead to inter-individual or ethnicity differences in responses and should be taken into account in an in vitro application.

References

Akhtar, Naseem, et al. (2011), 'The emerging role of P-glycoprotein inhibitors in drug delivery: a patent review', *Expert Opinion on Therapeutic Patents,* 21 (4), 561-76.

Akhtar, Saghir and Benter, Ibrahim F. (2007), 'Nonviral delivery of synthetic siRNAs in vivo', *The Journal of Clinical Investigation,* 117 (12), 3623-32.

Al-Nasiry, S., et al. (2007), 'The use of Alamar Blue assay for quantitative analysis of viability, migration and invasion of choriocarcinoma cells', *Human Reproduction,* 22 (5), 1304-09.

Alyaudtin, Renad N., et al. (2001), 'Interaction of Poly(butylcyanoacrylate) Nanoparticles with the Blood-Brain Barrier in vivo and in vitro', *Journal of Drug Targeting,* 9 (3), 209-21.

BD-biosciences (2011), 'Introduction to flow cytometry: A learning guide', <http://www.stemcell.umn.edu/prod/groups/med/@pub/@med/documents/asset/med_80691.pdf >, accessed February 20th.

Begley, David, et al. (2000), 'The Role of Brain Extracellular Fluid Production and Efflux Mechanisms in Drug Transport to the Brain', *The Blood-Brain Barrier and Drug Delivery to the CNS* (Informa Healthcare).

Bloomfield, Victor A. (1996), 'DNA condensation', *Current Opinion in Structural Biology,* 6 (3), 334-41.

Brinkmann, U. and Eichelbaum, M. (2001), 'Polymorphisms in the ABC drug transporter gene MDR1', *Pharmacogenomics J,* 1 (1), 59-64.

Buyens, Kevin, et al. (2010), 'Monitoring the disassembly of siRNA polyplexes in serum is crucial for predicting their biological efficacy', *Journal of Controlled Release,* 141 (1), 38-41.

Cerletti, Andrin, et al. (2000), 'Endocytosis and Transcytosis of an Immunoliposome-Based Brain Drug Delivery System', *Journal of Drug Targeting,* 8 (6), 435-46.

Claxton, NS., Fellers, TJ., Davidson, MW (2011), 'Laser Scanning Confocal Microscopy', <http://www.olympusfluoview.com/theory/LSCMIntro.pdf>, accessed March 10th.

Corsi, Karin, et al. (2003), 'Mesenchymal stem cells, MG63 and HEK293 transfection using chitosan-DNA nanoparticles', *Biomaterials,* 24 (7), 1255-64.

Dash, M., et al. (2011), 'Chitosan--A versatile semi-synthetic polymer in biomedical applications', *Progress in Polymer Science,* 36 (8), 981-1014.

de Fougerolles, Antonin, et al. (2007), 'Interfering with disease: a progress report on siRNA-based therapeutics', *Nat Rev Drug Discov,* 6 (6), 443-53.

De Paula, Daniel, Bentley, M. Vitória L.B., and Mahato, Ram I. (2007), 'Hydrophobization and bioconjugation for enhanced siRNA delivery and targeting', *RNA,* 13 (4), 431-56.

Dehousse, V., et al. (2010), 'Comparison of chitosan/siRNA and trimethylchitosan/siRNA complexes behaviour in vitro', *International Journal of Biological Macromolecules,* 46 (3), 342-49.

Edwards, Geoffrey (2003), 'Ivermectin: does P-glycoprotein play a role in neurotoxicity?', *Filaria Journal,* 2 (Suppl 1), S8.

Elbashir, Sayda M., Lendeckel, Winfried, and Tuschl, Thomas (2001), 'RNA interference is mediated by 21- and 22-nucleotide RNAs', *Genes & Development,* 15 (2), 188-200.

Elouahabi, Abdelatif and Ruysschaert, Jean-Marie (2005), 'Formation and Intracellular Trafficking of Lipoplexes and Polyplexes', *Mol Ther,* 11 (3), 336-47.

Fire, Andrew, et al. (1998), 'Potent and specific genetic interference by double-stranded RNA in Caenorhabditis elegans', *Nature,* 391 (6669), 806-11.
Franch, Harold A., et al. (2001), 'A Mechanism Regulating Proteolysis of Specific Proteins during Renal Tubular Cell Growth', *Journal of Biological Chemistry,* 276 (22), 19126-31.
Fromm, Martin F. (2004), 'Importance of P-glycoprotein at blood-tissue barriers', *Trends in Pharmacological Sciences,* 25 (8), 423-29.
Fuest, Christina, et al. (2009), 'In vivo down-regulation of mouse brain capillary P-glycoprotein: A preliminary investigation', *Neuroscience Letters,* 464 (1), 47-51.
GE-Lifesciences (2011), 'Fluorescence Theory', <http://www.gelifesciences.com/aptrix/upp00919.nsf/Content/618C37F7236EDF05C1257628001CEBF7/$file/Fluores_Theory_SPA.pdf>, accessed February 13th.
Gershon, Hezi, et al. (1993), 'Mode of formation and structural features of DNA-cationic liposome complexes used for transfection', *Biochemistry,* 32 (28), 7143-51.
Grimm, Dirk, et al. (2006), 'Fatality in mice due to oversaturation of cellular microRNA/short hairpin RNA pathways', *Nature,* 441 (7092), 537-41.
Han, Hee Dong, et al. (2010), 'Targeted Gene Silencing Using RGD-Labeled Chitosan Nanoparticles', *Clinical Cancer Research,* 16 (15), 3910-22.
Harish Prashanth, K. V. and Tharanathan, R. N. (2007), 'Chitin/chitosan: modifications and their unlimited application potential--an overview', *Trends in Food Science & Technology,* 18 (3), 117-31.
Hosoya, Ken-Ichi, et al. (2000), 'mRNA Expression and Transport Characterization of Conditionally Immortalized Rat Brain Capillary Endothelial Cell Lines; a New in vitro BBB Model for Drug Targeting', *Journal of Drug Targeting,* 8 (6), 357-70.
Howard, Kenneth A., et al. (2008), 'Chitosan/siRNA Nanoparticle-mediated TNF-[alpha] Knockdown in Peritoneal Macrophages for Anti-inflammatory Treatment in a Murine Arthritis Model', *Mol Ther,* 17 (1), 162-68.
Howard, Kenneth A., et al. (2006), 'RNA Interference in Vitro and in Vivo Using a Chitosan/siRNA Nanoparticle System', *Mol Ther,* 14 (4), 476-84.
Issa, Mohamed M., Köping-Höggård, Magnus, and Artursson, Per (2005), 'Chitosan and the mucosal delivery of biotechnology drugs', *Drug Discovery Today: Technologies,* 2 (1), 1-6.
Jackson, Aimee L. and Linsley, Peter S. (2004), 'Noise amidst the silence: off-target effects of siRNAs?', *Trends in Genetics,* 20 (11), 521-24.
Jackson, Aimee L. and Linsley, Peter S. (2010), 'Recognizing and avoiding siRNA off-target effects for target identification and therapeutic application', *Nat Rev Drug Discov,* 9 (1), 57-67.
Jackson, Aimee L., et al. (2006), 'Widespread siRNA “off-target” transcript silencing mediated by seed region sequence complementarity', *RNA,* 12 (7), 1179-87.
Jiang, H. L., et al. (2007), 'Galactosylated chitosan-graft-polyethylenimine as a gene carrier for hepatocyte targeting', *Gene Ther,* 14 (19), 1389-98.
Kasinathan, Ravi S., et al. (2010), 'Modulation of a Schistosoma mansoni multidrug transporter by the antischistosomal drug praziquantel', *The FASEB Journal,* 24 (1), 128-35.
Katas, Haliza and Alpar, H. Oya (2006), 'Development and characterisation of chitosan nanoparticles for siRNA delivery', *Journal of Controlled Release,* 115 (2), 216-25.

Kean, T. and Thanou, M. (2010), 'Biodegradation, biodistribution and toxicity of chitosan', *Advanced Drug Delivery Reviews,* 62 (1), 3-11.
Khalil, Ikramy A., et al. (2006), 'Uptake Pathways and Subsequent Intracellular Trafficking in Nonviral Gene Delivery', *Pharmacological Reviews,* 58 (1), 32-45.
Koping-Hoggard, M., et al. (2004), 'Improved chitosan-mediated gene delivery based on easily dissociated chitosan polyplexes of highly defined chitosan oligomers', *Gene Ther,* 11 (19), 1441-52.
Krohn, Randall I. (2001), *The Colorimetric Detection and Quantitation of Total Protein* (Current Protocols in Cell Biology: John Wiley & Sons, Inc.).
Kurita, Keisuke (2006), 'Chitin and Chitosan: Functional Biopolymers from Marine Crustaceans', *Marine Biotechnology,* 8 (3), 203-26.
Lai, Wing-Fu and Lin, Marie Chia-Mi (2009), 'Nucleic acid delivery with chitosan and its derivatives', *Journal of Controlled Release,* 134 (3), 158-68.
Lee, Minhyung, et al. (2001), 'Water-Soluble and Low Molecular Weight Chitosan-Based Plasmid DNA Delivery', *Pharmaceutical Research,* 18 (4), 427-31.
Lee, S. H. and Sinko, P. J. (2006), 'siRNA--Getting the message out', *European Journal of Pharmaceutical Sciences,* 27 (5), 401-10.
Liao, Zi-Xian, et al. (2010), 'Enhancement of efficiencies of the cellular uptake and gene silencing of chitosan/siRNA complexes via the inclusion of a negatively charged poly([gamma]-glutamic acid)', *Biomaterials,* 31 (33), 8780-88.
Liu, Xiudong, et al. (2007), 'The influence of polymeric properties on chitosan/siRNA nanoparticle formulation and gene silencing', *Biomaterials,* 28 (6), 1280-88.
Loscher, W. and H. Potschka (2005), 'Role of drug efflux transporters in the brain for drug disposition and treatment of brain diseases', *Progress in Neurobiology,* (76), 22-76.
Löscher, Wolfgang and Potschka, Heidrun (2005), 'Role of drug efflux transporters in the brain for drug disposition and treatment of brain diseases', *Progress in Neurobiology,* 76 (1), 22-76.
Lv, Hongtao, et al. (2006), 'Toxicity of cationic lipids and cationic polymers in gene delivery', *Journal of Controlled Release,* 114 (1), 100-09.
Malmo, Jostein, Vårum, Kjell M., and Strand, Sabina P. (2011), 'Effect of Chitosan Chain Architecture on Gene Delivery: Comparison of Self-Branched and Linear Chitosans', *Biomacromolecules,* 12 (3), 721-29.
Manzone, Timothy A., et al. (2007), 'Blood Volume Analysis: A New Technique and New Clinical Interest Reinvigorate a Classic Study', *J Nucl Med Technol,* 35 (2), 55-63.
Mao, Shirui, Sun, Wei, and Kissel, Thomas (2010), 'Chitosan-based formulations for delivery of DNA and siRNA', *Advanced Drug Delivery Reviews,* 62 (1), 12-27.
Martin, Scott E. and Caplen, Natasha J. (2007), 'Applications of RNA Interference in Mammalian Systems*', *Annual Review of Genomics and Human Genetics,* 8 (1), 81-108.
Martinez, Javier, et al. (2002), 'Single-Stranded Antisense siRNAs Guide Target RNA Cleavage in RNAi', *Cell,* 110 (5), 563-74.
Matranga, Christian, et al. (2005), 'Passenger-Strand Cleavage Facilitates Assembly of siRNA into Ago2-Containing RNAi Enzyme Complexes', *Cell,* 123 (4), 607-20.
Meng, Huan, et al. (2010), 'Engineered Design of Mesoporous Silica Nanoparticles to Deliver Doxorubicin and P-Glycoprotein siRNA to Overcome Drug Resistance in a Cancer Cell Line', *ACS Nano,* 4 (8), 4539-50.

Minderman, H., U. Vanhoefer, K. Toth, M. B. Yin, M. D. Minderman, C. Wrzosek, M. L. Slovak, and Y. M. Rustum. . . (1996), 'DiO2(3) is not a substrate for multidrug resistance protein (MRP)-mediated drug efflux.', *Cytometry,* (25), 14-20.

Mohammadi, Z., et al. (2011), 'Preparation and evaluation of chitosan-DNA-FAP-B nanoparticles as a novel non-viral vector for gene delivery to the lung epithelial cells', *International Journal of Pharmaceutics,* 409 (1-2), 307-13.

Nocker, Andreas, Cheung, Ching-Ying, and Camper, Anne K. (2006), 'Comparison of propidium monoazide with ethidium monoazide for differentiation of live vs. dead bacteria by selective removal of DNA from dead cells', *Journal of Microbiological Methods,* 67 (2), 310-20.

Pardridge, William M. (2007), 'Blood-brain barrier delivery', *Drug Discovery Today,* 12 (1-2), 54-61.

Pautina, OA., Mironova, NL., Popova, NA., Kaledin, VI., Nikolin, VP., Vlassov, VV., Zenkova, MA. (2010), 'The siRNA targeted to mdr1b and mdr1a mRNAs in vivo sentitizes murine lymphosarcoma to chemotherapy', *BMC Cancer,* 10.

Quanta-tech (2011), 'Confocal Microscopy', <http://opto.braggcell.com/uploads/files/CONFOCAL.pdf>, accessed March 10th.

Rahman, M (2011), 'Introduction to flow cytometry', <http://www.abdserotec.com/uploads/Flow-Cytometry.pdf >, accessed February 20th.

Rao, Donald D., et al. (2009), 'siRNA vs. shRNA: Similarities and differences', *Advanced Drug Delivery Reviews,* 61 (9), 746-59.

Ravi Kumar, Majeti N. V. (2000), 'A review of chitin and chitosan applications', *Reactive and Functional Polymers,* 46 (1), 1-27.

Regina, Anthony, et al. (1998), 'Mrp1 Multidrug Resistance-Associated Protein and P-Glycoprotein Expression in Rat Brain Microvessel Endothelial Cells', *Journal of Neurochemistry,* 71 (2), 705-15.

Reischl, Daniela and Zimmer, Andreas (2009), 'Drug delivery of siRNA therapeutics: potentials and limits of nanosystems', *Nanomedicine: Nanotechnology, Biology and Medicine,* 5 (1), 8-20.

Richardson, Simon C. W., Kolbe, Hanno V. J., and Duncan, Ruth (1999), 'Potential of low molecular mass chitosan as a DNA delivery system: biocompatibility, body distribution and ability to complex and protect DNA', *International Journal of Pharmaceutics,* 178 (2), 231-43.

Roberts, G.A. F (1992), *Chitin chemistry* (1 edn.; London: Macmillan).

Rojanarata, Theerasak, et al. (2008), 'Chitosan-Thiamine Pyrophosphate as a Novel Carrier for siRNA Delivery', *Pharmaceutical Research,* 25 (12), 2807-14.

Rossomando, AJ. (2011), 'Application of RNAi to block adventitious infections in bioprocessing', accessed March 20th.

Roux, Françoise and Couraud, Pierre-Olivier (2005), 'Rat Brain Endothelial Cell Lines for the Study of Blood–Brain Barrier Permeability and Transport Functions', *Cellular and Molecular Neurobiology,* 25 (1), 41-57.

Rudzinski, Walter E. and Aminabhavi, Tejraj M. (2010), 'Chitosan as a carrier for targeted delivery of small interfering RNA', *International Journal of Pharmaceutics,* 399 (1-2), 1-11.

Ruponen, Marika, Ylä-Herttuala, Seppo, and Urtti, Arto (1999), 'Interactions of polymeric and liposomal gene delivery systems with extracellular glycosaminoglycans:

physicochemical and transfection studies', *Biochimica et Biophysica Acta (BBA) - Biomembranes,* 1415 (2), 331-41.
Seetharaman, Seeta, et al. (1998), 'Multidrug Resistance-Related Transport Proteins in Isolated Human Brain Microvessels and in Cells Cultured from These Isolates', *Journal of Neurochemistry,* 70 (3), 1151-59.
Semwogerere, D., Weeks, ER (2011), 'Confocal microscopy', < http://www.physics.emory.edu/~weeks/lab/papers/ebbe05.pdf>, accessed February 21th.
Sharom, J.F (2006), 'Shedding light on drug transport: structure and function of the P-glycoprotein multidrug transporter (ABCB1)This paper is one of a selection of papers published in this Special Issue, entitled CSBMCB — Membrane Proteins in Health and Disease', *Biochemistry and Cell Biology,* 84 (6), 979-92.
Snustad, P and Simmons, MJ (2010), *Principles of genetics* (5 edn.: Wiley).
Stierlé, V., Laigle, A., Jollès, B. (2004), 'The Reduction of P-Glycoprotein Expression by Small Interfering RNAs Is Improved in Exponentially Growing Cells ', *Oligonucleotides* (14), 191-98.
Strand, Sabina P., et al. (2008), 'Tailoring of Chitosans for Gene Delivery: Novel Self-Branched Glycosylated Chitosan Oligomers with Improved Functional Properties', *Biomacromolecules,* 9 (11), 3268-76.
Su, Fengxi, et al. (2005), 'Psychological stress induces chemoresistance in breast cancer by upregulating mdr1', *Biochemical and Biophysical Research Communications,* 329 (3), 888-97.
Tahara, Kohei, et al. (2010), 'Chitosan-modified poly(d,l-lactide-co-glycolide) nanospheres for improving siRNA delivery and gene-silencing effects', *European Journal of Pharmaceutics and Biopharmaceutics,* 74 (3), 421-26.
Thanou, M., et al. (2002), 'Quaternized chitosan oligomers as novel gene delivery vectors in epithelial cell lines', *Biomaterials,* 23 (1), 153-59.
Thiebaut, F, et al. (1987), 'Cellular localization of the multidrug-resistance gene product P-glycoprotein in normal human tissues', *Proceedings of the National Academy of Sciences,* 84 (21), 7735-38.
Tokatlian, Talar and Segura, Tatiana (2010), 'siRNA applications in nanomedicine', *Wiley Interdisciplinary Reviews: Nanomedicine and Nanobiotechnology,* 2 (3), 305-15.
Twentyman, P. R., Rhodes, T., and Rayner, S. (1994), 'A comparison of rhodamine 123 accumulation and efflux in cells with P-glycoprotein-mediated and MRP-associated multidrug resistance phenotypes', *European Journal of Cancer,* 30 (9), 1360-69.
USU (2011), 'Introduction to Flow Cytometry', <http://www.usuhs.mil/bic/cytometry/pdf/tutorial.pdf>, accessed February 14th.
Volk, Holger A. and Löscher, Wolfgang (2005), 'Multidrug resistance in epilepsy: rats with drug-resistant seizures exhibit enhanced brain expression of P-glycoprotein compared with rats with drug-responsive seizures', *Brain,* 128 (6), 1358-68.
Wang, Xiaoying, et al. (2010), 'Chitosan-DNA-rectorite nanocomposites: Effect of chitosan chain length and glycosylation', *Carbohydrate Polymers,* 79 (3), 590-96.
Warnes, Gary (2011), 'Principles of fluorescence', <http://www.icms.qmul.ac.uk/flowcytometry/flowcytometry/principles/index.html>, accessed February 14th.
Whitehead, Kathryn A., Langer, Robert, and Anderson, Daniel G. (2009), 'Knocking down barriers: advances in siRNA delivery', *Nat Rev Drug Discov,* 8 (2), 129-38.

Wolff, Jon A. and Rozema, David B. (2007), 'Breaking the Bonds: Non-viral Vectors Become Chemically Dynamic', *Mol Ther,* 16 (1), 8-15.

Wong, Kokhou, et al. (2005), 'PEI-g-chitosan, a Novel Gene Delivery System with Transfection Efficiency Comparable to Polyethylenimine in Vitro and after Liver Administration in Vivo', *Bioconjugate Chemistry,* 17 (1), 152-58.

Wu, Hao, Hait, William N., and Yang, Jin-Ming (2003), 'Small Interfering RNA-induced Suppression of MDR1 (P-Glycoprotein) Restores Sensitivity to Multidrug-resistant Cancer Cells', *Cancer Research,* 63 (7), 1515-19.

Xu, Dong, et al. (2004), 'Strategies for Inhibition of MDR1 Gene Expression', *Molecular Pharmacology,* 66 (2), 268-75.

Xu, Sailong, et al. (2007), 'Direct Force Measurements between siRNA and Chitosan Molecules Using Force Spectroscopy', *Biophysical journal,* 93 (3), 952-59.

Yang, L (2011), 'Effect of Bile Salts on Drug Delivery to the Brain', <http://otago.ourarchive.ac.nz/bitstream/handle/10523/460/PhD%20thesis%20Lin%20Yang.pdf?sequence=1>, accessed April 20th.

Zaman, G J, et al. (1994), 'The human multidrug resistance-associated protein MRP is a plasma membrane drug-efflux pump', *Proceedings of the National Academy of Sciences,* 91 (19), 8822-26.

Appendices

Appendices

A Production numbers

Table 1. Producers and production numbers of the materials used.

Water, Mol biograde – Dnase, RNase and protease free	250010	5prime	**Propidium Iodide**	81845	Sigma
DPBS, Dulbecco's phosphate buffered saline	14190-094	Gibco	**Alexa fluor® 647 siRNA**		Molecular Probes™
DMEM, Dulbecco's modified eagle medium,	31053-028	Gibco	**GFP (eGFP) siRNA**	AM4626	Ambion
HBSS, Hank's balanced salt solution,	14025-050	Gibco	**Negative control siRNA**	4611G	
Trypsin/EDTA (0,25%/0,02%)	T-4049	Sigma	**GAPDH (human) siRNA**	AM605	Ambion
OptiMEM ® reduced serum medium	31985-062	Gibco	**GAPDH (human, mouse, rat) siRNA**	AM4624	Ambion
Mannitol	103304Y	AnalaR®	**Abcb1a/b siRNA**	4390771	Ambion
HEPES	H-3375	Sigma	**BCA protein assay kit™**	71285-3	Pierce
RPMI-1640 medium		Sigma	**KDalert™ GAPDH assay kit**	1639	Ambion
PEST, penicillin and streptomycin	P-0781	Sigma	**alamarBlue® assay kit**	DAL 1025	Biosource, Invitrogen
G418 disulfate salt solution	A1720-1G	Sigma			
FBS, Fetal bovine serum	10106-169	Gibco			
NEAA, non-essential amino acids	11140-035	Gibco			
αMEM medium	31095-029	Gibco			
BD biocoat™ collagen cell culture flasks	354462	BD biosciences			
BD Biocoat™ collagen 96 well plates	ref# 354407	BD biosciences			

B Formulation of polyplexes

The formulation of transfection mixtures was calculated for 4 or 6 wells using table 2 given below. Calculation is based on the following relationship:

- Conc siRNA in polyplexes, 1.2 µg/mL = 90.2 pmol/mL = 90.2 nM before hypertonic OPTImem addition; dose 30ng/well (2.25pmol)
- Polyplex of N/P =1 corresponds 0.584 mg chitosan (Fa 0) per 1 mg siRNA

Table 2 Polyplex formulation for 4 wells in 96-well plates.

N/P ratio	**10**	**20**	**30**	**40**	**60**
siRNA (µL), 66.5 ug/mL	2.26	2.26	2.26	2.26	2.26
Chitosan(µL), 0,1 mg/mL	8.76	17.52	26.29	35.05	52.57
MQ water (µL)	113.98	105.22	96.46	87.69	70.17
Total	125.00	125.00	125.00	125.00	125.00

C Uptake and knockdown in H1299 and RBE4 cells

C.1 Alexa 647 uptake in RBE4 and H1299 cells

Table 3. Raw flow cytometry data for Alexa 647 Uptake in H1299 cells.

Sample		Ctrl	C54 T	C54 T	C200 T	C200 T	C300 T	C300 T	Turbo T	siRNA
N/P			*10*	*30*	*10*	*30*	*10*	*30*	*3*	*-*
	Parallell									
Median FI	1	0.665	10.10	36.70	39.80	75.40	95.3	89.00	43.2	0.77
	2	0.671	8.95	48.10	44.80	60.20	88.7	98.80	67	0.83
avg		**0.67**	**9.53**	**42.40**	**42.30**	**67.80**	**92.00**	**93.90**	**55.10**	**0.80**
stdev		**0.00**	**0.81**	**8.06**	**3.54**	**10.75**	**4.67**	**6.93**	**16.83**	**0.04**

Table 4. Raw flow cytometry data for Alexa 647 Uptake in RBE4 cells.

Sample		C 250	C 250	C 300	C 300	C 400	C 400	C 810	C 810	siRNA	ctrl
	Parallell	*10*	*60*	*10*	*60*	*10*	*60*	*10*	*60*	*-*	
Median FI	1	69.1	177	101	214	125	205	12.3	143	1.43	1.74
	2	53.1	148	110	190	149	174	9.79	138	1.4	1.31
	3	47.7	*	*	165	168	210	11.4	159	1.42	1.89
avg		**56.63**	**162.50**	**105.50**	**189.67**	**147.33**	**196.33**	**11.16**	**146.67**	**1.42**	**1.65**
std		11.13	20.51	6.36	24.50	21.55	19.50	1.27	10.97	0.02	0.30

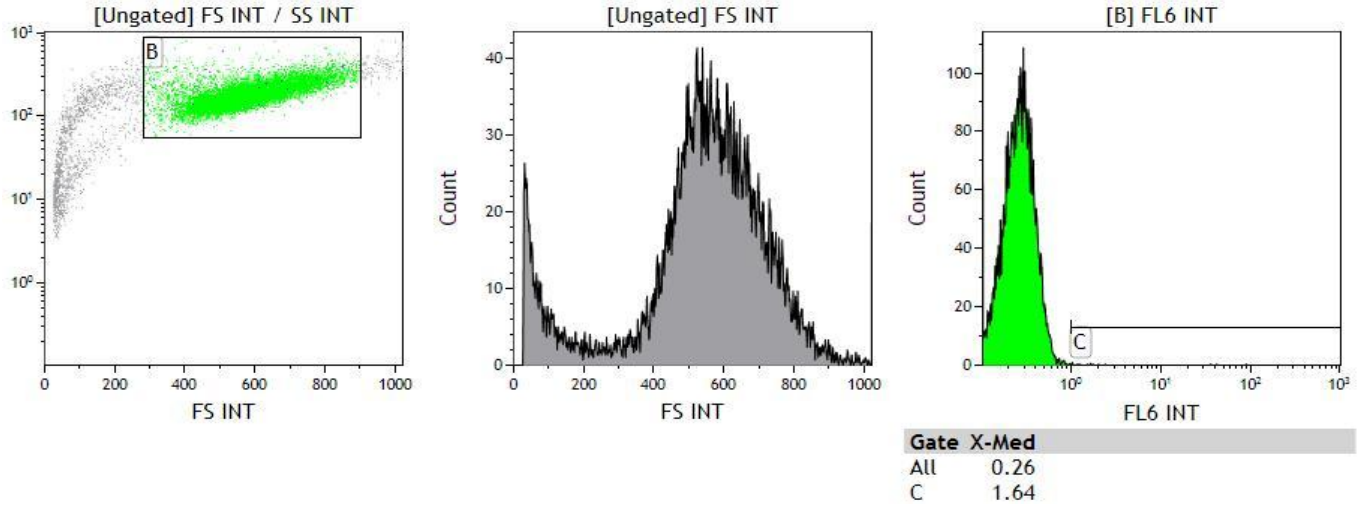

Figure 3. Alexa647 uptake in H1299 cells, siRNA control.

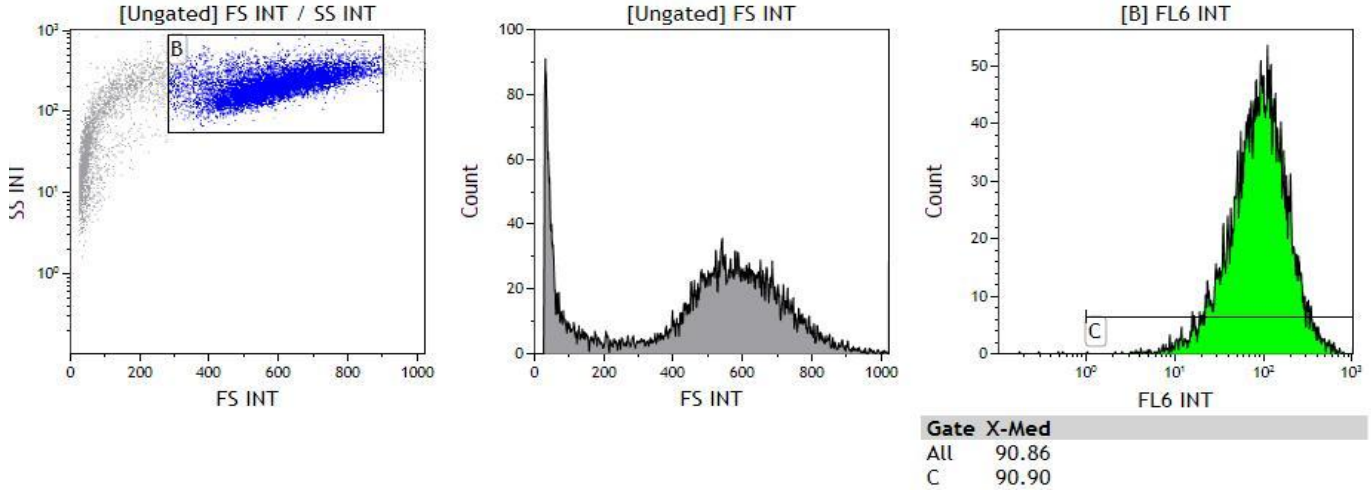

Figure 4. Alexa 647 uptake in H1299 cell treated with chitosan DPn 300 complexed with siRNA at N/P ratio 30

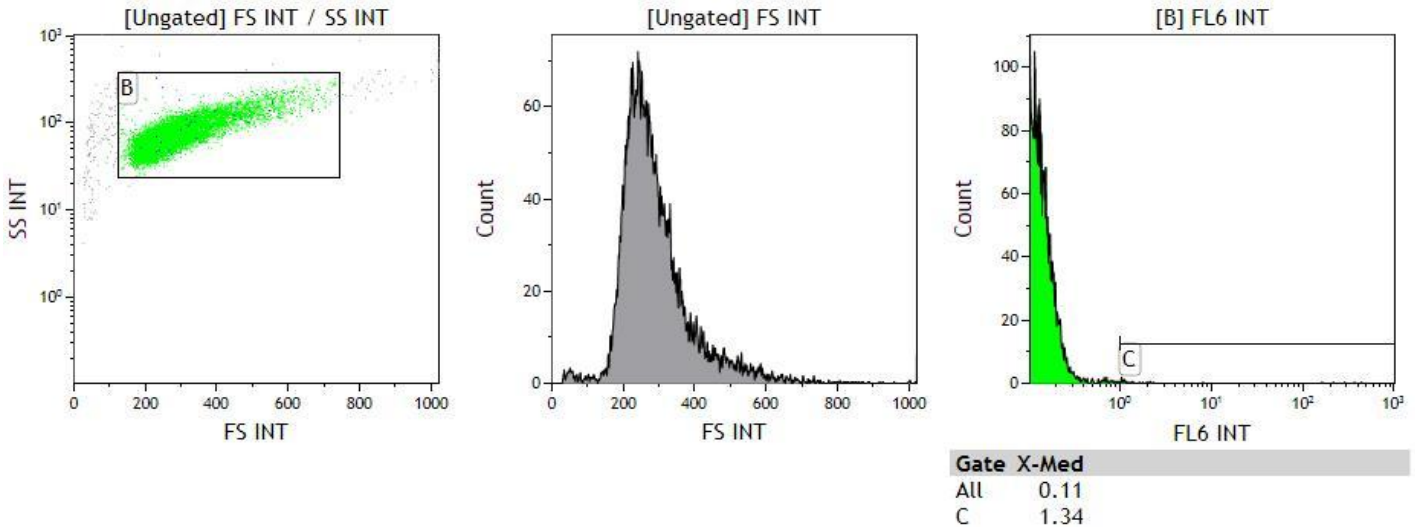

Figure 5. Uptake in RBE4 cells, Alexa647-siRNA control

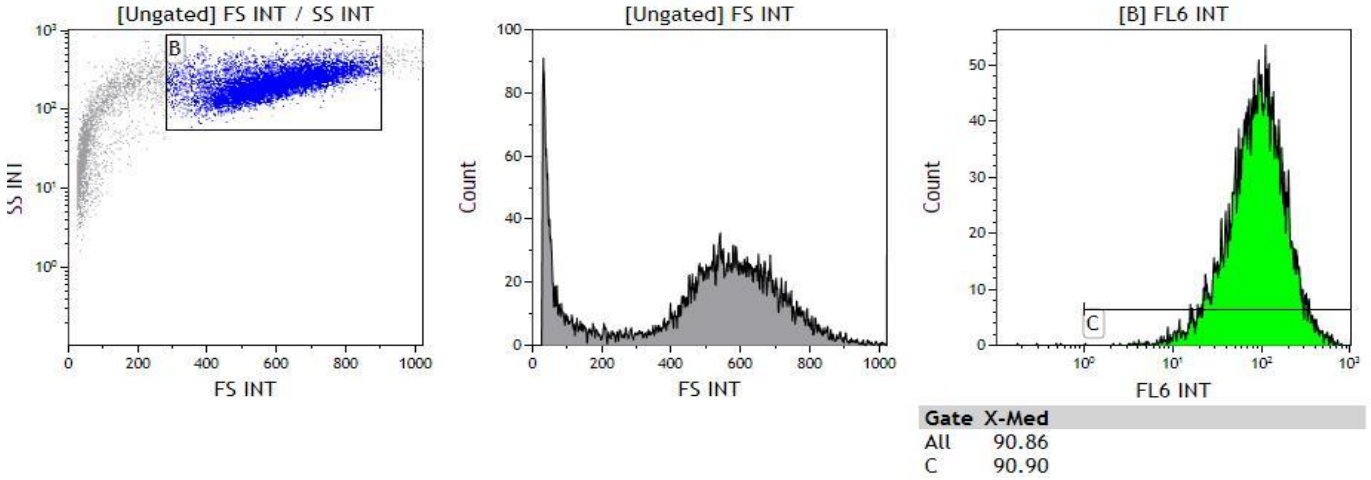

Figure 6. Uptake in RBE4 cells treated with chitosan Dpn300 complexed with Alexa647-siRNA in N/P ratio 30.

C.2 GFP knockdown in H1299 cells

Table 5. Raw and calculated flow cytometry data for H1299 GFP knockdown without serum incubation.

GFP Knockdown without serum													
Sample		**Ctrl**	**C 54 (T)**		**C54 (NT)**	**C 200 (T)**		**C200 (NT)**	**C 300 (T)**		**C300 (NT)**	**Turbofect T**	**Turbofect NT**
N/P			*10*	*30*	*30*	*10*	*30*	*30*	*10*	*30*	*30*	*3*	*3*
	Parallell												
Median FI	1	19.9	18.90	5.51	16.50	5.81	1.25	20.70	1.77	2.18	21.60	20.8	26.10
	2	18.9	18.00	5.46	18.50	4.85	1.23	20.80	7.02	2.56	22.20	22.6	24.50
	3	20.7	17.90	5.17	17.10	*	2.63	20.80	4.64	1.96	22.00	23	*
% median FI of ctrl	1	100.34	95.29	27.78	83.19	29.29	6.30	104.37	8.92	10.99	108.91	104.87	131.60
	2	95.29	90.76	27.53	93.28	24.45	6.20	104.87	35.39	12.91	111.93	113.95	123.53
	3	104.37	90.25	26.07	86.22	0.00	13.26	104.87	23.39	9.88	110.92	115.97	0.00
avg		**100.00**	**92.10**	**27.13**	**87.56**	**17.92**	**8.59**	**104.71**	**22.57**	**11.26**	**110.59**	**111.60**	**127.56**
stdev		4.55	2.78	0.93	5.17	15.70	4.05	0.29	13.25	1.53	1.54	5.91	5.70

Table 6. Raw and calculated flow cytometry data for H1299 GFP knockdown with serum incubation.

GFP knockdown with serum													
Sample		**Ctrl**	**C 54 (T)**		**C54 (NT)**	**C 200 (T)**		**C200 (NT)**	**C 300 (T)**		**C300 (NT)**	**Turbofect T**	**Turbofect NT**
N/P			10	30	30	10	30	30	10	30	30	3	3
	Parallell												
Median FI	1	11.3	14.9	13.4	14.7	13.4	4.05	11.1	15.2	1.69	15.6	8.63	10.6
	2	11.8	14.7	12.4	14.4	13.2	4.28	11	15.5	1.92	15.8	8.63	9.97
	3	10.6	14.2	11.6	14.2	13.4	3.91	11.1	14.9	1.89	14	8.71	8.95
% median FI of ctrl	1	100.59	132.64	119.29	130.86	119.29	36.05	98.81	135.31	15.04	138.87	76.82	94.36
	2	105.04	130.86	110.39	128.19	117.51	38.10	97.92	137.98	17.09	140.65	76.82	88.75
	3	94.36	126.41	103.26	126.41	119.29	34.81	98.81	132.64	16.82	124.63	77.54	79.67
avg		**100.00**	**129.97**	**110.98**	**128.49**	**118.69**	**36.32**	**98.52**	**135.31**	**16.32**	**134.72**	**77.06**	**87.60**
stdev		5.37	3.21	8.03	2.24	1.03	1.66	0.51	2.67	1.11	8.78	0.41	7.41

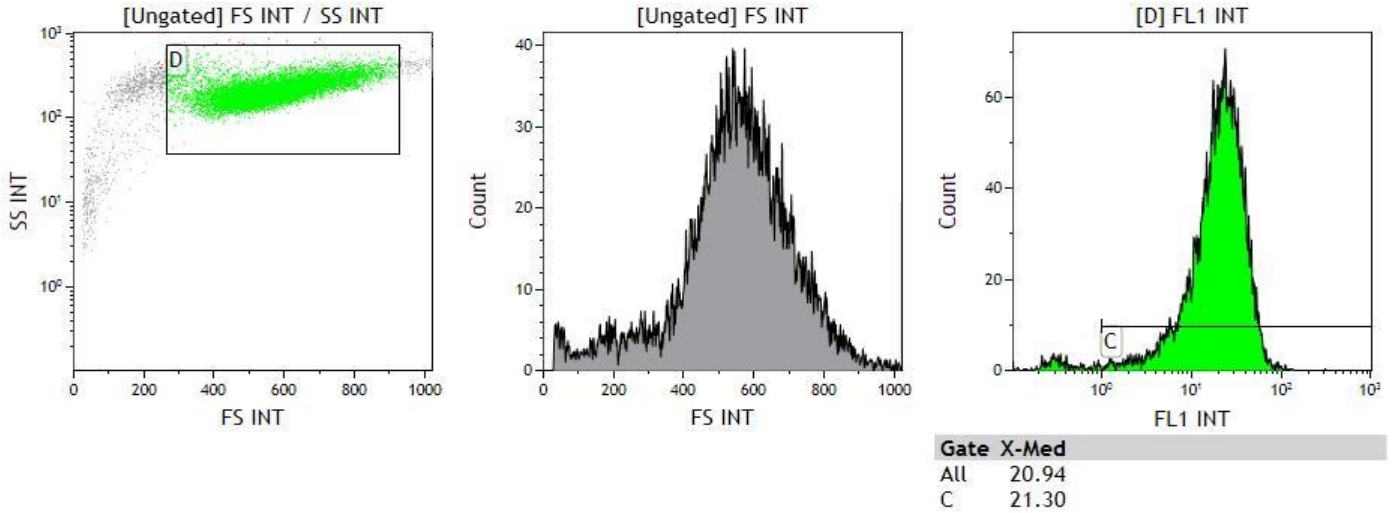

Figure 1. GFP expression in untreated control cells.

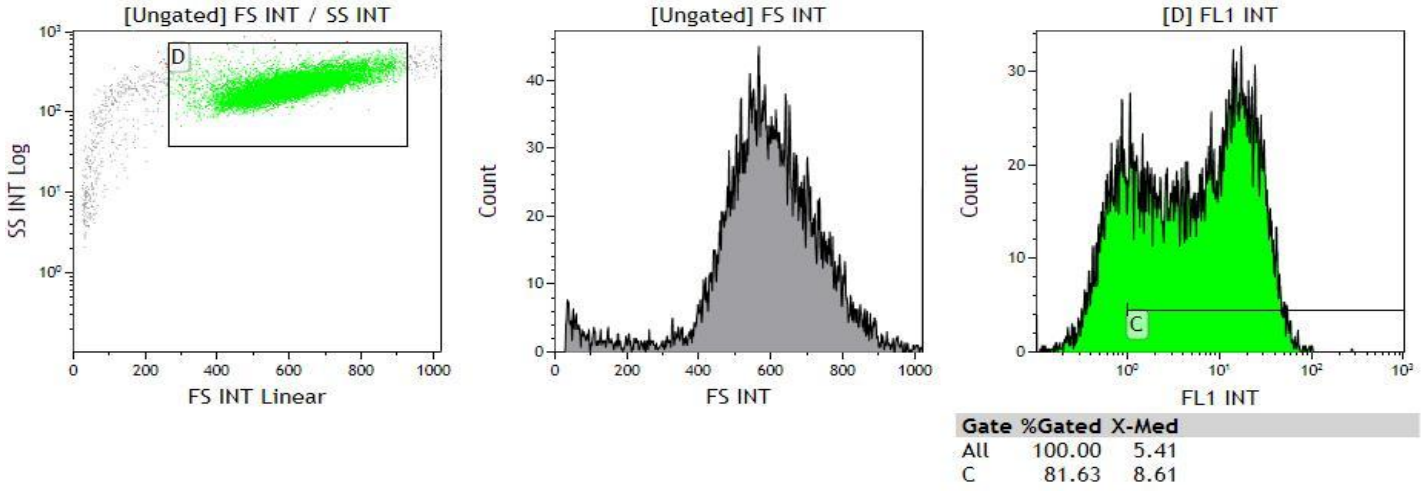

Figure 2. GFP expression in cells treated with Chitosan DPn 300 complexed with GFP siRNA at N/P ratio 30.

C.3 GAPDH knockdown in H1299 cells and RBE4 cells

Table 7. Raw and calculated data for GAPDH knockdown in H1299 cells.

Sample		C54	C54	C54 NT	C200	C200	C200 NT	C300	C300	C300 NT	Turbo T	Turbo NT	Ctrl	Blank
N/P		*10*	*30*	*30*	*10*	*30*	*30*	*10*	*30*	*30*	-	-	-	-
	Parallell													
Abs 615nm	1	0.154	0.355	0.168	0.471	0.535	0.205	0.524	0.537	0.260	0.621	0.647	0.087	0.666
	2	0.229	0.385	0.187	0.559	0.552	0.325	0.531	0.530	0.231	0.523	0.658	0.177	0.656
	3	0.191	0.385	0.221	0.558	0.589	0.300	0.483	0.537	0.216	0.661	0.584	0.179	0.738
Minus blank	1	-0.532	-0.332	-0.519	-0.215	-0.151	-0.481	-0.163	-0.150	-0.427	-0.066	-0.039	-0.599	
	2	-0.458	-0.301	-0.499	-0.128	-0.134	-0.362	-0.155	-0.157	-0.455	-0.163	-0.028	-0.509	
	3	-0.495	-0.301	-0.466	-0.129	-0.097	-0.387	-0.204	-0.149	-0.470	-0.025	-0.103	-0.507	
% reduced of ctrl	1	98.83	61.57	96.29	39.92	28.05	89.38	30.25	27.76	79.19	12.24	7.32	111.25	
	2	84.96	55.96	92.72	23.67	24.88	67.16	28.83	29.09	84.55		5.27	94.56	
	3	91.94	55.89	86.43	23.88	18.03	71.80	37.84	27.66	87.34	4.64		94.19	
Avg		**91.91**	**57.80**	**91.81**	**29.16**	**23.65**	**76.11**	**32.31**	**28.17**	**83.69**	**8.44**	**6.29**	**100.00**	
Std		6.93	3.26	4.99	9.32	5.12	11.72	4.84	0.80	4.14	5.37	1.44	9.75	

D Cytotoxicity data

D.1 Alamar blue Assay calculations and data

To determine the percent reduction of alamarBlue, the following equation was used:

$$\%\ \text{Reduced} = \frac{\textbf{CRED Test Well}}{\textbf{COX Negative Control Well}}$$

$$= \frac{(\varepsilon OX)\lambda 2\ A\lambda 1 - (\varepsilon OX)\ \lambda 1\ A\lambda 2}{(\varepsilon RED)\lambda 1\ A'\lambda 2 - (\varepsilon RED)\lambda 2\ A'\lambda 1} \times 100$$

eg: $$= \frac{(117{,}216)(.61) - (80{,}586)(.42)}{(155{,}677)(.64) - (14{,}652)(.44)} \times 100$$

$$= \frac{71{,}502 - 33{,}846}{99{,}633 - 6{,}447} \times 100$$

$$= 0.404 \times 100 = 40\%$$

Where:

CRED = concentration of reduced form alamarBlue
COX = oxidized form of alamarBlue
λ1 = 570**, λ2** = 600
(εOX)λ2 = 117,216 molar extinction coefficient of alamarBlue oxidized form
(εOX)λ1 = 80,586 molar extinction coefficient of alamarBlue oxidized form
(εRED)λ1 = 155,677 molar extinction coefficient of alamarBlue reduced form
(εRED)λ2 = 14,652 molar extinction coefficient of alamarBlue reduced form
Aλ1 = 0.61 ,absorbance reading for test well
Aλ2 = 0.42 ,absorbance reading for test well
A'λ2 = 0.64 ,absorbance reading for negative control well
A'λ1 = 0.44 ,absorbance reading for negative control well.

Table 8.1 Raw absorbance and calculated values from 5-days alamarBlue assay with H1299 cells.

Time		24hrs						48hrs						72hrs					
Sample		**Ctrl**	**C 200**	**C 200**	**C 200 (N)**	**siRNA**	**R-MAX**	**Ctrl**	**C 200**	**C 200**	**C 200 (N)**	**siRNA**	**R-MAX**	**Ctrl**	**C 200**	**C 200**	**C 200 (N)**	**siRNA**	**R-MAX**
N/P		*-*	*10*	*60*	*60*	*-*	*-*	*-*	*10*	*60*	*60*	*-*	*-*	*-*	*10*	*60*	*60*	*-*	*-*
Parallell																			
Abs 570	1	0.674	0.683	0.589	0.605	0.666	0.640	1.259	1.037	0.936	0.930	0.908	0.890	1.890	1.305	1.166	1.154	1.033	0.971
	2	0.938	0.838	0.826	0.843	0.737	0.743	1.062	1.023	1.017	1.015	1.210	1.010	1.053	0.985	0.972	0.984	0.949	0.976
	3	0.761	0.885	0.743	0.779	0.808	0.760	1.017	0.936	0.981	0.890	0.939	0.965	1.034	0.924	0.951	0.950	0.945	0.909
	4	0.880	0.842	0.882	1.004	0.851	0.661	0.965	0.979	0.900	0.930	0.953	0.960	1.049	0.994	0.972	1.010	1.022	1.058
Abs 600	1	0.393	0.448	0.422	0.418	0.481	0.430	0.705	0.318	0.301	0.293	0.339	0.315	1.241	0.576	0.504	0.507	0.355	0.354
	2	0.525	0.572	0.563	0.576	0.557	0.536	0.321	0.352	0.359	0.354	0.451	0.324	0.300	0.347	0.321	0.350	0.336	0.334
	3	0.511	0.577	0.516	0.540	0.590	0.523	0.319	0.361	0.352	0.367	0.431	0.329	0.361	0.357	0.363	0.361	0.392	0.350
	4	0.608	0.566	0.489	0.636	0.551	0.516	0.292	0.329	0.350	0.379	0.375	0.346	0.250	0.322	0.297	0.289	0.324	0.279
% reduced of ctrl	1	*	78.55	73.10	58.19	61.81	65.32	90.56	104.2	*	98.09	97.97	90.85	102.3	*	*	*	113.19	*
	2	109.7	*	*	*	*	*	110.1	*	109.36	107.8	108.1	*	105.8	*	105.70	106.4	105.29	101.63
	3	90.28	92.48	110.1	87.61	92.09	90.77	99.28	107.1	92.47	99.44	85.79	86.43	91.82	108.02	93.32	96.48	96.50	92.87
	4	*	*	110.3	*	*	115.1	*	73.82	92.47	*	*	67.13	*	74.42	65.58	65.16	68.85	67.88
avg		**100.0**	**85.51**	**97.87**	**87.61**	**97.32**	**90.41**	**100.0**	**95.07**	**98.10**	**101.8**	**97.29**	**81.47**	**100.0**	**91.22**	**88.20**	**89.36**	**95.96**	**87.46**
std		13.75	9.85	21.45	20.80	38.39	24.91	7.69	18.46	9.75	5.30	11.17	12.61	7.29	23.76	20.55	21.54	19.31	17.51

Table 8.2 Raw absorbance and calculated values from 5-days alamarBlue assay with H1299 cells.

Time		96hrs						120hrs					
Sample		Ctrl	C 200	C 200	C 200 (N)	siRNA	R-MAX	Ctrl	C 200	C 200	C 200 (N)	siRNA	R-MAX
N/P		-	*10*	*60*	*60*	-	-	-	*10*	*60*	*60*	-	-
	Parallell												
Abs 570	1	0.840	1.150	0.863	1.280	1.027	1.221	0.733	0.621	0.613	0.833	0.614	0.594
	2	0.884	0.802	0.857	0.871	0.828	0.837	0.609	0.589	0.629	0.670	0.574	0.606
	3	0.916	0.876	0.878	0.854	0.836	0.846	0.614	0.743	0.623	0.631	0.532	0.611
	4	0.854	0.873	0.862	0.883	0.819	0.841	0.632	0.615	0.625	0.636	0.596	0.605
Abs 600	1	0.474	0.717	0.473	0.826	0.753	0.802	0.234	0.210	0.217	0.247	0.215	0.196
	2	0.519	0.543	0.550	0.574	0.594	0.541	0.235	0.197	0.219	0.222	0.225	0.211
	3	0.533	0.556	0.551	0.575	0.630	0.543	0.217	0.231	0.203	0.213	0.197	0.214
	4	0.531	0.554	0.531	0.549	0.599	0.549	0.211	0.199	0.212	0.203	0.208	0.200
% reduced of ctrl	1	132.15	101.53					101.99		105.74	102.96		
	2	91.74	103.89	84.37	94.47	93.98	82.66	100.93	98.14	99.29	104.79	113.38	91.81
	3	93.92	108.91	97.97	98.92	91.02	80.02	94.68	94.77	119.31	98.58	98.79	80.97
	4	82.18	86.66	87.41	88.05	89.68	72.34	102.40	106.68	119.31	105.03	108.69	99.22
avg		**100.00**	**100.25**	**89.92**	**93.82**	**91.56**	**78.34**	**100.00**	**99.86**	**110.91**	**102.84**	**106.95**	**90.67**
std		22.03	9.56	7.14	5.47	2.20	5.36	3.60	6.14	10.04	2.99	7.45	9.18

Table. 8.3 Raw and calculated data for metabolic activity in RBE4 cells.

Sample		C 200		C 200 NT	C 300		C 300 NT	RNAiMAX	siRNA	ctrl	triton	blank
N/P		*10*	*60*	*60*	*10*	*60*	*60*	-	-	-	-	-
	Parallell											
Abs 570 nm	1	0.5937	0.563	0.5916	0.5792	0.5597	0.5897	0.5776	0.6124	0.5959	0.3854	0.622
	2	0.5802	0.5592	0.5807	0.6081	0.5648	0.583	0.5667	0.6106	0.6214	0.3832	0.5805
	3	0.5944	0.6006	0.6165		0.6112	0.6092	0.5019	0.604	0.6135	0.3854	0.6058
	4	0.5803	0.574	0.5963	0.6175	0.6123	0.5971	0.5222	0.6276	0.6202	0.3854	0.6853
Abs 600 nm	1	0.273	0.3116	0.2918	0.2787	0.3062	0.2651	0.3483	0.241	0.2587	0.5375	0.8688
	2	0.2759	0.3109	0.2851	0.2317	0.2766	0.2595	0.3699	0.2223	0.2117	0.5348	0.833
	3	0.2747	0.2849	0.2891	0.2665	0.248	0.241	0.3601	0.2411	0.2234	0.5394	0.8676
	4	0.2728	0.2915	0.2809	0.2273	0.2323	0.241	0.339	0.2229	0.2195	0.5385	0.8384
% reduced of ctrl	1	87.11	74.83	83.88	83.15	74.91	87.41	72.54	95.84	89.69	3.40	
	2	87.21	77.15	85.91	100.23	83.67	90.36	69.77	102.23	106.27	3.47	
	3	86.97	86.80	89.59		94.51	95.11	54.54	93.98	98.63	3.12	
	4	88.22	83.92	90.56	103.60	101.66	96.90	64.95	106.55	105.41	3.41	
Avg		**87.38**	**80.67**	**87.49**	**95.66**	**88.69**	**92.45**	**65.45**	**99.65**	**100.00**	**3.35**	
Std		0.57	5.62	3.13	10.96	11.79	4.35	7.92	5.80	7.68	0.15	

D.2 BSA assay calculations and data

The total protein concentration in cell samples can be deducted from a BCA standard curve. The concentrations used for this experiment was prepared as given in table 4 (volumes adjusted to number of samples):

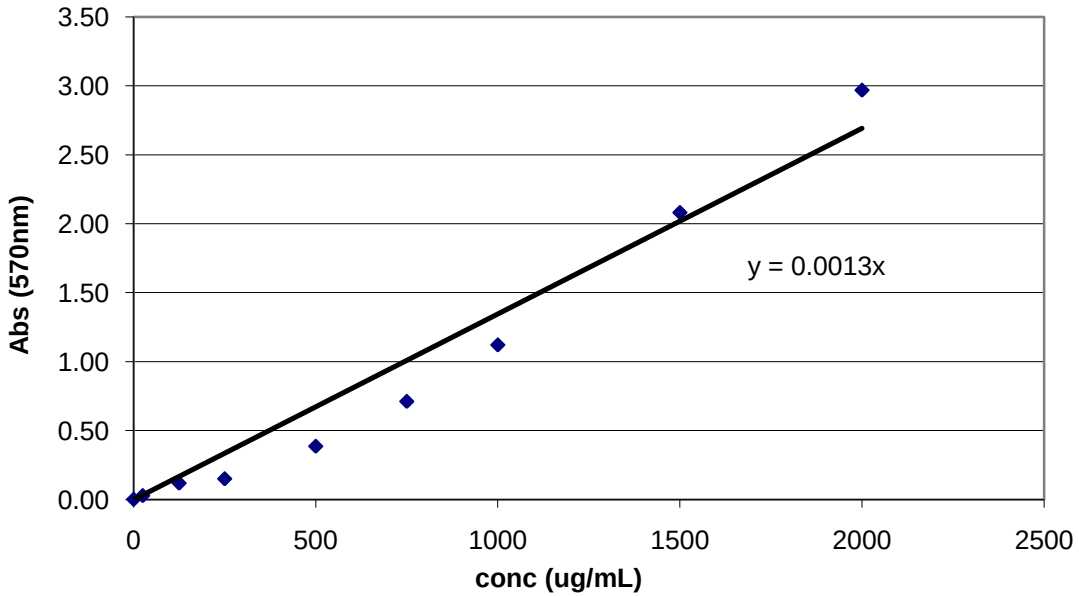

Figure 3 BSA standard curve, absorbance plot against BSA concentration (0-2000 ug/mL).

Table 6.1 Dilution series of BSA stock solution for standard

Vial	Lysis buffer	BSA source	Conc	Abs (570nm)
A	0 uL	300 uL stock solution	2,000 ug/mL	3.065
B	125 uL	375 uL stock solution	1,500 ug/mL	2.177
C	325 uL	325 uL stoc solution	1000 ug/mL	1.217
D	175 uL	175 uL from vial B	750 ug/mL	0.807
E	325 uL	325 uL from vial C	500 ug/mL	0.482
F	325 uL	325 uL from vial E	250 ug/mL	0.246
G	325 uL	325 uL from vial F	125 ug/mL	0.214
H	400 uL	100 uL from vial G	25 mg/mL	0.124
I	400 uL	0 uL	0 mg/mL	0.096

Calculation of total cellular protein was done by subtracting the blank measurements and adjusting for lysis volume used followed by division of slope from std curve (y-value given in figure 3)

eg. **abs-blank/Y*0.01**
= 0.148-0.096/0.0013*0.01
= <u>0.064</u> ug protein/mL cell lysate

Table 9.1 Raw and calculated absorbance data for five-day BSA assay experiment on H1299 cells.

Time		24 hrs						48 hrs						72 hrs					
Sample		**C200**	**C200**	**C200 (N)**	**siRNA**	**R-MAX**	**Ctrl**	**C200**	**C200**	**C 200 (N)**	**siRNA**	**R-MAX**	**Ctrl**	**C200**	**C200**	**C 200 (N)**	**siRNA**	**R-MAX**	**Ctrl**
N/P		*10*	*60*	*60*	-	-	-	*10*	*60*	*60*	-	-	-	*10*	*60*	*60*	-	-	-
Parallell																			
Raw data	1	0.105	0.105	0.102	0.104	0.106	0.107	0.242	0.253	0.241	0.237	0.233	0.234	0.409	0.394	0.403	0.382	0.322	0.391
	2	0.101	0.103	0.101	0.103	0.107	0.104	0.226	0.220	0.220	0.226	0.219	0.239	0.450	0.362	0.395	0.410	0.364	0.418
	3	0.104	0.104	0.102	0.104	0.104	0.114	0.225	0.225	0.233	0.232	0.218	0.231	0.384	0.413	0.391	0.362	0.359	0.363
	4	0.104	0.104	0.102	0.104	0.106	0.112	0.194	0.204	0.189	0.195	0.179	0.190	0.398	0.417	0.373	0.383	0.382	0.379
Blank subtracted	1	0.008	0.008	0.006	0.008	0.010	0.011	0.145	0.157	0.144	0.141	0.137	0.137	0.313	0.297	0.306	0.285	0.226	0.294
	2	0.005	0.006	0.005	0.006	0.010	0.008	0.130	0.123	0.123	0.129	0.123	0.142	0.353	0.266	0.298	0.313	0.268	0.321
	3	0.008	0.007	0.005	0.007	0.008	0.017	0.128	0.128	0.137	0.136	0.122	0.134	0.287	0.316	0.295	0.266	0.263	0.266
	4	0.007	0.008	0.006	0.007	0.010	0.015	0.097	0.108	0.093	0.098	0.082	0.093	0.301	0.320	0.276	0.286	0.286	0.282
Divided by slope	1	0.064	0.065	0.044	0.061	0.076	0.083	1.116	1.206	1.111	1.082	1.053	1.057	2.405	2.286	2.357	2.193	1.735	2.263
	2	0.036	0.046	0.037	0.046	0.079	0.061	0.998	0.947	0.949	0.993	0.943	1.094	2.719	2.046	2.293	2.410	2.060	2.469
	3	0.059	0.056	0.040	0.056	0.058	0.132	0.988	0.986	1.053	1.042	0.936	1.032	2.209	2.434	2.266	2.043	2.019	2.048
	4	0.056	0.059	0.043	0.056	0.073	0.118	0.746	0.830	0.713	0.756	0.634	0.719	2.318	2.462	2.126	2.203	2.198	2.170
Avg prot/mL cell lys		**0.054**	**0.056**	**0.041**	**0.055**	**0.072**	**0.098**	**0.962**	**0.992**	**0.956**	**0.968**	**0.891**	**0.976**	**2.412**	**2.307**	**2.261**	**2.212**	**2.003**	**2.238**
Std prot/mL cell lys		0.012	0.008	0.003	0.006	0.010	0.032	0.155	0.157	0.176	0.147	0.180	0.173	0.219	0.191	0.097	0.151	0.194	0.178

Table 9.2 Raw and calculated absorbance data for five-day BSA assay experiment on H1299 cells.

Time		96 hrs						120hrs					
Sample		**C200**	**C200**	**C 200 (N)**	**siRNA**	**R-MAX**	**Ctrl**	**C200**	**C200**	**C 200 (N)**	**siRNA**	**R-MAX**	**Ctrl**
N/P		*10*	*60*	*60*	-	-	-	*10*	*60*	*60*	-	-	-
	Parallell												
Raw data	1	0.463	0.481	0.513	0.479	0.426	0.516	0.495	0.468	0.504	0.508	0.527	0.513
	2	0.449	0.444	0.510	0.606	0.483	0.485	0.397	0.513	0.561	0.486	0.419	0.469
	3	0.524	0.493	0.482	0.560	0.461	0.484	0.511	0.518	0.528	0.453	0.492	0.701
	4	0.507	0.500	0.536	0.511	0.583	0.456	0.389	0.466	0.504	0.495	0.454	0.507
Blank subtracted	1	0.367	0.384	0.417	0.383	0.330	0.420	0.398	0.372	0.408	0.411	0.431	0.417
	2	0.353	0.347	0.414	0.510	0.386	0.388	0.300	0.417	0.464	0.389	0.322	0.372
	3	0.428	0.396	0.385	0.463	0.364	0.388	0.414	0.422	0.432	0.357	0.396	0.604
	4	0.410	0.403	0.439	0.414	0.486	0.360	0.292	0.370	0.408	0.399	0.357	0.411
Divided by slope + lysate adjustment	1	2.821	2.956	3.206	2.943	2.536	3.229	3.064	2.861	3.137	3.165	3.312	3.207
	2	2.715	2.672	3.183	3.922	2.971	2.985	2.308	3.207	3.572	2.995	2.477	2.862
	3	3.289	3.046	2.965	3.562	2.802	2.982	3.186	3.244	3.321	2.743	3.045	4.648
	4	3.157	3.103	3.380	3.188	3.742	2.766	3.122	2.844	3.135	3.068	2.748	3.158
Avg protein/mL cell lysate		**2.995**	**2.944**	**3.183**	**3.404**	**3.012**	**2.990**	**2.853**	**3.039**	**3.291**	**2.993**	**2.896**	**3.469**
STDEV protein/mL cell lysate		0.272	0.192	0.170	0.429	0.518	0.190	0.476	0.216	0.207	0.180	0.362	0.801

D.3 Cell count data

Table 10. Estimated raw data for cellular proliferation in H1299 cells over 5-days after counting with bürker chambers.

Time		24hrs						48hrs					
Sample		**C200**	**C200**	**C 200 (N)**	**siRNA**	**R-MAX**	**Ctrl**	**C200**	**C200**	**C 200 (N)**	**siRNA**	**R-MAX**	**Ctrl**
N/P		10	60	60				10	60	60			
Cell count	Parallell												
	1	9000	6750	7650	8550	6300	10350	15000	10500	11700	14700	9000	16500
	2	9450	5850	8100	9000	5400	11250	14400	9600	11400	14100	8700	17400
Avg		**9225**	**6300**	**7875**	**8775**	**5850**	**10800**	**14700**	**10050**	**11550**	**14400**	**8850**	**16950**
Std		318.198	636.396	318.198	318.198	636.396	636.396	424.264	636.396	212.132	424.264	212.132	636.396

Time		72hrs						96hrs					
Sample		**C200**	**C200**	**C 200 (N)**	**siRNA**	**R-MAX**	**Ctrl**	**C200**	**C200**	**C 200 (N)**	**siRNA**	**R-MAX**	**Ctrl**
N/P		10	60	60				10	60	60			
Cell count	Parallell												
	1	29700	21600	22800	30000	18000	32400	45000	33000	33900	44700	29700	48000
	2	29100	21000	22500	28800	19200	33600	43500	33600	34500	46500	29100	49200
Avg		**29400**	**21300**	**22650**	**29400**	**18600**	**33000**	**44250**	**33300**	**34200**	**45600**	**29400**	**48600**
Std		424.264	424.264	212.132	848.528	848.528	848.528	1060.660	424.264	424.264	1272.792	424.264	848.528

Time		120hrs					
Sample		**C200**	**C200**	**C 200 (N)**	**siRNA**	**R-MAX**	**Ctrl**
N/P		10	60	60			
Cell count	Parallell						
	1	48600	35400	35100	48300	30600	51300
	2	49800	35700	36000	48000	30300	52500
Avg		**49200**	**35550**	**35550**	**48150**	**30450**	**51900**
Std		848.528	212.132	636.396	212.132	212.132	848.528

D.4 PI staining flow cytometry data

Table 11.1 Raw and calculated flow cytometry data for 5-days PI staining experiment.

Time		24hrs						48hrs					
Sample		C200	C200	C 200 (N)	siRNA	R-MAX	Ctrl	C200	C200	C 200 (N)	siRNA	R-MAX	Ctrl
N/P		10	60	60	-	-	-	10	60	60	-	-	-
	Parallell												
Median FI	1	2.06	5.99	7.66	7.19	9.3	4.79	7	10.71	11.98	8.88	22.95	4.89
	2	2.17	8.04	10.55	8.68	9.62	*	7.15	7.51	14.98	8.89	23.37	*
%of ctrl	1	43.01	125.05	159.92	150.10	194.15	100.00	143.15	219.02	244.99	181.60	469.33	100.00
	2	45.30	167.85	220.25	181.21	200.84	*	146.22	153.58	306.34	181.80	477.91	*
Average		**44.15**	**146.45**	**190.08**	**165.66**	**197.49**	**100.00**	**144.68**	**186.30**	**275.66**	**181.70**	**473.62**	**100.00**
STDEV		1.62	30.26	42.66	22.00	4.72	0.00	2.17	46.27	43.38	0.14	6.07	0.00
Time		**72hrs**						**96hrs**					
Sample		C200	C200	C 200 (N)	siRNA	R-MAX	Ctrl	C200	C200	C 200 (N)	siRNA	R-MAX	Ctrl
N/P		10	60	60	-	-	-	10	60	60	-	-	-
	Parallell												
Median FI	1	6.32	17.55	16.54	18.34	34.06	4.95	3.37	6.53	6.28	15.23	16.66	5.24
	2	15.83	15.9	17.18	9.1	31.26	6.7	5.56	6.46	7.27	9.78	16.5	5.11
%of ctrl	1	108.5	301.29	283.9	314.8	584.721	84.979	231.3	303.57	175.1	242.5121	310.5314	101.3
	2	271.76	272.96	294.9	156.2	536.6524	115.02		198.45	176.2	231.3043	297.971	98.74
Average		**190.13**	**287.12**	**289.4**	**235.5**	**560.6867**	**100**	**231.3**	**251.01**	**175.7**	**236.9082**	**304.2512**	**100**
STDEV		115.44	20.03	7.769	112.2	33.98968	21.244	0	74.332	0.82	7.925062	8.881534	1.776

Table 11.2 Raw and calculated flow cytometry data for 5-days PI staining experiment.

Time		120hrs					
Sample		C200	C200	C 200 (N)	siRNA	RNAiMAX	Ctrl
N/P		10	60	60	-	-	-
	Parallell						
Median FI	1	11.97	15.71	9.06	12.55	16.07	4.99
	2	*	10.27	9.12	11.97	15.42	*
%of ctrl	1	239.88	314.83	181.563126	251.5	322.0441	100
	2	0	205.81	182.765531	239.9	309.018	*
Average		239.88	260.32	182.164329	245.7	315.5311	100
STDEV		0	77.087	0.85022859	8.219	9.21081	0

E Rho 123 efflux data

E.1 mdr1 downregulation in RBE4 cells

Table 11 Raw and calculated flow cytometry data for Rho 123 efflux in RBE4 cells

Sample		C 300 T	C 300 T	C 300 NT	C 400 T	C 400 T	C 400 NT	siRNA	ctrl	ctrl + Verapamil
N/P		*10*	*10*	*10*	*10*	*10*	*10*	-	-	*10 uM*
siRNA		mdr1a	mdr1b		mdr1a	mdr1b		mdr1a	-	
	Parallell									
Median FI	1	6.19	3.01	3.45	6.19	3.3	4.05	3.15	3.84	42.4
	2	7.21	3.27	3.12	6.02	3.77	3.18	3.18	2.41	68.3
	3	7.08	3.27	2.96	5.49	3.88	4.02	3.07	2.52	49
% of Verapamil ctrl	1	11.15	5.42	6.21	11.15	5.94	7.29	5.67	6.92	76.36
	2	12.99	5.89	5.62	10.84	6.79	5.73	5.73	4.34	123.01
	3	12.75	5.89	5.33	9.89	6.99	7.24	5.53	4.54	88.25
avg		**12.07**	**5.66**	**5.92**	**11.00**	**6.37**	**6.51**	**5.70**	**5.63**	**100.00**
stdev		1.30	0.33	0.42	0.22	0.60	1.11	0.04	1.82	21.44

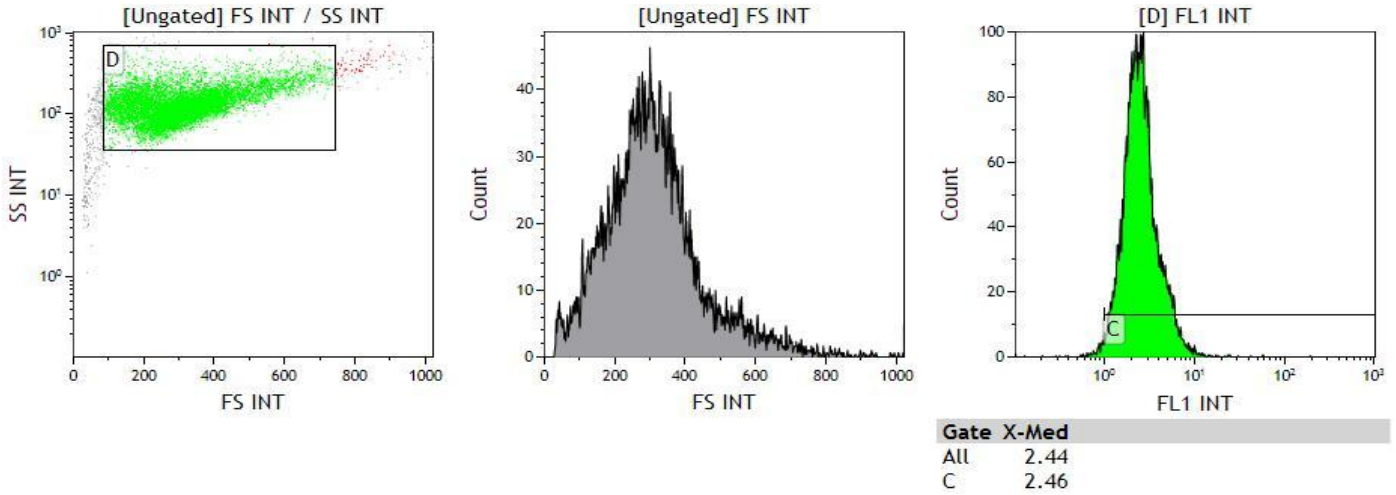

Figure 7. Rho123 acumulation in RBE4 cells, untreated control

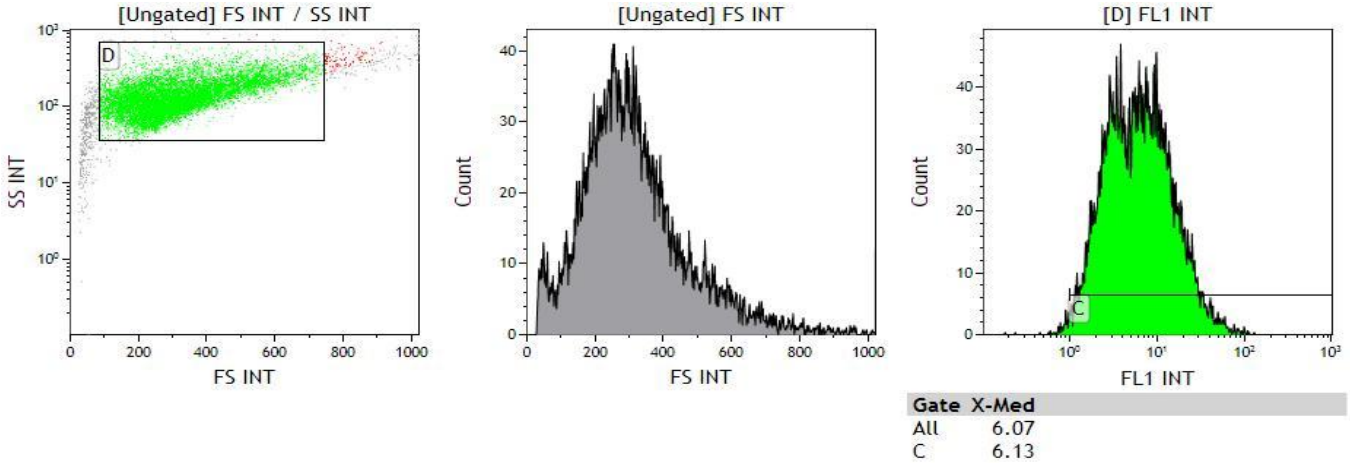

Figure 8. Rho123 accumuation in RBE4 cells treated with chitosan DPn300 complexed with mdr1a-siRNA at N/P ratio 10

E.2 Verapamil and siRNA concenctration effect on Rho123 efflux

Table 13. Raw and calculated flow cytometry data for temporal Verapamil concentration dependent Rho123 efflux in RBE4 cells.

Time		1hrs						1,5 hrs					
Concentration		**0uM**	**5uM**	**10uM**	**25um**	**50uM**	**250uM**	**0uM**	**5uM**	**10uM**	**25um**	**50uM**	**250uM**
	Parallell												
Median FI	1	152	224	234	218	512	708	72	64.7	81	*	357	566
	2	156	268	182	280	424	768	68.3	79.6	139	139	348	636
	3	139	293	230	315	464	768	63	101	155	155	*	*
avg		**149.00**	**261.67**	**215.33**	**271.00**	**468.00**	**738.00**	**67.77**	**81.77**	**125.00**	**147.00**	**352.50**	**601.00**
std		8.89	34.93	28.94	49.12	62.23	42.43	4.52	18.25	38.94	11.31	6.36	49.50

Time		2hrs					
Concentration		**0uM**	**5uM**	**10uM**	**25um**	**50uM**	**250uM**
	Parallell						
Median FI	1	*	*	*	*	*	*
	2	65.9	87.9	121	158	216	470
	3	*	*	78.2	*	377	*
avg		**65.90**	**87.90**	**99.60**	**158.00**	**296.50**	**470.00**
std		0.00	0.00	30.26	0.00	113.84	0.00

Table 14 Raw and calculated flow cytometry data for Verapamil concentration dependent Rho123 efflux in RBE 4 cells

Concentration		**0uM**	**5uM**	**10uM**	**25um**	**50uM**	**250uM**
	Parallell						
Median FI	1	3.88	256	293	381	428	571
	2	4.36	304	299	402	455	608
	3	3.95	299	374	440	*	636
avg		**4.06**	**286.33**	**322.00**	**407.67**	**441.50**	**605.00**
std		0.26	26.39	45.13	29.91	19.09	32.60

Table 15 Raw flow cytometry data for siRNA concentration dependent Rho123 efflux I RBE4 cells.

Sample		C500	C500 NT	C500	C500 NT	C500	C500 NT	C500	C500 NT	C500	C500 NT	C500	C500 NT	vera	ctrl
Conc (nM)		**96**	**96**	**48**	**48**	**24**	**24**	**12**	**12**	**6**	**6**	**3**	**3**	-	
Median FI	1	28.9	4.24	16.8	3.27	10.7	3.36	6.71	4.68	5.55	4.52	4.17	4.4	5.26	3.91
	2	*	4.77	24.7	3.24	13.5	3.33	6.24	5.46	5.03	4.85	4.2	4.68	5.97	**4.52**
	3	*	4.48	19.90	3.36	*	3.27	5.46	4.48	6.36	4.44	4.90	3.67	*	3.4
avg		**28.9**	**4.5**	**20.5**	**3.3**	**12.1**	**3.3**	**6.1**	**4.9**	**5.6**	**4.6**	**4.4**	**4.3**	**5.6**	**3.9**
std		0	0.265	3.980	0.062	1.980	0.046	0.631	0.518	0.670	0.217	0.413	0.521	0.502	0.566